MECHANISMS CONTROLLING THE DIRECTION EPITHELIAL CELLS EXTRUDE AND AN EMERGING ROLE FOR BASAL EXTRUSION IN TUMOR CELL INVASION

by

Gloria Slattum

A dissertation submitted to the faculty of
The University of Utah
in partial fulfillment of the requirements for the degree of

Doctor of Philosophy

Department of Oncological Sciences

The University of Utah

August 2015

The University of Utah Graduate School

STATEMENT OF DISSERTATION APPROVAL

The dissertation of **Gloria Slattum**

has been approved by the following supervisory committee members:

Jody Rosenblatt	, Chair	**09-22-2014** Date Approved
Charles Murtaugh	, Member	**09-22-2014** Date Approved
Rodney Stewart	, Member	**09-22-2014** Date Approved
Katharine Ullman	, Member	**09-22-2014** Date Approved
Bryan Welm	, Member	**09-22-2014** Date Approved

and by **Bradley R Cairns** , Chair/Dean of the Department/College/School of **Oncological Sciences**

and by David B. Kieda, Dean of The Graduate School.

ABSTRACT

Epithelia provide a protective barrier for the organs they encase, yet the cells compromising the epithelia constantly turn over via cell death and cell division. Our lab has identified a process by which cells are removed from an epithelial layer without compromising its barrier function called 'epithelial cell extrusion'. To extrude, a cell emits the bioactive lipid Sphingosine 1 Phosphate (S1P), which binds the $S1P_2$ receptor in the neighboring cells and triggers them to form an actomyosin ring that contracts to squeeze the cell out of the epithelial layer. Although extrusion removes apoptotic cells in response to damage, typically during homeostasis, epithelia extrude live cells that later die by anoikis. Wild type cells extrude predominantly apically and are eliminated through the lumen; however, we found that some cells extrude basally, back into the tissue the epithelium encases. Because most cells extrude while alive and many aggressive tumors override anoikis signaling to enhance survival outside the epithelium, the direction a cell extrudes has important consequences to its later fate. Transformed cells that extrude apically would be eliminated through the lumen; however, those extruding basally could potentially invade into the stroma. My goal was to elucidate the mechanisms that control the direction a cell extrudes from epithelia. My first study showed that apical extrusion requires microtubules and that they target p115 RhoGEF in the cells surrounding an extruding cell to the basolateral surface of the live/extruded cell interface to activate Rho-mediated actin/myosin contraction basolaterally. Blocking this mechanism by microtubule disrupters causes cells to instead contract apically and extrude basally. In my second study, I found that cells

expressing oncogenic K-Ras shift extrusion basally and enable extruded cells to survive and proliferate. In this situation, basal extrusion results from degradation of S1P due to autophagy that is highly upregulated in oncogenic K-Ras cells. Although $S1P_2$ also becomes slightly downregulated in K-Ras expressing cells too, disruption of the autophagy flux is sufficient to rescue both S1P levels and apical extrusion. Similarly, several aggressive tumors that are driven by K-Ras mutations lack $S1P_2$. $S1P_2$ deficient epithelia are extrusion deficient, which results in neoplastic masses that are chemoresistant, basal extrusion, and poor barrier function both *in vitro* and *in vivo*, all properties that could contribute to tumor formation and progression. Currently, I am developing an *in vivo* model system in zebrafish epidermis to investigate if basal cell extrusion can drive invasion of oncogenic K-Ras cells. The transparency of zebrafish allows us for the first time to directly follow extrusion, invasion, and migration of individual cells without invasive techniques intrinsic to most current cancer models.

To my family in Colombia and my new family in the States

TABLE OF CONTENTS

ABSTRACT iii

LIST OF FIGURES viii

ACKNOWLEDGEMENTS xi

Chapters

1. INTRODUCTION -TUMOR CELL INVASION: AN EMERGING ROLE FOR BASAL EPITHELIAL CELL EXTRUSION 1

1.1 Mechanisms of Epithelial Cell Extrusion 2
1.2 Apical Versus Basal Extrusion 2
1.3 Diverting Extrusion Basally 3
1.4 Basal Extrusion and Tumour Invasion 5
1.5 Concluding Remarks 6
1.6 References 7

2. P115 RHOGEF AND MICROTUBULES DECIDE THE DIRECTION APOPTOTIC CELLS EXTRUDE FROM AN EPITHELIUM 9

2.1 Introduction 11
2.2 Results and Discussion 12
2.3 Materials and Methods 18
2.4 References 19
2.5 Supplemental Materials 21

3. AUTOPHAGY IN ONCOGENIC K-RAS PROMOTES BASAL EXTRUSION OF EPITHELIAL CELLS BY DEGRADING S1P 26

3.1 Summary 27
3.2 Introduction 27
3.3 Results 28
3.4 Discussion 32
3.5 References 35
3.6 Supplemental Materials 37

4. DEFECTIVE APICAL EXTRUSION SIGNALING CONTRIBUTES TO AGGRESIVE TUMOR HALLMARKS 46

4.1 Abstract 47
4.2 Introduction 47
4.3 Results 48
4.4 Discussion 57
4.6 Materials and Methods 59
4.7 References 62

5. CONCLUSIONS AND FUTURE DIRECTIONS 64

5.1 Expression of Oncogenic K-Ras in the Developing Zebrafish Epidermis .. 67
5.2 Do Cells Expressing K-Ras^{V12} Extrude from the Developing Zebrafish Epidermis? 67
5.3 Is Invasion and Survival of K-Ras^{V12} Cells Enhanced by Loss of p53? 68
5.4 Developing Tools to Spatially and Temporally Control K-Ras Expression. 69
5.5 Perspectives to Spatially and Temporally Control K-Ras Expression 70
5.6 Expressing K-Ras in Other Cell Types 71
5.7 Can Small Molecule Inhibitors Selectively Target K-Ras Expressing Cell to Extrude and Die? 71
5.8 References 76

LIST OF FIGURES

1.1 The Direction in which a Cell Extrudes Has Important Consequences for Its Fate 3

1.2 Modes of Diverting Extrusion Basally 4

1.3 Alternative Mechanisms to Divert Extrusion Basally 5

1.4 Model of Single and Collective Cell-Autonomous Basal Extrusion of Tumour Cells During Tumour Invasion 7

2.1 Hallmarks of Apical and Basal Apoptotic Cell Extrusion 13

2.2 Localization of Active Myosin IIA but not Intrinsic Polarity Markers Are Altered when Cells Are Extruded Apically or Basally 14

2.3 The Growing Ends of Microtubules Point Toward the Actin/Myosin Ring During Extrusion 15

2.4 Disruption of Microtubules Alters the Direction a Cell Extrudes 16

2.5 P115 RhoGEF is Required for Apical Extrusion 17

S.2.1 Disruption of Microtubules with Nocodazole or Taxol Mislocalizes Both Myosin IIA and Phospho-myosin II in 16-HBE-14o Cell Monolayers 21

S.2.2 Freezing Microtubules with Taxol Drives Extrusion Basally in Zebrafish Larval Epidermis 22

S.2.3 siRNA-Mediated Knockdown of other RGS-RhoGEFs Has no Effect on the Direction of Extrusion 23

3.1 Epithelial Cells Expressing K-Ras^{V12} Extrude Basally in a Cell-Autonomous Manner 65

3.2 K-Ras^{V12} Does Not Affect Direction of Extrusion by Altering Microtubule Dynamics or Cell Intrinsic Polarity 28

3.3 S1P and the S1P Receptor 2 Signal Apical but Not Basal Extrusion and Are Misregulated in K-Ras^{V12}-Expressing Cells 29

3.4 K-Ras^{V12}-Extruding Cells Express High Levels of the Autophagy Marker LC3A/LC3B..... 30

3.5 Blocking Autophagy in K-Ras^{V12} Cells Rescues S1P Localization and Apical Extrusion..... 33

3.6 Basally Extruded K-RasV12 Cells Survive and Proliferate in 3D Cultures..34

S.3.1 Extruding K-Ras^{V12} Cells Lack S1P and Extrude Basally Under Homeostatic Conditions..... 38

S.3.2 Inducing Autophagy in Control MDCK Cells Induces Basal Extrusion..... 39

S.3.3 Chloroquine Blocks Autophagic Flux and Drives Extrusion Apically. 40

S.3.4 Chloroquine-Mediated Inhibition of Autophagy Does not Rescue S1P2 Levels in K-Ras^{V12} cells. 41

S.3.5 siRNA-Mediated Knockdown of ATG5 in K-Ras^{V12} Cells Rescues Apical Extrusion..... 42

S.3.6 K-Ras^{V12} Cells Grown in 3-D Form Mini-cysts by Extruding Live Cells Basally 43

4.1 Loss of S1P2 and Extrusion Leads to Accumulation of Epithelial Cell Masses 49

4.2 Disruption of S1P2 Extrusion Signaling Reduces Apoptotic Response 50

4.3 Decrease Apoptosis is due to blocked extrusion rather than S1P Signaling..... 51

4.4 Pancreatic Cancer Cell Line HPAF II Accumulates into Masses and Extrude Basally.....52

4.5 Exogenous Expression of $S1P_2$ Rescues Apical Extrusion and Cell Death 53

4.6 Inhibition of FAK Activity Specifically Increases Cell Death in Epithelial Cells Lacking S1P..... 55

4.7 FAK Inhibitors Eliminate Epidermal Cell Masses in $S1P_2$ Zebrafish Mutants and Improve Epidermal Barrier Function WIthout Affecting Wild Type Zebrafish..... 56

4.8 Exogenous $S1P_2$ Expression Reduces Orthotopic Pancreatic Tumors and Rate of Metastasis in Mice 57

4.9 Human Pancreatic Tumors Have Reduced S1P2 Expression.....58

4.10 Model For How Extrusion Can Promote Cell Death and Supress Tumor Formation.....59

5.1 Expressing Oncogenic K-Ras in the Developing Zebrafish Epidermis Results in the Formation of Cell Masses 73

5.2 Expression of CK:EGFP-K-Ras^{V12} Causes Cells to Extrude Basally.....74

5.3 Loss of p53 Enhanced Survival and Invasion of CK:EGFP-K-Ras^{V12} Cells.....75

ACKNOWLEDGEMENTS

I am grateful to my mentor Jody Rosenblatt for accepting me into her lab first as a lab manager and then as a graduate student. I thank her for giving me scientific freedom and trusting me to carry out a project on my own from day one. I thank her for taking me to my first ASCB meeting to present our work when I was still her technician. That was one of the experiences that made me want to earn a Ph.D. As a graduate advisor, Jody provided me with essential guidance at all points in my training. She gave me freedom to think, support when I failed, and motivation to continue on a path of becoming an independent scientist. I thank her for believing in me and for helping me navigate through my insecurities so I could believe in myself. Jody is one of the most sassy, intelligent, and well-rounded scientists I have known. I am deeply thankful for the opportunity of being trained by her.

My thesis committee members challenged me to think critically and to come up with new perspectives and interpretations of my research. They helped me move projects forward and gave me helpful input for my publications; for that I am immensely grateful to Charles Murtaugh, Rodney Stewart, Katharine Ullman, and Bryan Welm. I thank them for taking time to talk to me when needed and for helping me to find a new home for my postdoctoral training.

I thank all past and present Rosenblatt lab members for endless amounts of help and for all the good times. Special mention to Jimmy Delalande, George Eisenhoffer and Tom Marshall for help during the preliminatory exams and Yapeng Gu for fruitful collaborative projects. Thanks to my high school students Brenda

Martinez and Ian Gorrell-Brown for the contagious fascination about science and for keeping me young…at heart. I would like to thank the HCI administration for providing a wonderful environment that I will miss. Special thanks to my fifth floor "sister labs" the Beckerle and Ullman labs for friendship, technical assistance, advice, and reagents. I am grateful to the University of Utah Developmental Biology Training Grant community for monetary support and for being my second scientific family at the UofU. Special thanks to Joe Yost and Richard Dorsky for intellectual support.

During my time in Salt Lake City, I have formed many wonderful relationships with fellow graduate students, researchers, and other friends outside academia. I know our associations will remain lifelong friendships regardless of our geographical location. I thank all my friends for keeping me sane, healthy, and entertained.

Finally, I would not be where I am today without the love and support of both my family back in Colombia and my new family in the States. I was the first person in my family to go to college thanks to the tenacity of my mother Ofelia Londono. -Gracias Mama por tus sacrificios-. Thanks to my sister Juliana Martis for her unconditional support -siempre contigo- and to my uncle Dario Londono for being the father figure in my life. I would like to give credit to my grandma and my aunt "Las Julias" for teaching me how to cook and for allowing me to perform scary experiments in their kitchens. Many thanks to my lovely in-laws Ingrid and Larry Slattum for welcoming me into their family and for raising such a wonderful son. Most of all, I thank my rock, my love, my best friend, and my husband Paul Slattum. He put up with me during the high and low points of the past six years. Paul always encouraged me to pursue my passion and helped me not only emotionally but also in many practical ways such as reading and discussing my scientific manuscripts. Paul's love, kindness, and understanding

of this training process helped me to accomplish this work and for that there are really no words to express my gratitude towards him. I am thrilled to see what new adventures await for us.

CHAPTER 1

INTRODUCTION: TUMOUR CELL INVASION: AN EMERGING ROLE FOR BASAL EPITHELIAL CELL EXTRUSION

Reprinted with permission from Nature Reviews Cancer. Gloria M. Slattum and Jody Rosenblatt (2014). Tumour cell invasion: an emerging role for basal epithelial cell extrusion. Nat. Rev. Can. 14 (7): 495-501.

Chapter 1 is a published article.

OPINION

Tumour cell invasion: an emerging role for basal epithelial cell extrusion

Gloria M. Slattum and Jody Rosenblatt

Abstract | Metastasis is the leading cause of cancer-related deaths, but it is unclear how cancer cells escape their primary sites in epithelia and disseminate to other sites in the body. One emerging possibility is that transformed epithelial cells could invade the underlying tissue by a process called cell extrusion, which epithelia use to remove cells without disrupting their barrier function. Typically, during normal cell turnover, live cells extrude apically from the epithelium into the lumen and later die by anoikis; however, several oncogenic mutations shift cell extrusion basally, towards the tissue that the epithelium encases. Tumour cells with high levels of survival and motility signals could use basal extrusion to escape from the tissue and migrate to other sites within the body.

A crucial primary step for cancer metastasis is invasion, but we know very little about the mechanisms that govern it. As metastasis is the main reason that patients succumb to cancer, understanding the mechanisms that initiate metastasis will be crucial for targeting aggressive tumours. Because it has been difficult to directly follow tumour cell invasion from the epithelia, where most human cancers arise, we do not yet have a clear picture of the mechanisms that drive this process. In considering how tumour cells invade, it is helpful to understand how normal epithelia function and behave. Epithelia form a selective and protective barrier for all of the tissues that they encase. The polarized epithelium contains an apical surface that faces the lumen (external environment) and a basal surface that faces the basement membrane. Epithelia are the first line of defence against pathogens and toxins and, therefore, the cells that constitute epithelia are exposed to potential damage. As a result, many epithelia constantly turn over by cell division and death. We found that to maintain homeostatic epithelial cell numbers, when epithelia become too crowded owing to cell division elsewhere in the layer, some cells extrude and later die[1]. By extruding, cells that are destined for death are seamlessly ejected from the monolayer by concerted contraction of the cells that surround them[2]. Typically, because these cells extrude apically, they detach from the matrix and its associated survival signals, and die by anoikis. However, because metastatic tumour cells can, in some cases, override anoikis by upregulating survival signalling[3,4], we propose that extrusion could enable them to escape the epithelium. Normally, epithelia extrude cells apically into the lumen, which would function to remove any transformed cells, thereby essentially suppressing tumorigenesis. Intriguingly, we have found that oncogenic signalling can alter normal apical extrusion and cause cells to instead extrude basally under the epithelium. In this way, basal extrusion could enable transformed cells that are refractory to cell death to invade the underlying stroma. In this Opinion article, we discuss how misregulation of extrusion and normal epithelial survival mechanisms could enable tumours to initiate metastasis by subverting a process that normally triggers epithelial cell death.

Mechanisms of epithelial cell extrusion

Dying cells could pose a threat to the tight barrier that epithelia form, but they do not. Instead, epithelial cells that are destined to die are extruded by contraction of an actin and myosin ring in the surrounding cells, which squeeze cells out of the epithelium while closing the potential gap that could have formed from the exit of the cells (FIG. 1). All of the epithelia that have been observed, across animals from *Drosophila melanogaster*, zebrafish, mice and humans, extrude epithelial cells through what seems to be a highly conserved mechanism[1,2,5–8]. For a cell to extrude, it produces and secretes the bioactive lipid sphingosine-1-phosphate (S1P), which then binds to S1P receptor 2 (S1P2; also known as S1PR2; a G protein-coupled receptor) in the surrounding cells[9] to contract an intercellular actomyosin band that squeezes the cell out of the epithelium[2]. Additionally, we and others have observed that the cell being extruded also contracts, thereby aiding in its removal[10]. Epithelia extrude either live cells during homeostasis or dying cells in response to apoptotic stimuli[1,2,6,11]. We have found that epithelia maintain cell number homeostasis by extruding live cells once cells at a given site become up to 1.6-fold to 1.8-fold more crowded[1]. Crowding-induced extrusion occurs through activation of the mechanosensitive ion channel, PIEZO1, which presumably triggers calcium currents[12] to activate S1P-dependent extrusion of live cells, which later die by anoikis. Apoptotic stimuli, such as chemotherapies, toxins or pathogens that trigger cell death can also activate cell extrusion through the S1P–S1P2 pathway[9], possibly in response to caspase activation[11]. Thus, both during natural cell turnover and following the induction of apoptosis, the S1P–S1P2 pathway activates cells to extrude in a manner that ensures no gaps form in the epithelia as cells are expelled.

Apical versus basal extrusion

Normally, epithelia extrude cells apically into the lumen, but in some situations, cells can also extrude basally into the underlying tissue. The direction in which a cell extrudes depends on where the actomyosin band contracts in neighbouring cells[13]. To extrude a cell apically, contraction occurs towards the base of the cell, whereas to extrude it basally, contraction

occurs at the apex (FIG. 1). The direction in which a cell extrudes can have important consequences for the fate of the cell, especially when live, transformed cells are extruded. Apical extrusion eliminates cells with upregulated survival signalling through the lumen (FIG. 1). For example, in the intestine, apical extrusion would remove putative tumour cells into the waste canal. Similarly, transient mosaic expression of oncogenic *HRAS*^{V12} or v-*src* transforms cells and causes them to self-segregate away from the wild-type epithelium in a process that is similar to but different from extrusion, which essentially removes them[14,15]. In mammary or prostate glands, apical extrusion could lead to carcinoma *in situ* — a tumour type with good prognosis in which cells accumulate in the luminal space and are generally non-invasive[16,17]. However, basal extrusion preserves live cells within the organ (FIG. 1). During development, basal extrusion could enable cells to dedifferentiate from the epithelium and then differentiate into new cell types, as during neuroblast delamination in *D. melanogaster*[18]. For tumours, basal extrusion could enable transformed cells to invade the tissue that the epithelium encases to initiate metastasis. Intriguingly, oncogenic mutations can subvert the normal extrusion pathway, shifting the direction of extrusion from apical to basal, and this suggests a link between basal extrusion and invasiveness. A basally extruded cell could either divide and accumulate beneath the epithelium or invade, depending on its ability to cross the basement membrane by either degrading or invading the underlying matrix[19]. Many tumours express various matrix metalloproteinases, which suggests that matrix degradation may be intrinsic to transformation, enabling basally extruded transformed cells to transit through the basement membrane. However, *in vivo* studies have suggested that cancer cells can breach the basement membrane without degrading it, by extending invadopodia that squeeze through gaps in the matrix and push it apart[20,21]. Determining whether basally extruded cells can breach the basement membrane and how they do so will be important goals for future *in vivo* studies.

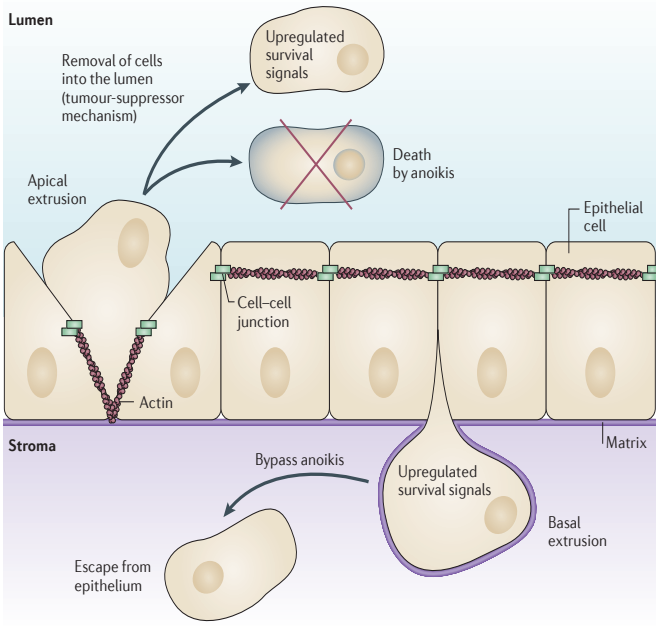

Figure 1 | **The direction in which a cell extrudes has important consequences for its fate.** Extrusion removes either live or dying epithelial cells in response to crowding during homeostasis or apoptotic stimuli, respectively. Typically, live cells extrude apically from the epithelium into the lumen by contracting an intercellular actomyosin band basolaterally to squeeze the cell out (left). Apically extruded cells generally die in the lumen by the loss of survival signals from the matrix — a process called anoikis (top). Tumour cells with upregulated survival signalling could still be eliminated through the lumen by apical extrusion, which could function like a tumour-suppressor mechanism (top). Less frequently, cells extrude basally by apical contraction (right), back into the tissue that the epithelium encases. Several oncogenic mutations disrupt apical extrusion, thereby driving cells to extrude basally instead. Because basally extruded cells with upregulated survival signals can bypass anoikis, this may provide a novel mechanism to enable oncogenic cells with upregulated survival signalling to initiate invasion (bottom).

Apical extrusion seems to require at least two activities: S1P–S1P2 signalling and microtubule dynamics. Microtubules reorient to the basolateral interfaces of both the extruding and neighbouring cells to localize RHO guanine nucleotide exchange factor 1 (ARHGEF1; also known as p115RHOGEF) and thereby activate RHO-mediated actomyosin contraction under the extruding cell, driving it out apically[13] (FIG. 2a). Disruption of microtubule dynamics shifts extrusion basally[13]. Although microtubules reorient in both the extruding cell and its neighbours, cell-autonomous knockdown of a crucial microtubule regulator, adenomatous polyposis coli (APC), suggests that the direction in which a cell extrudes requires dynamic microtubules only within the extruding cell[22]. Because the S1P–S1P2–RHO pathway controls only apical but not basal extrusion[23], one possibility is that, in the extruding cell, microtubules target S1P to restrict contraction and membrane recycling basolaterally, where it is needed to drive apical extrusion (FIG. 2a). When any machinery that controls apical extrusion is aberrant, cell-autonomous contraction of cortical actin and myosin at existing apical junctions could enable a cell to extrude basally. Recent studies show that cell-autonomous apical contraction precedes the basolateral contraction in the neighbouring cells, and this suggests that loss of basolateral contraction would naturally lead to basal extrusion[10]. However, how complete apical contraction is controlled is still unknown, as are other signals and mechanisms that might collaborate to control apical extrusion.

Diverting extrusion basally

Oncogenic signalling. Although there is no direct proof that basal extrusion drives tumour cell invasion, we have found that oncogenic mutations can manipulate apical extrusion, a process that normally promotes cell death, into a process that could allow cells to escape into the stroma. Mutations that disrupt the

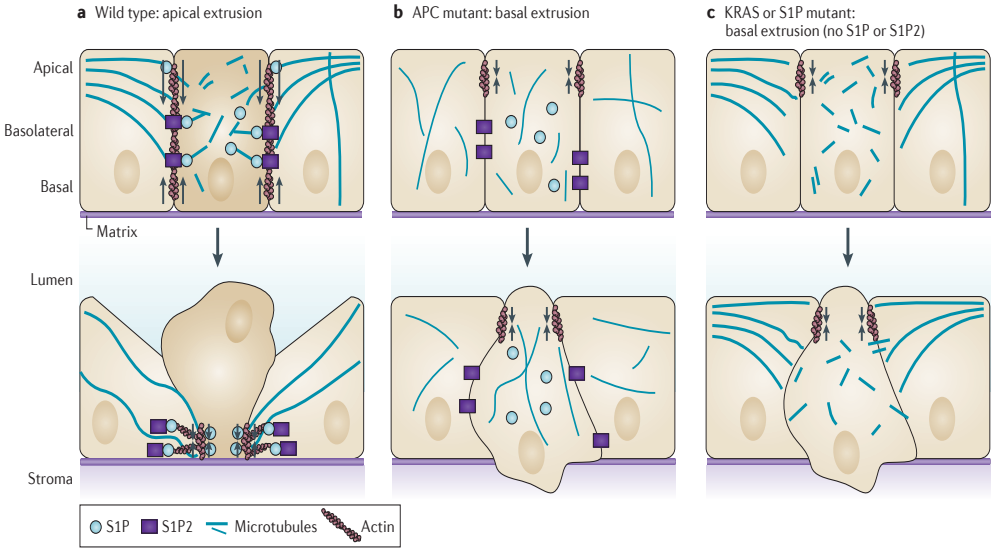

Figure 2 | **Modes of diverting extrusion basally.** **a** | During wild-type apical extrusion, the cell that is destined for extrusion (dark beige), as well as its neighbouring cells (light beige), reorient their microtubules to the basolateral interface. Reorientation of microtubules in the cell destined for extrusion is required for apical extrusion and presumably restricts the biologically active lipid sphingosine-1-phosphate (S1P) to the basolateral surface, where it binds to S1P receptor 2 (S1P2) expressed in the neighbouring cells to trigger apical extrusion. Microtubule reorientation in the neighbouring cells might reinforce RHO-mediated actomyosin contraction (arrows) at the basolateral surface. **b** | Mutations in the tumour suppressor adenomatous polyposis coli (APC) that disrupt microtubule dynamics can function cell-autonomously in the extruding cell to drive extrusion basally. Cell-autonomous apical contraction of cortical actin and myosin (arrows) at apical epithelial cell junctions can extrude the cell basally into the basement membrane. **c** | Oncogenic KRAS disrupts apical extrusion by downregulating both S1P and S1P2. Autophagy degrades S1P, and both S1P puncta and apical extrusion can be rescued by disrupting autophagy. Without apical extrusion signalling, junctional apical actin and myosin contraction (arrows) results in basal extrusion.

tumour-suppressive function of APC or constitutively activate KRAS disrupt normal apical extrusion by disrupting either cytoskeletal dynamics or S1P signalling, respectively (FIG. 2b,c). *APC* is mutated or lost in >80% of colorectal cancers and is downregulated in some breast and prostate cancers[24–26]. We found that cells preferentially extruded basally when a truncated form of APC associated with tumour formation was expressed in either cell lines or in zebrafish epidermis[22]. The APC truncation mutant lacks the carboxyl terminus that binds to both microtubules and F-actin[27–29]. Because apical extrusion relies on coupling microtubules to cortical actin to control where contraction occurs, loss of this domain disrupts this targeting, thereby driving extrusion basally. APC functions cell-autonomously to drive apical extrusion, as expression of the microtubule-binding domain of APC in the extruding cell alone is sufficient to rescue apical extrusion in colorectal cancer cell lines expressing the truncation mutant. This suggests that single cells accumulating sporadic *APC* mutations could extrude basally. This new function for APC in controlling the direction of extrusion could collaborate with its known function in driving uncontrolled proliferation through upregulated WNT signalling[30,31], thereby enabling *APC*-mutant cells to both invade and proliferate.

Oncogenic *KRAS* mutations are crucial drivers of aggressive tumours, such as those of the pancreas, lung and colon[32–34]. When we expressed the oncogenic $KRAS^{V12G}$ mutation in MDCK (canine kidney epithelial cell) monolayers, they predominantly extruded basally in a cell-autonomous manner[23]. When grown in three-dimensional cysts surrounded by matrix, the basally extruded oncogenic *KRAS*-mutant cells proliferated into smaller cysts or migrated away as single cells. Similarly, constitutive mosaic expression of oncogenic *HRAS* in MCF-10A mammary epithelial cell cysts caused cells to either basally extrude or lead collective cell migration of the neighbouring wild-type cells within the cyst[35]. Although three-dimensional cultures are more representative of *in vivo* epithelia than monolayers, it is not clear how well the Matrigel that surrounds these cysts mimics the underlying matrix and stroma in real tissue. Therefore, the compelling behaviour of basally extruded cells from cysts will ultimately need to be assessed *in vivo* to determine whether basally extruded transformed cells can also escape beneath the epithelium in real tissue. We have found that unlike mutated APC, which disrupts microtubules, cells that express oncogenic *KRAS* degrade S1P and partially downregulate S1P2, both of which are required for apical extrusion. S1P is degraded owing to high levels of autophagy, specifically in extruding KRAS-transformed cells. Disruption of autophagy (either genetically or chemically) rescued S1P accumulation and apical extrusion[23]. Because cells expressing oncogenic *KRAS* rely on autophagy for their increased survival[36,37], current clinical trials are using chloroquine (an autophagy inhibitor) to target these cells. This treatment could also prevent tumour invasion by promoting apical

extrusion[38]. Chloroquine treatment has already shown promising results in overcoming chemotherapy resistance in human HER2 (also known as ERBB2)-positive breast cancers that are also addicted to autophagy[39]. However, mouse models of genetically engineered pancreatic cancers that lack p53 have found that chloroquine treatment can actually exacerbate tumour growth[40], suggesting some human tumours driven by KRAS mutants might also be chloroquine-resistant.

Alternative mechanisms to divert extrusion basally. Apart from APC and KRAS, other factors that are typically associated with poor cancer prognosis could also shift the direction in which cells extrude from epithelia. Proteins controlling epithelial cell polarity, such as those in the scribble homologue (SCRIB)–lethal giant larvae homologue (LGL)–discs large homologue (DLG) and partitioning defective 6 homologue (PAR6)–PAR3–atypical protein kinase C (aPKC) complexes, are mutated in numerous carcinomas[41] and have been linked to their progression and metastasis[42]. Disruption of epithelial polarity could randomize the direction in which a cell extrudes, thereby increasing the incidence of basal extrusion (FIG. 3a). Another possibility is that activation of basal extrusion alone could occur without invoking other signals that activate apical extrusion (FIG. 3b). In several studies, basal extrusion seems to occur as a default pathway when apical extrusion fails[10,23]. Although it is not clear what controls basal extrusion, one candidate could be hyperactivation of RHO, which is associated with tumour cell migration[43,44,20]. It is plausible that simply activating RHO would cause cells to contract at the apical cell–cell junctions, where most actin and myosin II exists. In addition, comparatively weaker cell–cell or cell–matrix adhesions could cause some cells to preferentially detach (FIG. 3c). Studies of nanomechanical forces of single cells, both *in vitro* and from human breast cancer biopsies, revealed that metastatic breast tumour cells are less stiff than the rest of the tumour or surrounding normal tissue[45], and this can substantially enhance their motility *in vitro*[46]. Similarly, reduced cell–cell adhesion by decreased expression of E-cadherin that is found in some metastatic tumours[47] could make these cells more susceptible to extrusion than others. Although reduced tension of a single cell within an epithelium under expansion forces could make that cell spread, under intrinsic crowding forces in regions of extrusion[1], it would instead be more likely to extrude. Loss of E-cadherin and reduced cell stiffness have been linked to metastatic tumours, but it is unclear whether these factors drive cell extrusion or are a consequence of losing contact with the epithelium following extrusion. Therefore, further studies will need to identify what makes a cell susceptible to extrusion and whether factors that promote extrusion do so in a preferentially apical or basal manner.

Basal extrusion and tumour invasion

We propose that tumour cells could exploit epithelial extrusion as a mechanism to

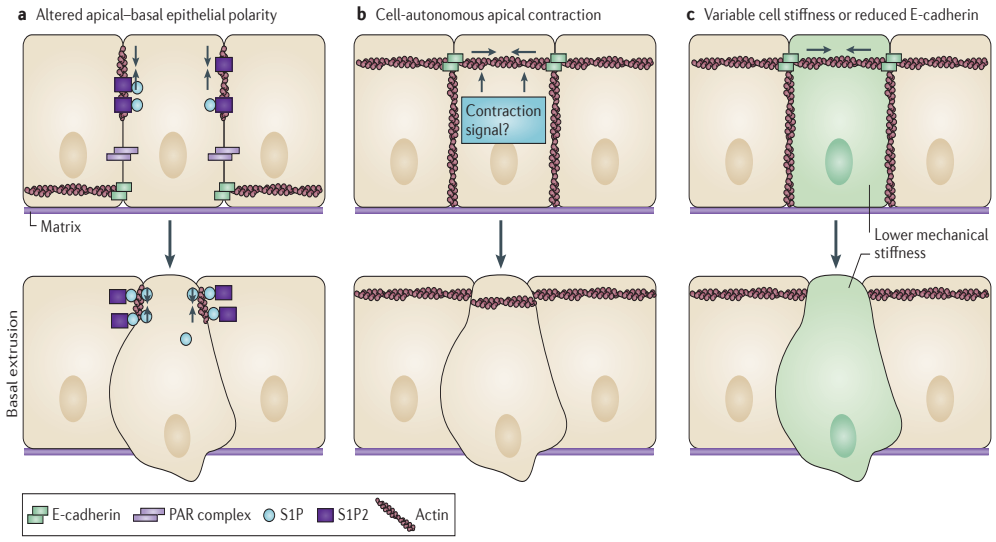

Figure 3 | **Alternative mechanisms to divert extrusion basally.** **a** | Improper localization or disruption of proteins controlling apical–basal epithelial cell polarity could increase basal extrusion by randomizing the direction in which a cell extrudes and disrupting apical extrusion. For example, E-cadherin and partitioning defective (PAR) protein complexes, which are crucial for localizing actin and myosin at apical contacts, could organize actin elsewhere if polarity is disrupted. **b** | Cell-autonomous apical contraction (arrows) alone could result in basal extrusion. Although it is not clear what activates contraction during basal extrusion, one candidate could simply be activation of RHO, which would cause actin and myosin — which are typically concentrated apically at adherens junctions — to contract at the top of the cell. **c** | Stiffness of tumour cells has been shown to have an important role during cell invasion. Under compressive forces, Cells that are less stiff (green), would be more primed to extrude than neighbouring, stiffer cells. Similarly, reduced E-cadherin levels, which are also associated with metastatic cells, would result in reduced attachment to surrounding cells, and these cells with lower E-cadherin levels might be more likely to become detached by extrusion. Although either of the above mechanisms could enable cells to extrude apically or basally, cells may be more likely to extrude basally, which seems to be the default direction in the absence of canonical extrusion signalling. S1P, sphingosine-1-phosphate; S1P2, S1P receptor 2.

initiate invasion into the underlying stroma. Current models for how cells escape the primary tumour to initiate metastasis fit into two broad categories: collective cell and single cell invasion[21,48,49]. The main difference between these modes of invasion is whether or not tumour cells maintain intracellular contacts as they migrate through the stroma and matrix (BOX 1). Histological sections showing streams of cells and single cells emanating from the tumour lend support to both types of motility[21]. In considering the hypothesis that tumour cells can invade using basal extrusion, it is important to establish the fate of transformed cells after they have extruded basally. When we transform MDCK cells with oncogenic *KRAS*, cells that extrude basally from cysts show two different behaviours: they either migrate away singly (FIG. 4a) or they proliferate, thereby forming a smaller cyst that is attached to the parent cyst[23] (FIG. 4b). Therefore, basal extrusion of transformed cells could enable cells to potentially migrate to other sites using either mode of invasion. It may be that some cells are primed to lose E-cadherin after extrusion to become more mesenchymal-like or stem cell-like (FIG. 4a). Basal extrusion seems to drive cells to dedifferentiate during development, as is the case during neuroblast delamination from the neuroepithelium in *D. melanogaster* or blood stem cell budding from the endothelia of many vertebrates[50,18]. Similarly, in cancer, tumour-initiating cells may bud from the epithelium by basal extrusion, thereby increasing their ability to proliferate and survive in foreign sites. Alternatively, basally extruded cells may retain their E-cadherin, as suggested by the ability of extruded cells expressing oncogenic *KRAS* to form new intact cysts. As seen in MCF-10A cysts, an initial basally extruded cell with an *HRAS* mutation could lead the collective cell migration of other attached cells[35]. Cells that do not lose E-cadherin expression after basal extrusion may still be less differentiated, having more intrinsic ability to divide, but restricted to an epithelial rather than a mesenchymal or pluripotent cell fate. Given the right cues *in vivo*, these cells could undergo collective cell migration rather than simply divide (FIG. 4b). Although epithelia that are cultured in three dimensions behave more like epithelia *in vivo*, they lack the complex components of real tissue. Thus, future work will need to determine whether basal extrusion could drive either single or collective cell migration in an *in vivo* model system.

An important point that distinguishes basal extrusion from the other models is that extrusion of cells can occur away from the main tumour mass (FIG. 4a,b). We have found that although oncogenic *KRAS* can drive cells to lose contact inhibition, the sites where cells basally extrude are not necessarily the same as the areas where masses form[23]. This could account for why pancreatic, colon and lung tumours that are driven by KRAS are typically metastatic with poor prognosis. The idea that tumours could metastasize independently of a primary tumour is alarming but not unheard of[51,52]. Indeed, molecular profiling of different tumour types suggests that some tumours develop with higher likelihoods of metastasizing than others[53–56]. Although transformed cells could invade at sites that are distinct from the primary mass using epithelial-to-mesenchymal transition (EMT) or collective cell migration, the invasive aspects in these models typically derive from general loss of epithelial organization and compressive forces that arise in surrounding tissue owing to growth of the primary tumour.

Concluding remarks

It is not clear why some tumours metastasize, whereas others do not. Our understanding of tumour invasion is mitigated by our ability to capture the natural formation and invasion of a tumour from an epithelium *in vivo*. Two-photon confocal intravital imaging of mammary mouse tumours has provided unprecedented resolution of migrating tumour cells *in vivo*[57–62]. One caveat to this approach, however, is the necessary introduction of a wound to provide a window for microscope access to the tumour, which could result in signalling and inflammation that is not present in naturally occurring tumours[63]. Future studies using zebrafish could provide an excellent animal model to directly visualize tumours invading directly from epithelia, as embryos are transparent and can be readily imaged without the invasive techniques that are intrinsic to current tumour models[64]. The zebrafish epidermis provides an excellent model for the epithelial bilayer that encases lungs and

Box 1 | **Current models of carcinoma invasion**

EMT: invasion of single tumour cells from a mass

Epithelial-to-mesenchymal transition (EMT) might provide a mechanism by which some single cells disseminate from an epithelial tumour mass[47,67,68] (see the figure, part **a**). During EMT, tumour cells downregulate E-cadherin (thereby weakening cell–cell adhesions) and migrate away as single cells. The loss of E-cadherin and activation of matrix-degrading proteases changes cell behaviour to be more mesenchymal, which allows these cells to adapt and survive in different parts of the body, independently of normal epithelial survival signals. EMT could promote the dedifferentiation of cells into stem cells in development and cancer[67,69]. Mesenchymal cells could then transdifferentiate to an epithelial phenotype in different sites within the body to promote metastatic outgrowth. Several types of carcinomas with poor prognosis express various inducers of EMT, such as snail homologue 1 (SNAI1) and SLUG (also known as SNAI2), TWIST, and zinc finger E-box-binding homeobox 1 (ZEB1) and ZEB2, which downregulate E-cadherin, and this supports the idea that tumours use EMT to initiate invasion.

Collective tumour cell invasion from a mass

Tumour cells have been seen emanating in streams from a tumour cell mass in what is termed collective cell migration[21,48,70] (see the figure, part **b**). Cells can migrate as a continuous mass that disseminates from the primary tumour or as smaller discontinuous cohorts of nearby cells. Unlike single cells that invade by EMT, these cells maintain cell–cell adhesions and are cohesive as they migrate. Migration of a cell front requires degradation of the matrix and the secretion of matrix-degrading proteases. Owing to histological evidence and the fact that most metastases retain E-cadherin, most metastatic carcinomas are thought to migrate collectively.

In addition, it is thought that metastatic cells may alter their ability to migrate singly or collectively, depending on the matrix and the tissue that they encounter.

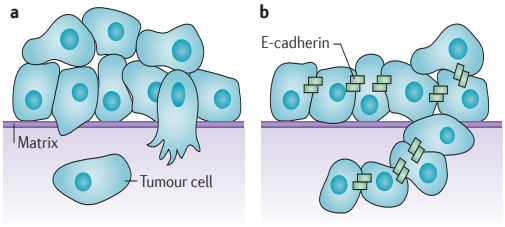

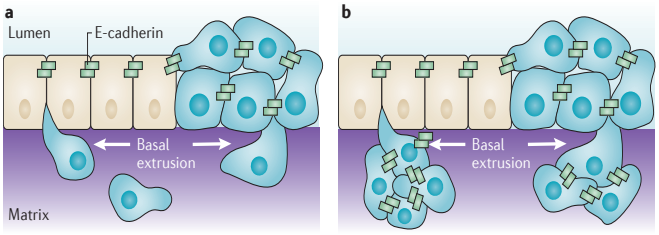

Figure 4 | **Model of single and collective cell-autonomous basal extrusion of tumour cells during tumour invasion.** Transformed cells (blue) could invade by basal extrusion, either when surrounded by wild-type cells (beige) or from homogenously transformed neighbouring cells (blue). **a** | Basally extruded cells could downregulate E-cadherin once they lose contact with other epithelial cells and migrate away as single cells. **b** | Basally extruded cells could retain E-cadherin expression and proliferate and migrate together by collective cell migration.

mammary glands. We are developing tools to label, knock down and express genes in single cells, where we can directly follow cells dividing, migrating and invading from the epithelium *in situ* (G.M.S., A. V. Gardner, G. Eisenhoffer and J.R., unpublished observations). Additionally, a new method to test the metastatic potential of human tumours has been developed in zebrafish embryos[65,66]. In this model, within only 48 hours after injecting cancer cells into the yolk sacs of 2-day-old zebrafish embryos, the metastatic potential was found to mimic mouse xenografts that were observed over the course of 2 months[54], and this zebrafish model allows tumour cell dissemination to be filmed live.

Once a tumour cell has gained access to the circulation, the extravasation, survival and establishment of micrometastases in a distal organ are thought to be surprisingly efficient[4]. Therefore, identifying whether tumour cells use basal extrusion to initiate invasion into the underlying stroma before entering the circulation is of crucial importance to our understanding of metastasis. Understanding the molecular and genetic profiles of cells that can extrude basally and survive might help us to define the metastatic potential of some tumours. Furthermore, identifying whether basal extrusion might be enhanced with zinc finger E-box-binding homeobox 1 (ZEB1), snail homologue 1 (SNAI1) and SLUG (also known as SNAI2), which drive EMT, or with matrix metalloproteinases, which are typically upregulated with collective cell migration, will be important to determine the relationship of extrusion to these previously defined invasion modes. New imaging methods that allow us to follow metastases from their initial local invasion to their colonization in distant organs will also be important for determining how cells invade and migrate and whether basal extrusion is a crucial step in this process. A better understanding of how different tumours invade will be essential for preventing their spread.

Gloria M. Slattum and Jody Rosenblatt are at the Huntsman Cancer Institute, University of Utah, 2000 Circle of Hope, Salt Lake City, Utah 84112, USA. Correspondence to J.R.
e-mail: Jody.Rosenblatt@hci.utah.edu
doi:10.1038/nrc3767
Published online 19 June 2014

1. Eisenhoffer, G. T. *et al.* Crowding induces live cell extrusion to maintain homeostatic cell numbers in epithelia. *Nature* **484**, 546–549 (2012).
2. Rosenblatt, J., Raff, M. C. & Cramer, L. P. An epithelial cell destined for apoptosis signals its neighbors to extrude it by an actin- and myosin-dependent mechanism. *Curr. Biol.* **11**, 1847–1857 (2001).
3. Hanahan, D. & Weinberg, R. A. Hallmarks of cancer: the next generation. *Cell* **144**, 646–674 (2011).
4. Valastyan, S. & Weinberg, R. A. Tumor metastasis: molecular insights and evolving paradigms. *Cell* **147**, 275–292 (2011).
5. Kiehart, D. P., Galbraith, C. G., Edwards, K. A., Rickoll, W. L. & Montague, R. A. Multiple forces contribute to cell sheet morphogenesis for dorsal closure in *Drosophila*. *J. Cell Biol.* **149**, 471–490 (2000).
6. Marinari, E. *et al.* Live-cell delamination counterbalances epithelial growth to limit tissue overcrowding. *Nature* **484**, 542–545 (2012).
7. Madara, J. L. Maintenance of the macromolecular barrier at cell extrusion sites in intestinal epithelium: physiological rearrangement of tight junctions. *J. Membr. Biol.* **116**, 177–184 (1990).
8. Guan, Y. *et al.* Redistribution of the tight junction protein ZO-1 during physiological shedding of mouse intestinal epithelial cells. *Am. J. Physiol. Cell Physiol.* **300**, C1404–C1414 (2011).
9. Gu, Y., Forostyan, T., Sabbadini, R. & Rosenblatt, J. Epithelial cell extrusion requires the sphingosine-1-phosphate receptor 2 pathway. *J. Cell Biol.* **193**, 667–676 (2011).
10. Kuipers, D. *et al.* Epithelial repair is a two-stage process driven first by dying cells and then by their neighbours. *J. Cell Sci.* **127**, 1229–1241 (2014).
11. Andrade, D. & Rosenblatt, J. Apoptotic regulation of epithelial cellular extrusion. *Apoptosis* **16**, 491–501 (2011).
12. Coste, B. *et al.* Piezo1 and Piezo2 are essential components of distinct mechanically activated cation channels. *Science* **330**, 55–60 (2010).
13. Slattum, G., McGee, K. M. & Rosenblatt, J. P115 RhoGEF and microtubules decide the direction apoptotic cells extrude from an epithelium. *J. Cell Biol.* **186**, 693–702 (2009).
14. Hogan, C. *et al.* Characterization of the interface between normal and transformed epithelial cells. *Nature Cell Biol.* **11**, 460–467 (2009).
15. Kajita, M. *et al.* Interaction with surrounding normal epithelial cells influences signalling pathways and behaviour of Src-transformed cells. *J. Cell Sci.* **123**, 171–180 (2010).
16. Donker, M. *et al.* Breast-conserving treatment with or without radiotherapy in ductal carcinoma in situ: 15-year recurrence rates and outcome after a recurrence, from the EORTC 10853 randomized Phase III trial. *J. Clin. Oncol.* **31**, 4054–4059 (2013).
17. Bleyer, A. & Welch, H. G. Effect of three decades of screening mammography on breast-cancer incidence. *N. Engl. J. Med.* **367**, 1998–2005 (2012).
18. Hartenstein, V., Younossi-Hartenstein, A. & Lekven, A. Delamination and division in the *Drosophila* neurectoderm: spatiotemporal pattern, cytoskeletal dynamics, and common control by neurogenic and segment polarity genes. *Dev. Biol.* **165**, 480–499 (1994).
19. Kelley, L. C., Lohmer, L. L., Hagedorn, E. J. & Sherwood, D. R. Traversing the basement membrane *in vivo*: a diversity of strategies. *J. Cell Biol.* **204**, 291–302 (2014).
20. Wyckoff, J. B., Pinner, S. E., Gschmeissner, S., Condeelis, J. S. & Sahai, E. ROCK- and myosin-dependent matrix deformation enables protease-independent tumor-cell invasion *in vivo*. *Curr. Biol.* **16**, 1515–1523 (2006).
21. Friedl, P., Locker, J., Sahai, E. & Segall, J. E. Classifying collective cancer cell invasion. *Nature Cell Biol.* **14**, 777–783 (2012).
22. Marshall, T. W., Lloyd, I. E., Delalande, J. M., Nathke, I. & Rosenblatt, J. The tumor suppressor adenomatous polyposis coli controls the direction in which a cell extrudes from an epithelium. *Mol. Biol. Cell* **22**, 3962–3970 (2011).
23. Slattum, G., Gu, Y., Sabbadini, R. & Rosenblatt, J. Autophagy in oncogenic K-Ras promotes basal extrusion of epithelial cells by degrading S1P. *Curr. Biol.* **24**, 19–28 (2014).
24. Clevers, H. Wnt breakers in colon cancer. *Cancer Cell* **5**, 5–6 (2004).
25. Oving, I. M. & Clevers, H. C. Molecular causes of colon cancer. *Eur. J. Clin. Invest.* **32**, 448–457 (2002).
26. van Es, J. H., Giles, R. H. & Clevers, H. C. The many faces of the tumor suppressor gene APC. *Exp. Cell Res.* **264**, 126–134 (2001).
27. Kita, K., Wittmann, T., Nathke, I. S. & Waterman-Storer, C. M. Adenomatous polyposis coli on microtubule plus ends in cell extensions can promote microtubule net growth with or without EB1. *Mol. Biol. Cell* **17**, 2331–2345 (2006).
28. Mogensen, M. M., Tucker, J. B., Mackie, J. B., Prescott, A. R. & Nathke, I. S. The adenomatous polyposis coli protein unambiguously localizes to microtubule plus ends and is involved in establishing parallel arrays of microtubule bundles in highly polarized epithelial cells. *J. Cell Biol.* **157**, 1041–1048 (2002).
29. Zumbrunn, J., Kinoshita, K., Hyman, A. A. & Nathke, I. S. Binding of the adenomatous polyposis coli protein to microtubules increases microtubule stability and is regulated by GSK3 β phosphorylation. *Curr. Biol.* **11**, 44–49 (2001).
30. Minde, D. P., Anvarian, Z., Rudiger, S. G. & Maurice, M. M. Messing up disorder: how do missense mutations in the tumor suppressor protein APC lead to cancer? *Mol. Cancer* **10**, 101 (2011).
31. Schepers, A. & Clevers, H. Wnt signaling, stem cells, and cancer of the gastrointestinal tract. *Cold Spring Harb. Perspect. Biol.* **4**, a007989 (2012).
32. Neuzillet, C., Hammel, P., Tijeras-Raballand, A., Couvelard, A. & Raymond, E. Targeting the Ras-ERK pathway in pancreatic adenocarcinoma. *Cancer Metastasis Rev.* **32**, 147–162 (2013).
33. Aviel-Ronen, S., Blackhall, F. H., Shepherd, F. A. & Tsao, M. S. K-*ras* mutations in non-small-cell lung carcinoma: a review. *Clin. Lung Cancer* **8**, 30–38 (2006).
34. Jiang, Y., Kimchi, E. T., Staveley-O'Carroll, K. F., Cheng, H. & Ajani, J. A. Assessment of K-*ras* mutation: a step toward personalized medicine for patients with colorectal cancer. *Cancer* **115**, 3609–3617 (2009).
35. Liu, J. S., Farlow, J. T., Paulson, A. K., Labarge, M. A. & Gartner, Z. J. Programmed cell-to-cell variability in Ras activity triggers emergent behaviors during mammary epithelial morphogenesis. *Cell Rep.* **2**, 1461–1470 (2012).

36. White, E. Exploiting the bad eating habits of Ras-driven cancers. *Genes Dev.* **27**, 2065–2071 (2013).
37. Mathew, R. & White, E. Autophagy, stress, and cancer metabolism: what doesn't kill you makes you stronger. *Cold Spring Harb. Symp. Quant. Biol.* **76**, 389–396 (2011).
38. Mancias, J. D. & Kimmelman, A. C. Targeting autophagy addiction in cancer. *Oncotarget* **2**, 1302–1306 (2011).
39. Cufi, S. *et al.* The anti-malarial chloroquine overcomes primary resistance and restores sensitivity to trastuzumab in HER2-positive breast cancer. *Sci. Rep.* **3**, 2469 (2013).
40. Rosenfeldt, M. T. *et al.* p53 status determines the role of autophagy in pancreatic tumour development. *Nature* **504**, 296–300 (2013).
41. Royer, C. & Lu, X. Epithelial cell polarity: a major gatekeeper against cancer? *Cell Death Differ.* **18**, 1470–1477 (2011).
42. Macara, I. G. & McCaffrey, L. Cell polarity in morphogenesis and metastasis. *Phil. Trans. R. Soc. B* **368**, 20130012 (2013).
43. Gildea, J. J. *et al.* RhoGDI2 is an invasion and metastasis suppressor gene in human cancer. *Cancer Res.* **62**, 6418–6423 (2002).
44. Struckhoff, A. P., Rana, M. K. & Worthylake, R. A. RhoA can lead the way in tumor cell invasion and metastasis. *Front. Biosci.***16**, 1915–1926 (2011).
45. Plodinec, M. *et al.* The nanomechanical signature of breast cancer. *Nature Nanotechnol.* **7**, 757–765 (2012).
46. Lee, M. H. *et al.* Mismatch in mechanical and adhesive properties induces pulsating cancer cell migration in epithelial monolayer. *Biophys. J.* **102**, 2731–2741 (2012).
47. Yang, J. & Weinberg, R. A. Epithelial-mesenchymal transition: at the crossroads of development and tumor metastasis. *Dev. Cell* **14**, 818–829 (2008).
48. Sahai, E. Mechanisms of cancer cell invasion. *Curr. Opin. Genet. Dev.* **15**, 87–96 (2005).
49. Yilmaz, M., Christofori, G. & Lehembre, F. Distinct mechanisms of tumor invasion and metastasis. *Trends Mol. Med.* **13**, 535–541 (2007).
50. Kissa, K. & Herbomel, P. Blood stem cells emerge from aortic endothelium by a novel type of cell transition. *Nature* **464**, 112–115 (2010).
51. Rhim, A. D. *et al.* EMT and dissemination precede pancreatic tumor formation. *Cell* **148**, 349–361 (2012).
52. Chambers, K. F. *et al.* Stroma regulates increased epithelial lateral cell adhesion in 3D culture: a role for actin/cadherin dynamics. *PLoS ONE* **6**, e18796 (2011).
53. Sorlie, T. *et al.* Gene expression patterns of breast carcinomas distinguish tumor subclasses with clinical implications. *Proc. Natl Acad. Sci. USA* **98**, 10869–10874 (2001).
54. Perez-Enciso, M. & Tenenhaus, M. Prediction of clinical outcome with microarray data: a partial least squares discriminant analysis (PLS-DA) approach. *Hum. Genet.* **112**, 581–592 (2003).
55. Livasy, C. A. *et al.* Phenotypic evaluation of the basal-like subtype of invasive breast carcinoma. *Mod. Pathol.* **19**, 264–271 (2006).
56. Prat, A., Ellis, M. J. & Perou, C. M. Practical implications of gene-expression-based assays for breast oncologists. *Nature Rev. Clin. Oncol.* **9**, 48–57 (2012).
57. Zomer, A. *et al.* Intravital imaging of cancer stem cell plasticity in mammary tumors. *Stem Cells* **31**, 602–606 (2013).
58. Wang, W. *et al.* Coordinated regulation of pathways for enhanced cell motility and chemotaxis is conserved in rat and mouse mammary tumors. *Cancer Res.* **67**, 3505–3511 (2007).
59. Nakasone, E. S. *et al.* Imaging tumor-stroma interactions during chemotherapy reveals contributions of the microenvironment to resistance. *Cancer Cell* **21**, 488–503 (2012).
60. Condeelis, J. & Weissleder, R. *In vivo* imaging in cancer. *Cold Spring Harb. Perspect. Biol.* **2**, a003848 (2010).
61. Roussos, E. T. *et al.* Mena deficiency delays tumor progression and decreases metastasis in polyoma middle-T transgenic mouse mammary tumors. *Breast Cancer Res.* **12**, R101 (2010).
62. Boimel, P. J. *et al.* Contribution of CXCL12 secretion to invasion of breast cancer cells. *Breast Cancer Res.* **14**, R23 (2012).
63. Elinav, E. *et al.* Inflammation-induced cancer: crosstalk between tumours, immune cells and microorganisms. *Nat. Rev. Cancer* **13**, 759–771 (2013).
64. White, R., Rose, K. & Zon, L. Zebrafish cancer: the state of the art and the path forward. *Nature Rev. Cancer* **13**, 624–636 (2013).
65. Jung, D.-W. *et al.* A novel zebrafish human tumor xenograft model validated for anti-cancer drug screening. *Mol. BioSyst.* **8**, 1930–1939 (2012).
66. Konantz, M. *et al.* Zebrafish xenografts as a tool for *in vivo* studies on human cancer. *Ann. NY Acad. Sci.* **1266**, 124–137 (2012).
67. Thiery, J. P., Acloque, H., Huang, R. Y. & Nieto, M. A. Epithelial-mesenchymal transitions in development and disease. *Cell* **139**, 871–890 (2009).
68. Kalluri, R. & Weinberg, R. A. The basics of epithelial-mesenchymal transition. *J. Clin. Invest.* **119**, 1420–1428 (2009).
69. Nieto, M. A. The early steps of neural crest development. *Mech. Dev.* **105**, 27–35 (2001).
70. Wang, W. *et al.* Tumor cells caught in the act of invading: their strategy for enhanced cell motility. *Trends Cell Biol.* **15**, 138–145 (2005).

Acknowledgements
The authors thank the US National Institutes of Health (NIH) for an Innovator Award DP2OD002056-01 and an RO1 1R01GM102169-01 to J.R., and for an NIH Developmental Biology Training Grant 5T32 HDO7491 to G.M.S.

Competing interests statement
The authors declare no competing interests.

CHAPTER 2

P115 RHOGEF AND MICROTUBULES DECIDE THE DIRECTION APOPTOTIC CELLS EXTRUDE FROM AN EPITHELIUM

Reprinted with permission from the Journal of Cell Biology. *Slattum, G., McGee, K.M., and Rosenblatt, J. (2009). P115 RhoGEF and microtubules decide the direction apoptotic cells extrude from an epithelium. The Journal of Cell Biology. Sep 7;186(5):693-702 *Cover

Chapter 2 is a published article. Both Gloria Slattum and Karen McGee contributed to this work equally.

JCB
THE JOURNAL OF CELL BIOLOGY
VOL. 186, NO. 5, SEPTEMBER 7, 2009

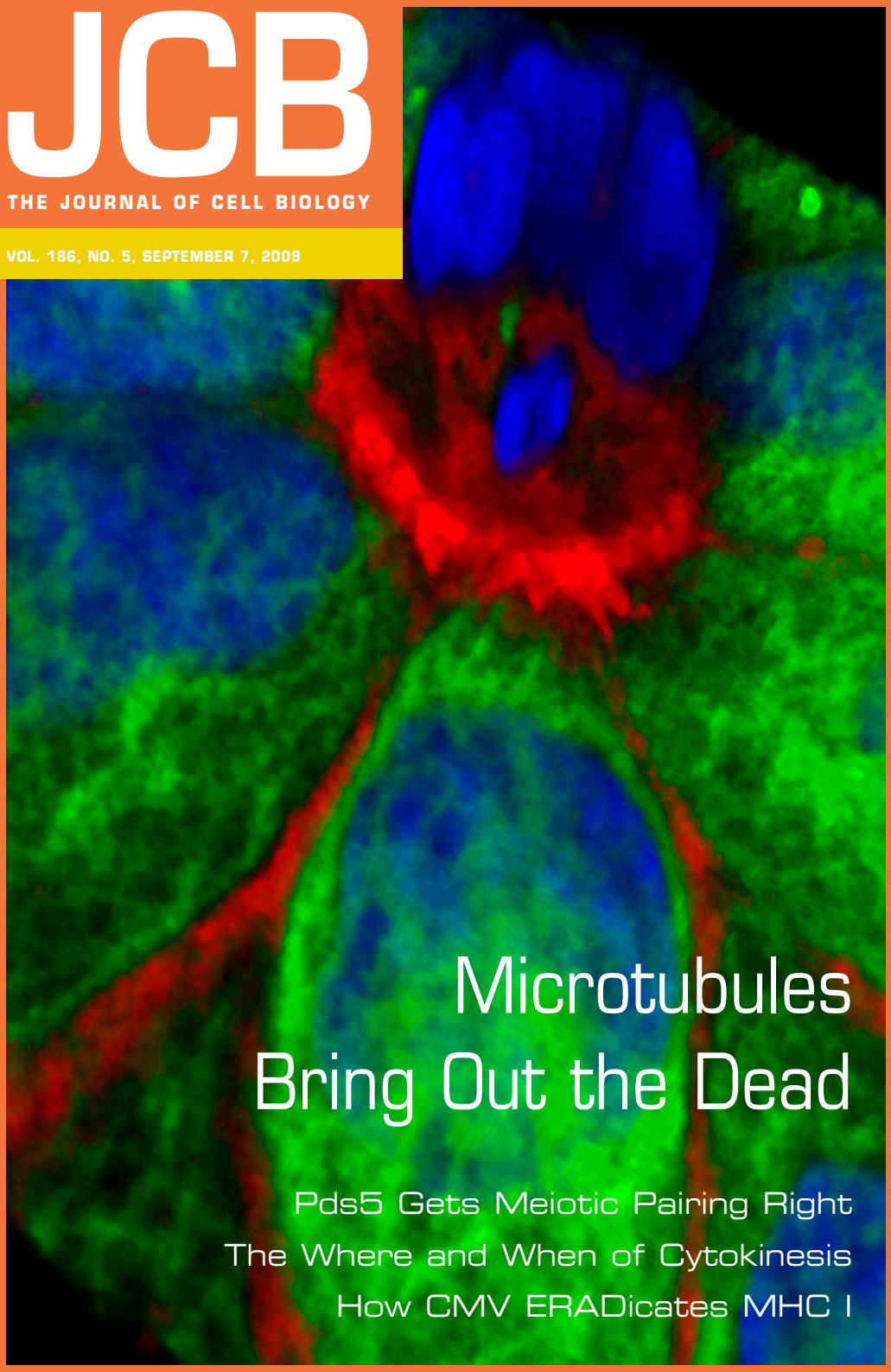

Microtubules Bring Out the Dead

Pds5 Gets Meiotic Pairing Right

The Where and When of Cytokinesis

How CMV ERADicates MHC I

www.jcb.org

Published August 31, 2009

JCB: REPORT

P115 RhoGEF and microtubules decide the direction apoptotic cells extrude from an epithelium

Gloria Slattum,[1] Karen M. McGee,[1,2] and Jody Rosenblatt[1]

[1]Department of Oncological Sciences, Huntsman Cancer Institute, University of Utah, Salt Lake City, UT 84112
[2]Institute of Ophthalmology, London EC1V 9EL, England, UK

To preserve epithelial barrier function, dying cells are squeezed out of an epithelium by "apoptotic cell extrusion." Specifically, a cell destined for apoptosis signals its live neighboring epithelial cells to form and contract a ring of actin and myosin II that squeezes the dying cell out of the epithelial sheet. Although most apoptotic cells extrude apically, we find that some exit basally. Localization of actin and myosin IIA contraction dictates the extrusion direction: basal extrusion requires circumferential contraction of neighboring cells at their apices, whereas apical extrusion also requires downward contraction along the basolateral surfaces. To activate actin/myosin basolaterally, microtubules in neighboring cells reorient and target p115 RhoGEF to this site. Preventing microtubule reorientation restricts contraction to the apex, driving extrusion basally. Extrusion polarity has important implications for tumors where apoptosis is blocked but extrusion is not, as basal extrusion could enable these cells to initiate metastasis.

Introduction

To preserve epithelial barrier function during cell turnover, dying cells are shoved out of the epithelium by a process we have termed "apoptotic cell extrusion" (Rosenblatt et al., 2001). Here, the cell destined for apoptosis signals its live neighboring epithelial cells to form a ring of actin and myosin II that contracts to squeeze the dying cell out of the epithelial sheet. This contraction not only ejects the dying cell out of the layer but also closes any gaps that may have resulted from the dying cell's exit.

Importantly, cells can be extruded either apically into the lumen or basally back into the tissue the epithelia encases. Previously, we only detected apical extrusion of apoptotic cells from the epithelia encasing vertebrate embryos and adult organs. However, we find that basal extrusion occurs occasionally in vertebrates and commonly in *Drosophila* embryonic epithelia (also see Gibson and Perrimon, 2005; Vidal et al., 2006; Ninov et al., 2007). The direction a cell is extruded is important for its fate, as corpses extruded basally must be engulfed, whereas those extruded apically may be expelled or trapped in the lumen. Extrusion direction is likely more important in cases where cells are blocked from death but still extrude. Apical extrusion would still eliminate these cells, whereas basal extrusion could allow live cells to be retained in the tissue to potentially migrate elsewhere. Because this decision is critical for the extruded cell's fate, we sought to identify the molecular mechanism that determines the direction a cell will extrude.

Although our previous work had established the fact that apoptotic cell extrusion requires Rho-mediated contraction of an intercellular actin/myosin II ring in the cells surrounding the dying cell (Rosenblatt et al., 2001), we did not examine how actin/myosin contraction is organized to squeeze the dying cell out apically into the lumen. Further, we did not notice the minor populations of apoptotic cells that extruded basally in tissue culture monolayers. Here, we analyze how actin and myosin contraction is regulated differently when cells extrude apically versus basally using cultured epithelial monolayers from canine kidney, MDCK, or human bronchia (16-HBE-14o), as well as the epidermis of live zebrafish. We find that apical extrusion requires reorientation of microtubules and associated p115 RhoGEF basolaterally, which activates Rho to contract actin/myosin basally and squeeze the dying cell out.

G. Slattum and K.M. McGee contributed equally to this paper.

Correspondence to Jody Rosenblatt: jody.rosenblatt@hci.utah.edu

Abbreviations used in this paper: CCD, charge-coupled device; DIC, differential interference contrast; DMEM, Dulbecco's minimum essential medium; LARG, leukemia-associated RhoGEF; RGS, regulator of G protein signaling.

The Rockefeller University Press $30.00
J. Cell Biol. Vol. 186 No. 5 693–702
www.jcb.org/cgi/doi/10.1083/jcb.200903079

THE JOURNAL OF CELL BIOLOGY

Published August 31, 2009

Results and discussion

Using MDCK and 16-HBE-14o epithelial lines treated with UV^{254} to induce apoptosis, we found that although most apoptotic cells extrude apically, a small fraction extrudes basally. The direction of extrusion is apparent in the stills from phase videos (Fig. 1 and associated Videos 1–3). During apical extrusion, the cell body is pushed out of the monolayer into the medium (Fig. 1 a and Video 1), whereas during basal extrusion, the cell becomes trapped between the monolayer and the cover glass and migrates underneath the monolayer (Fig. 1 b and Videos 2 and 3). Because epithelial monolayers in culture may have artificially strong adhesion to glass, we wanted to assess if similar ratios of apical versus basal extrusion also occurred in vivo. We have found that zebrafish larval epidermises provide an excellent model system to follow extrusion live, which can also be manipulated with inhibitors. G-418 treatment of 4-d-old zebrafish larvae induces dying cells that predominantly extrude apically from the epidermis (Fig. 1 c and Video 4). Apically extruded cells exit into the fish water, whereas basally extruded cells become trapped beneath the epidermis (Fig. 1 d and Video 5).

We visually scored apical versus basal extrusion in UV-treated, fixed monolayers (referred to as "extruding monolayers") and zebrafish epidermises by assessing the location of the actin-extruding ring compared with the extruded body, marked by compacted DNA and activated caspase-3 staining (see Fig. 1, e and f for examples of apical and basal extrusion in MDCKs; and see Videos 6 and 7 and Fig. S2 for examples in zebrafish). During apical extrusion, the actin ring is thicker and extends to the base of the cell, whereas active caspase-3 and DNA (marking the extruded cell) are apical to the ring. In contrast, during basal extrusion, the actin ring is apical and similar in intensity to the cortical actin at adherens junctions in the live cells, and the caspase-3 and DNA are basal to the contracted apical ring. Using these hallmarks for examining the polarity of extrusion, we found that zebrafish and tissue culture epithelia predominantly extrude apoptotic cells apically. 89 ± 2.3% (SEM) from >500 extruding cells (n = 4 experiments) from zebrafish epidermises, 80 ± 6% (SEM) of 1,250 extruding cells (n = 5 experiments) from MDCK monolayers, and 79 ± 9% (SEM) of 700 extruding cells (n = 7 experiments) from 16-HBE-14o monolayers extruded apoptotic cells apically; the remainder extruded basally.

What determines whether cells are extruded apically or basally? Two models for differentially regulating the direction are: (1) the intrinsic polarity of neighboring cells may be altered or lost, positioning cortical actin differentially; or (2) actin and myosin may be independently localized apically or basally. To examine if polarity was altered when cells extruded apically versus basally, we immunostained extruding monolayers for the apical tight junction protein, ZO-1, and the basolateral adherens junction protein, β-catenin (Yu et al., 2005). ZO-1 remained apical and β-catenin basal during either apical or basal extrusion (Fig. 2, a and b, respectively). The preserved localization of polarized adhesion markers suggests that epithelial polarity is not markedly altered when cells extrude basally versus apically.

To examine where actin/myosin contraction occurred, we immunostained extruding monolayers with a phospho-myosin II antibody that recognizes only actively contracting myosin II (Matsumura et al., 1998). We find that myosin IIA contraction is active along the basolateral interface between the apoptotic cell and its neighboring cells during apical extrusion but is restricted to the apical interface during basal extrusion (Figs. 2 c and S1, control). Localization of phospho-myosin II and videos of extrusion suggest that all extrusion events require coordinated, circumferential contraction of the cortical actin and myosin II at the cell–cell contacts that interface with the dying cell. The difference in whether extrusion occurs apically rather than basally appears to be linked to whether basolateral contraction also occurs at this ring.

If extrusion direction corresponds to where myosin II assembles and contracts, what controls its localization? Because microtubules have been found to activate or inhibit myosin II contraction in cytokinesis and other contractile processes (Wittmann and Waterman-Storer, 2001; Matsumura, 2005), we examined whether microtubules regulate myosin II contraction during extrusion. Live 3D videos of mApple-actin and GFP-tubulin show that microtubules dynamically reorient toward the actin-extruding ring early and throughout extrusion process, but retract once extrusion is complete during both apical and basal extrusion (see Videos 8 and 9, respectively). Because microtubules grow dynamically toward the ring, we reasoned that the plus ends of microtubules reorient toward the ring and activate myosin II contraction. To confirm that microtubule plus ends abut where actin and myosin contract during both apical and basal extrusion, we immunostained fixed, extruding monolayers for EB1, a plus-end microtubule-binding protein (Carvalho et al., 2003), myosin II, and DNA. Many EB1 spots localized to the basolateral surface during apical extrusion (Fig. 3 A, 3–6 µm from base), whereas far fewer EB1 spots localize to the apex during basal extrusion (Fig. 3 B, ≥6 µm from the base). Quantification confirmed that more EB1 spots localized to the basolateral surface (0–4 µm from base) than the apical surface (4–8 µm from base) of the actin ring during apical extrusion compared with basal extrusion or to live cell–cell contacts, labeled "junction" (Fig. 3 C). These experiments suggest that microtubules in the cells surrounding an apoptotic cell dynamically reorient toward the basolateral surface that contacts the dying cell during apical extrusion.

To test if microtubule reorientation toward the dying cell is required for basolateral contraction during apical extrusion, we used inhibitors to disrupt microtubules and analyzed fixed, immunostained extruding monolayers. Destabilizing microtubules with nocodazole reduced the number of apoptotic cells that extruded (no contraction) and increased the percentage that extruded basally (Fig. 4, a and b). To block the reorientation of microtubules toward the basal surface during apical extrusion, we treated extruding monolayers with the microtubule-stabilizing drug taxol.

Published August 31, 2009

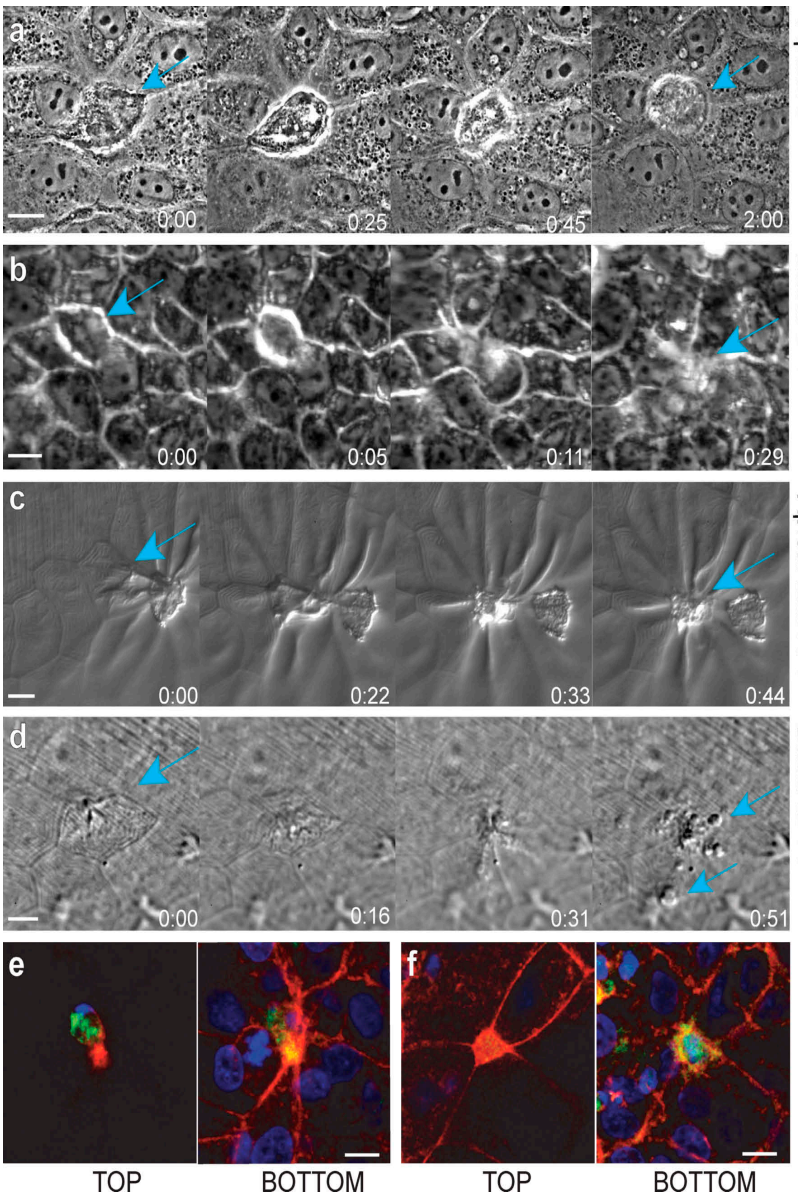

Figure 1. **Hallmarks of apical and basal apoptotic cell extrusion.** Stills from phase videos of apoptotic cells extruding apically (a and c) and basally (b and d) in an MDCK cell culture epithelium (a and b) and from a zebrafish larval epidermis (c and d; teal arrows denote extruding cells). Time is given in hours and minutes. (e and f) An apoptotic cell extruding apically (e) and basally (f), immunostained for active caspase-3 (green), actin (red), and DNA (blue). Note that caspase and DNA are in the top z plane and a thick actin ring is in the bottom plane when a cell is extruded apically (e), whereas the actin ring is in the top plane and caspase and DNA are in bottom plane when extruding basally (f). Bars, 10 µm.

In contrast to control-treated cells, taxol treatment blocked microtubule reorientation toward the base of the dying cell (Fig. 4 a). Additionally, taxol treatment of monolayers shifted the direction of extrusion from predominantly apical to basal (Fig. 4 b). We found that disruption of microtubule dynamics shifted the balance of extrusions from apical to basal even more dramatically in zebrafish larval epidermises (from 89 ± 2.3% [SEM] to 27 ± 1.3% [SEM] in control vs. taxol treatments, from >900 extruding cells over four separate experiments, $P < 0.0001$). The drug treatments suggest that

Published August 31, 2009

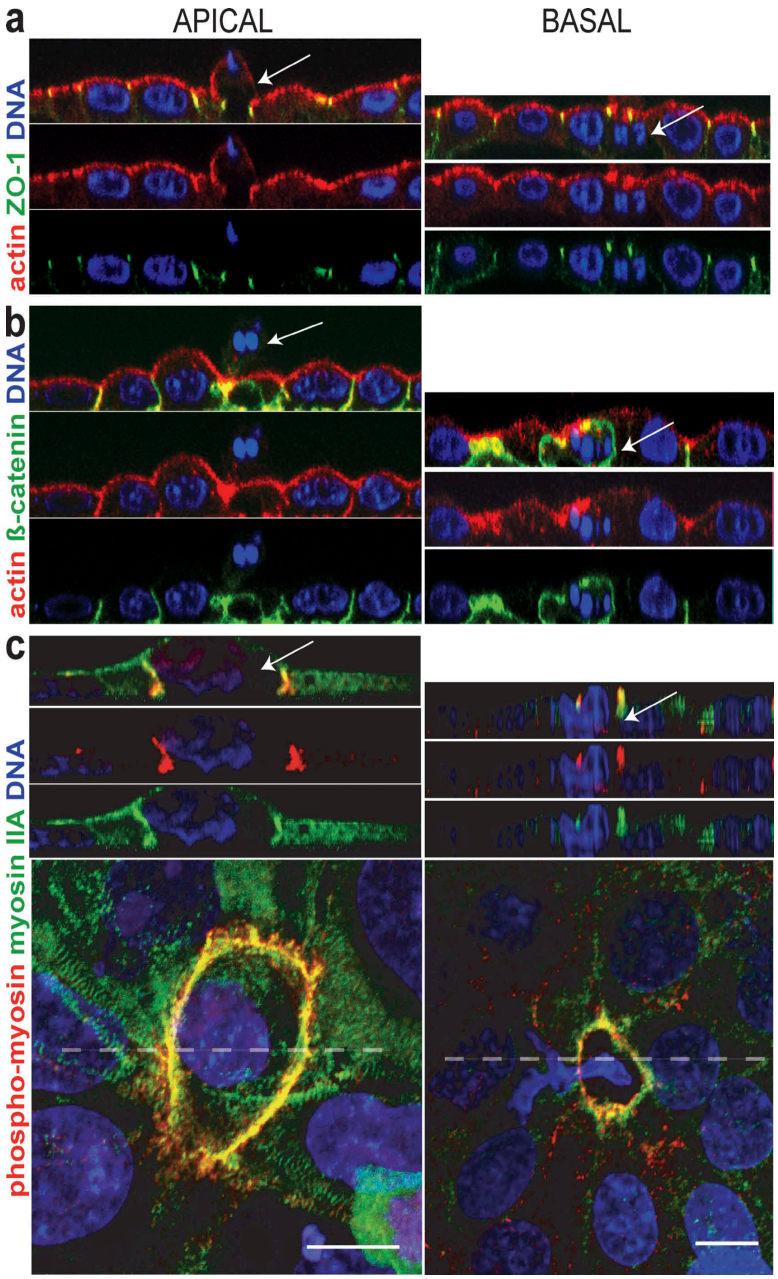

Figure 2. **Localization of active myosin IIA but not intrinsic polarity markers are altered when cells are extruded apically or basally.** (a and b) Cross sections of tight junction protein Z0-1 (a), which remains apical, and β-catenin (b), which remains basal. (c) Myosin IIA and phospho-myosin II are basolateral during apical extrusion and apical during basal extrusion. Cross sections are taken from the broken line in pictures of 3D confocal reconstructions of MDCK cells. Arrows point to dying, extruded cells in each case. Bars, 10 μm.

actin and myosin II contract at sites where microtubules contact the cortex. When microtubules are frozen at the apex, actin/myosin II contract at the apex and drive extrusion basally, but if microtubules are allowed to reorient toward the base, contraction occurs along the basolateral surface, driving extrusion apically.

Published August 31, 2009

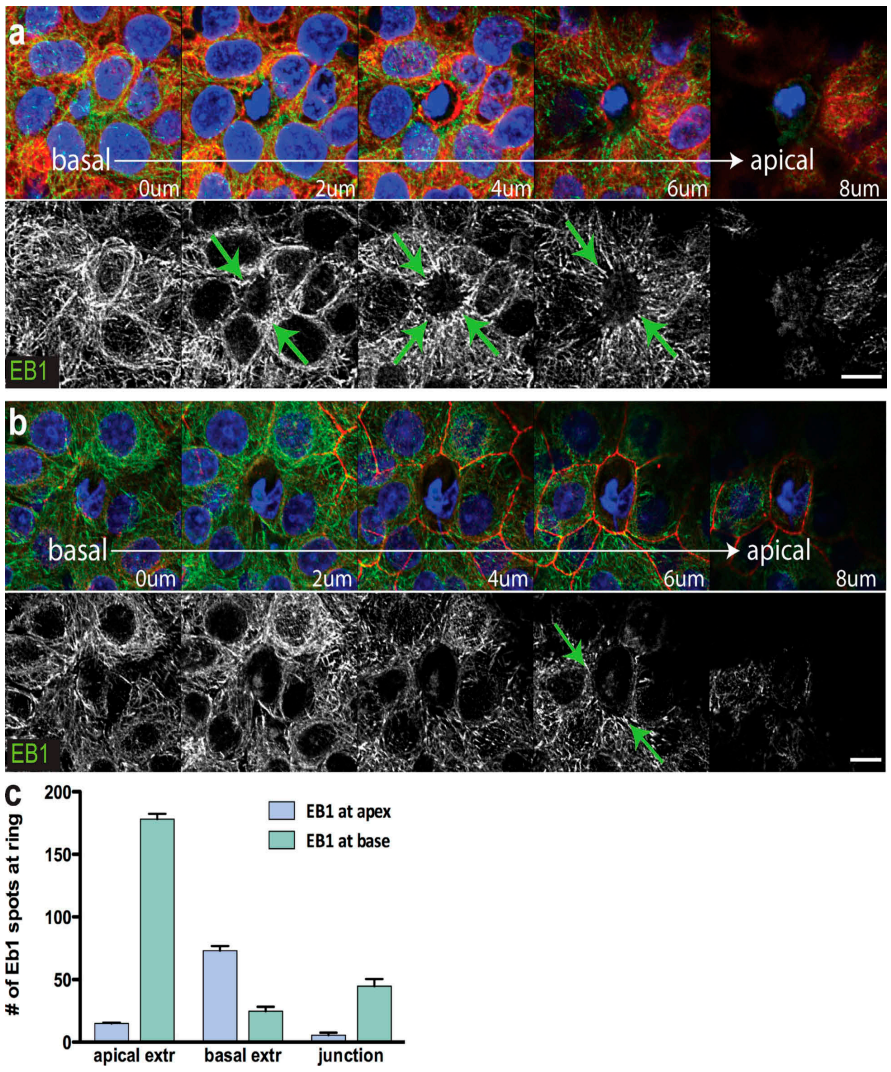

Figure 3. **The growing ends of microtubules point toward the actin/myosin ring during extrusion.** (a and b) EB1 (green), a plus-end microtubule-binding protein, colocalizes with the myosin II (red) ring during apical (a) and basal (b) extrusion. Arrows point to sites where EB1 abuts the myosin II ring. Note that most EB1 is from 0–4 µm from the base during apical extrusion, whereas during basal extrusion, only limited amounts of EB1 are seen at the apex (6 µm from the base). Bars, 10 µm. (c) Quantification of EB1 localization (>170 spots for each) from 12 extrusions each of apically extruding cells, basally extruding cells, and live junctions. Error bars indicate SEM and $P < 0.0001$, comparing spots from apical extrusion to basal extrusion.

To determine if basolateral microtubule reorientation localizes myosin II or its activators to this surface, we immunostained extruding monolayers treated with nocodazole or taxol for myosin II and phospho-myosin II. Both myosin II and phospho-myosin II localized to the extruding ring in control-treated monolayers but were substantially reduced in the presence of nocodazole, and restricted to the apex in the presence of taxol (Fig. S1). Disruption of both myosin II localization and activation with microtubule inhibitors suggests that microtubules promote both assembly and activation of the actin/myosin ring.

Because Rho activation in neighboring cells is required for extrusion contraction (Rosenblatt et al., 2001) and because microtubules can regulate several RhoGEFs (Krendel et al., 2002; Rogers et al., 2004), we hypothesized that microtubules could regulate extrusion direction by locally activating Rho. Total RhoA protein localized throughout the live–dead cell interface, although myosin II contraction occurred only at the bottom of the actin/myosin ring during apical extrusion (Fig. 5 a, bottom), suggesting that Rho activation is restricted to the basolateral surface. Because the *Drosophila*

Published August 31, 2009

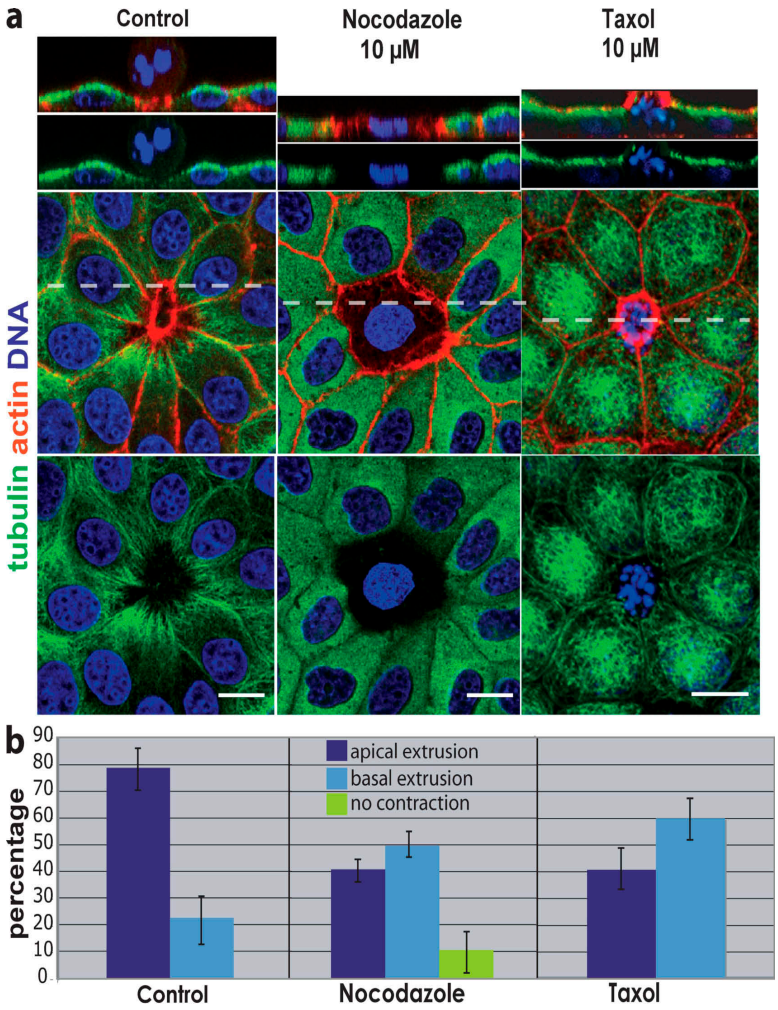

Figure 4. **Disruption of microtubules alters the direction a cell extrudes.** (a) In control (DMSO-treated) MDCK monolayers, microtubules dip down toward the basolateral surface of the actin ring, whereas nocodazole either blocks contraction of the ring (as shown) or drives extrusion basally. Stabilizing microtubules with taxol freezes microtubules at the apex compared with control and drives extrusion basally. Broken lines indicate the site of cross sections from 3D confocal reconstructions above. Bars, 10 μm. (b) Quantification of drug-treatments from six experiments, n = 1,350 extruding cells per treatment. P-values for apical and basal extrusions, respectively, were 0.0011 and 0.0066 for nocodazole and 0.0023 and 0.0023 for taxol. Error bars indicate SEM.

RhoGEF2 associates with microtubule plus ends to drive Rho-mediated actin/myosin contraction during gastrulation (Rogers et al., 2004), we investigated whether members of the regulator of G protein signaling (RGS) family of RhoGEFs, mammalian homologues of RhoGEF2 (Fukuhara et al., 2001), were required for apical extrusion. We treated 16-HBE-14o monolayers with siRNAs directed against PDZ RhoGEF, p115 RhoGEF, and leukemia-associated RhoGEF (LARG), and assayed the direction of extrusion in the resulting monolayers. Knockdown of PDZ and LARG RhoGEFs had no obvious effect on extrusion direction (Fig. S3, a and b). However, knockdown of p115 RhoGEF dramatically reduced the percentage of apically extruding cells, whereas scrambled p115 RhoGEF siRNA had no effect on extrusion direction (Fig. 5 b). The percentage of cells that shifted from predominantly apical to basal was similar to that seen with taxol treatment, which is consistent with p115 RhoGEF and microtubules acting in the same pathway.

Moreover, p115 RhoGEF, unlike RhoA, localizes only to sites of active myosin II contraction during both apical and basal extrusion. p115 RhoGEF appears in fibers that point to the base of the extruding ring during apical extrusion (Fig. 5 a, top; and Fig. 5 c). Unlike RhoGEF2 that localizes to microtubule tips (Rogers et al., 2004), we found that p115 RhoGEF colocalizes along microtubules, suggesting that it either associates with microtubules or with a microtubule-associated

Published August 31, 2009

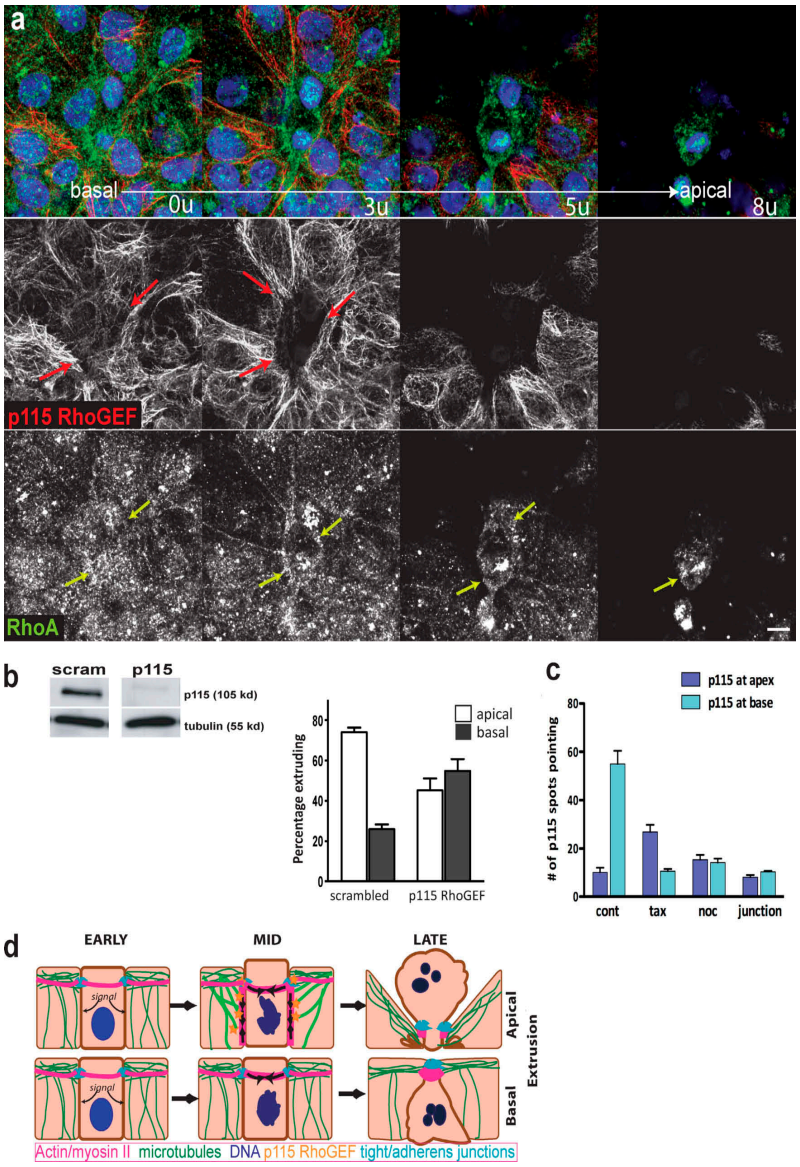

Figure 5. **p115 RhoGEF is required for apical extrusion.** (a) p115 RhoGEF (red; separate middle panel) form filaments that point toward the basolateral surface of the extruding ring during apical extrusion, whereas RhoA (green; bottom panel) is present through the apical and basal regions of the ring. Corresponding colored arrows indicate sites of interaction with the actin/myosin ring. Bar, 10 µm. (b) siRNA-mediated knockdown of p115 RhoGEF (above, lanes from one immunoblot) disrupts apical extrusion, whereas scrambled siRNA does not. The graph shows the percentage of apical versus basal extrusion from >1,000 cells from four siRNAs experiments, where $P < 0.0001$. (c) p115 RhoGEF localizes to the base of the extruding ring during apical extrusion, whereas it does not when microtubules are disrupted with nocodazole or taxol, or in control live junctions, where P-values are <0.0001 for control versus each treatment; $n = 10$ extrusions per treatment. (d) Model for how microtubules might control extrusion direction. An early apoptotic cell sends signals to its live neighboring epithelial cells, which react by reorienting microtubules toward the basolateral surfaces of the cells that contact the dying cell. p115 RhoGEF, by association with microtubules, assembles and activates Rho-mediated actin and myosin II contraction along the basolateral surface, extruding the cell apically (top). Basal extrusion occurs if the microtubules do not reorient or if p115 RhoGEF is absent (bottom).

Published August 31, 2009

matrix (Fig. S3 c). To test if p115 RhoGEF localization was dependent on microtubules, we quantified the number of p115 RhoGEF fibers in control-extruding monolayers compared with nocodazole or taxol-treated monolayers. Compared with control-treated monolayers, taxol treatment restricted p115 RhoGEF to the apex (Figs. 5 c and S3 d, for a representative picture), whereas nocodazole treatment eliminated p115 RhoGEF at the dying cell, similar to levels seen at live cell–cell junctions (Figs. 5 c and S3 e). These results suggest that microtubules localize p115 RhoGEF to activate basolateral contraction during apical extrusion. Although Rho exists throughout the ring, and microtubules and p115 span the extruding live cells, Rho is activated only at sites where it intersects with p115 RhoGEF.

Based on the effects of disrupting microtubules and p115 RhoGEF on the direction of extrusion, we propose a model for how microtubules control the direction of extrusion (Fig. 5 d). When cells are extruded apically (Fig. 5 d, top), the cells surrounding a cell destined to die reorient their microtubules toward the basolateral surfaces that interface with the dying cell. Microtubules target p115 RhoGEF to the basolateral surface, where it activates Rho, present at the live–dead cell interface, to assemble and activate myosin IIA contraction. The extrusion ring contracts circumferentially around the dying cell as well as basolaterally to squeeze the apoptotic cell out apically. Failure of p115 RhoGEF to target to the basolateral surface, either by its knockdown or by disruption of microtubule reorientation, results in basal extrusion (Fig. 5 d, bottom). Here, actin and myosin IIA already present at apical adherens junctions could readily contract circumferentially around the dying cell. However, because basolateral actin/myosin contraction is absent, contraction is restricted to the apex, forcing the apoptotic cell out basally. During both types of extrusion, adherens and tight junctions are maintained above the sites of contraction, which preserves the barrier function of the epithelium throughout the extrusion process (as seen in Fig. 2, a and b).

Although we have found that microtubule reorientation is important for apical extrusion, microtubule disruption did not reverse the extrusion direction in 100% of cells, which suggests that other factors may also contribute to extrusion polarity. The extrusion polarity effects from taxol treatment were more dramatic in zebrafish than in culture, which suggests that this decision is regulated more tightly in vivo. Other factors affecting extrusion polarity may include matrix, intrinsic polarity, or cell height. A more adhesive surface may encourage apical extrusion, whereas basal extrusion might dominate in monolayers on a less adhesive substratum. Taller epithelia, such as in the gut, would likely show more dramatic effects in extrusion polarity than would flatter epithelia.

Several observations suggest that extrusion may not be limited to apoptotic cells, but could be a common mechanism for living cells to exit an epithelium without disrupting epithelial function. Apoptotic extrusion looks morphologically similar to developmental events where single cells exit the epithelium, such as neuroblast delamination in *Drosophila melanogaster* (Hartenstein et al., 1994). Here, cells exit the neuroepithelium and, instead of dying, divide asymmetrically before differentiating into neurons. We have previously found that blocking cell death with a caspase inhibitor does not block cell extrusion (Rosenblatt et al., 2001). Further, many high-grade epithelial tumors have mutations in apoptosis (Yang et al., 2003; Schulze-Bergkamen and Krammer, 2004; Meulmeester and Jochemsen, 2008) that would block apoptosis at steps we predict would not block extrusion.

In situations where cells can extrude without dying, the direction a cell extrudes is pivotal for its fate. In cancer, apical extrusion could act as a tumor suppressor, eliminating tumor cells through the lumen. Even in cases where tumors cells accumulate in a closed lumen, such as in breast ductal carcinoma in situ, they rarely invade and metastasize (Kopans et al., 2003). Basal extrusion, however, could provide an exit path for these tumor cells to initiate metastasis and migrate to other sites in the body. Evidence for basal extrusion promoting invasion exists in *Drosophila* larvae and pupae when cell death is blocked, as extrusion in these tissues occurs almost exclusively basally (Pagliarini and Xu, 2003; Gibson and Perrimon, 2005; Thompson et al., 2005; Vidal et al., 2006; Ninov et al., 2007; Hogan et al., 2009). Further work will test if basal extrusion of tumor cells could enable their invasion and metastasis through the matrix and into the bloodstream in vertebrates. Our results identifying a role for microtubules in regulating the direction of extrusion in zebrafish will allow us to follow the fate of basally extruded live cells in a vertebrate model where single cells can be readily imaged and tracked (Redd et al., 2006).

Materials and methods

Cell culture

MDCK II cells (gift from K. Matlin, University of Chicago, Chicago, IL) were cultured in Dulbecco's minimum essential medium (DMEM) high glucose with 5% FBS and 100 µg/ml penicillin/streptomycin (all from Invitrogen) at 5% CO_2, 37°C. 16-HBE-14o (provided by D. Gruenert [California Pacific Medical Center, San Francisco, CA] and J. Porter [University College London, London, England, UK]) were cultured in MEM containing Earle's salts, 1 g/liter glucose, 2.2 g/liter $NaHCO_3$, L-glutamine, 10% FBS, and 100 µg/ml penicillin-streptomycin (Invitrogen) in a flask coated with human fibronectin type I (BD), bovine collagen I (Purecol; Inamed biomaterials), and BSA (Invitrogen) at 5% CO_2, 37°C.

Transfections

siRNAs were synthesized at the University of Utah oligo and peptide synthesis core to the following sequences: p115 RhoGEF (5′-GCAGCUCUGAGAACGGCAA-3′), LARG RhoGEF (5′-GAAACUCGUCGCAUCUUCC-3′), PDZ RhoGEF (5′-ACUGAAGUCUCGGCCAGCU-3′), and scrambled control siRNA (5′-UUCUCCGAACGUGUCACGU-3′). Antisense and sense duplexes LARG RhoGEF and P115 RhoGEF were annealed in 100 mM potassium acetate, 30 mM Hepes-KOH, 2 mM magnesium acetate, pH 7.4, and PDZ RhoGEF duplexes in 50 mM Tris, pH 8.0, and 100 mM NaCl at 90°C for 1 min and 37°C for 1 h. 50 pMol (LARG and P115) or 30 pMol (PDZ) siRNAs were transfected by nucleofection using the solution V-program G016 (Amaxa) or by RNAimax Reverse Transfection according to the manufacturer's instructions (Invitrogen). We also confirmed our results using two independent shRNAs directed against p115, PDZ, and LARG RhoGEFs (gift from A. Jaffe [Novartis, Boston, MA] and A. Hall [Memorial Sloan Kettering Cancer Center, New York, NY]).

Cell staining

For EB1 and myosin IIA staining, cells were fixed with 100% methanol at −20°C for 45 s. For RhoGEF p115 staining, monolayers were prepermeablized with PBS with 0.1% Triton X-100 containing 1 µg/ml phalloidin for 60 s before fixation with 4% formaldehyde in PBS at 37°C for 20 min. For all other immunostainings, cells were fixed with 4% formaldehyde in PBS at 37°C for 20 min. Fixed cells were rinsed three times in PBS, permeabilized for 5 min with PBS containing 0.5% Triton

Published August 31, 2009

X-100, and blocked in AbDil (PBS with 0.1% Triton X-100 and 2% BSA), then incubated in primary antibody (in AbDil) for 1 h, washed three times with PBS with 0.1% Triton X-100, and incubated in secondary antibodies. Antibody concentrations used for immunostaining were: 1:200 anti-tubulin ascites (DM1α; Sigma-Aldrich); 1:50 anti-EB1 monoclonal clone 5 (BD); 1:50 nonmuscle myosin IIA polyclonal antibody (Sigma-Aldrich); 1:50 phosphomyosin II antibody (Cell Signaling Technology); 1:100 mouse β-catenin antibody (BD), 1:25 anti-Rho A (BD), or 1:500 rabbit anti–ZO-1 (Zymed); and 1:100 rabbit anti–active caspase-3 (Cell Signaling Technology). Actin was detected using 0.1 µg/ml Alexa Fluor 568–phalloidin (Invitrogen) or with 1:200 actin polyclonal antibody (A2066 [Sigma-Aldrich] when fixed with methanol). Alexa Fluor 488 goat anti–mouse and Alexa Fluor 568 goat anti–rabbit IgG were used as secondary antibodies (Invitrogen). DNA was detected with 1 µg/ml Hoechst 33342 (Sigma-Aldrich) or 5 µm DRAQ5 (Axxora) in all fixed cell experiments.

Zebrafish staining

To score the percentage of epidermal cells extruding apically versus basally, we treated 4-d zebrafish larvae with 450 µg/ml G-418 (Invitrogen) and 20 µM taxol or 0.2% DMSO in fish water (60 mg Instant Ocean mix per liter of distilled H_2O) for 1 or 2 h. Larvae were then fixed in 4% formaldehyde, 0.15% glutaraldehyde, 1 mM $MgCl_2$, 0.2% Triton X-100, and 25 mM Pipes, pH 6.9, for 2 h, blocked in 0.25% casein overnight, and stained with active caspase-3 antibody and Alexa Fluor 594–phalloidin + DAPI or DRAQ5 overnight with three washes of 0.5% Triton X-100 in PBS between each incubation. Tails were cut and mounted between a coverslip and slide in ProLong Gold (Invitrogen).

Drug and UV treatment

Cells were treated with 10 µM nocodazole, 10 µM taxol, or 0.1% DMSO (for control) for 10 min before UV treatment. To induce apoptosis, monolayers plated on glass coverslips were exposed to 1,200 µJ/cm^2 UV^{254} irradiation in a UV series II (Spectroline) and incubated for 2 h before fixation.

Image and video acquisition

For live fluorescent imaging, MDCK cells transfected with GFP-tubulin (Clontech Laboratories, Inc.) and mApple-actin-7 (a gift from Michael W. Davidson, Florida State University, Tallahassee, FL) were grown to confluence on glass-bottom delta T culture dishes (Bioptechs) in DMEM. After 48 h, DMEM was replaced with DMEM/F12 without phenol red or Hepes buffer (Invitrogen) + 5% FBS. Medium was maintained at 37°C, 5% CO_2, and 3% humidity using a Ludin Cube and Brick (Life Imaging Services) fitted to the microscope and stage. Cells were treated with 800–1,000 µJ/cm^2 UV^{254} irradiation, then imaged with a spinning disc confocal system (Andor Technologies) mounted on an inverted microscope (TE300; Nikon) with a 60× 1.4 NA Plan-Apochromat lens (Nikon). Solid-state 488 nm and 568 nm lasers (Melles Griot) were used to excite GFP and mApple fluorophores, respectively. Images were acquired with an electron-multiplied cooled charge-coupled device (CCD) camera (DV887 1004X1002; Andor Technologies) driven by Andor IQ imaging software, and 4D movies were assembled with IQ software (Andor Technologies) and processed further with MetaMorph (GE Healthcare) and QuickTime Pro (Apple) software. A sample thickness of 9 µm in 4 z steps of 2.25 µm each was imaged every 2 min for 44 min.

For live phase video microscopy, cultured monolayers were imaged using a microscope (90i; Nikon) with a 40× phase lens. Images were acquired with a cooled CCD camera (Roper Scientific) driven by MetaMorph software. For filming zebrafish extrusion, larvae were treated with 450 µg/ml G-418 (Invitrogen) and 20 µM taxol or 0.2% DMSO for 15 min and mounted in 1% low melt agarose in the same treatment mix with 0.2% tricaine covered with fish water and a coverslip. Zebrafish videos were filmed using a 40× water immersion fluor differential interference contrast (DIC) lens on an upright microscope (Eclipse 90i). One frame per minute was captured for 2 h for all videos. MetaMorph software was used to analyze data.

Confocal sections were taken using a TCS SP5 microscope (Leica) using a 63× oil lens at 1,024 × 1,024 resolution. For montage pictures of EB1/myosin II and p115 RhoGEF/Rho, we made stacks from four (p115) or five (EB1) projections of five (EB1) or six (p115) consecutive 0.35-µm z slices from LSM confocal scans of each extrusion event. We displayed consecutive projections using the "montage" function on MetaMorph software. All images were processed further using Image J, Photoshop (Adobe), and Illustrator (Adobe).

Quantification of EB1 and p115 RhoGEF

To assess quantitatively the distribution of EB1 in 16-HBE-14o cells, we analyzed the abundance of EB1 fluorescent spots at actin/myosin rings in 12 randomly selected cell extrusions (>170 z sections). The number of EB1 spots at the base was averaged from the bottom 12 of 24 z sections and at the apex from the top 12 of 24 z sections, where the error bars indicate SEM from the variation of 12 separate apical and basal extrusions, and 12 cell–cell contacts where p-values from a *t* test are <0.0001 for apical versus basal extrusion. For quantification of p115 RhoGEF fibers intersecting with the extruding ring, we created montages (as described in the image acquisition section) and manually counted the number of p115 RhoGEF spots abutting the extrusion ring in the first 0–4 µm (base) and the next 4–8 µm (apex) from the bottom of the cell. Statistical analysis was done on 10 separate extrusions from control, nocodazole, taxol, and junctions from each, where error bars represent the SEM and the p-values from a *t* test are <0.0001 for each compared with the control.

Online supplemental material

Fig. S1 shows that disruption of microtubules mislocalizes myosin IIA and phospho-myosin II in 16-HBE-14o cell monolayers. Fig. S2 shows that taxol treatment induces basal extrusion in zebrafish larval epidermis. Fig. S3 shows that siRNA-mediated knockdown of other RGS-RhoGEFs has no effect on the direction of extrusion, and that disruption of microtubules disrupts localization of RhoGEF p115. Videos 1–3 show typical basal and apical extrusion from MDCK cell monolayers. Videos 4–7 shows apical and basal extrusion from the epidermis of 4-d-old zebrafish. Videos 8–9 show apical and basal extrusion, respectively, in MDCK cells expressing mApple-actin and GFP-tubulin. Online supplemental material is available at http://www.jcb.org/cgi/content/full/jcb.200903079/DC1.

We thank Aron Jaffe and Alan Hall for shRNAs of several RhoGEFs, Karl Matlin for MDCK cells, Dieter Gruenert, and Jo Porter for 16-HBE-14o cells, Carl Thummel for use of his LSM confocal microscope, and Michael Davidson for mApple-actin 7. We also give thanks to Katie Ullman, Mark Metzstein, and Julie Kadrmas for helpful comments.

This work was supported by Cancer Research UK project grant No. C8836/A3275, Biotechnology and Biological Sciences Research project grant No. 31/C18722, and a National Institutes of Health Innovator Award No. DP2 OD002056-01 to J. Rosenblatt, and P30 CA042014 awarded to the Huntsman Cancer Institute for core facilities.

Submitted: 17 March 2009
Accepted: 10 August 2009

References

Carvalho, P., J.S. Tirnauer, and D. Pellman. 2003. Surfing on microtubule ends. *Trends Cell Biol.* 13:229–237.

Fukuhara, S., H. Chikumi, and J.S. Gutkind. 2001. RGS-containing RhoGEFs: the missing link between transforming G proteins and Rho? *Oncogene.* 20:1661–1668.

Gibson, M.C., and N. Perrimon. 2005. Extrusion and death of DPP/BMP-compromised epithelial cells in the developing *Drosophila* wing. *Science.* 307:1785–1789.

Hartenstein, V., A. Younossi-Hartenstein, and A. Lekven. 1994. Delamination and division in the *Drosophila* neurectoderm: spatiotemporal pattern, cytoskeletal dynamics, and common control by neurogenic and segment polarity genes. *Dev. Biol.* 165:480–499.

Hogan, C., S. Dupré-Crochet, M. Norman, M. Kajita, C. Zimmermann, A.E. Pelling, E. Piddini, L.A. Baena-López, J.P. Vincent, Y. Itoh, et al. 2009. Characterization of the interface between normal and transformed epithelial cells. *Nat. Cell Biol.* 11:460–467.

Kopans, D.B., E. Rafferty, D. Georgian-Smith, E. Yeh, H. D'Alessandro, R. Moore, K. Hughes, and E. Halpern. 2003. A simple model of breast carcinoma growth may provide explanations for observations of apparently complex phenomena. *Cancer.* 97:2951–2959.

Krendel, M., F.T. Zenke, and G.M. Bokoch. 2002. Nucleotide exchange factor GEF-H1 mediates cross-talk between microtubules and the actin cytoskeleton. *Nat. Cell Biol.* 4:294–301.

Matsumura, F. 2005. Regulation of myosin II during cytokinesis in higher eukaryotes. *Trends Cell Biol.* 15:371–377.

Matsumura, F., S. Ono, Y. Yamakita, G. Totsukawa, and S. Yamashiro. 1998. Specific localization of serine 19 phosphorylated myosin II during cell locomotion and mitosis of cultured cells. *J. Cell Biol.* 140:119–129.

Meulmeester, E., and A.G. Jochemsen. 2008. p53: a guide to apoptosis. *Curr. Cancer Drug Targets.* 8:87–97.

Ninov, N., D.A. Chiarelli, and E. Martín-Blanco. 2007. Extrinsic and intrinsic mechanisms directing epithelial cell sheet replacement during *Drosophila* metamorphosis. *Development.* 134:367–379.

Published August 31, 2009

Pagliarini, R.A., and T. Xu. 2003. A genetic screen in *Drosophila* for metastatic behavior. *Science.* 302:1227–1231.

Redd, M.J., G. Kelly, G. Dunn, M. Way, and P. Martin. 2006. Imaging macrophage chemotaxis in vivo: studies of microtubule function in zebrafish wound inflammation. *Cell Motil. Cytoskeleton.* 63:415–422.

Rogers, S.L., U. Wiedemann, U. Häcker, C. Turck, and R.D. Vale. 2004. Drosophila RhoGEF2 associates with microtubule plus ends in an EB1-dependent manner. *Curr. Biol.* 14:1827–1833.

Rosenblatt, J., M.C. Raff, and L.P. Cramer. 2001. An epithelial cell destined for apoptosis signals its neighbors to extrude it by an actin- and myosin-dependent mechanism. *Curr. Biol.* 11:1847–1857.

Schulze-Bergkamen, H., and P.H. Krammer. 2004. Apoptosis in cancer—implications for therapy. *Semin. Oncol.* 31:90–119.

Thompson, B.J., J. Mathieu, H.H. Sung, E. Loeser, P. Rørth, and S.M. Cohen. 2005. Tumor suppressor properties of the ESCRT-II complex component Vps25 in *Drosophila*. *Dev. Cell.* 9:711–720.

Vidal, M., D.E. Larson, and R.L. Cagan. 2006. Csk-deficient boundary cells are eliminated from normal *Drosophila* epithelia by exclusion, migration, and apoptosis. *Dev. Cell.* 10:33–44.

Wittmann, T., and C.M. Waterman-Storer. 2001. Cell motility: can Rho GTPases and microtubules point the way? *J. Cell Sci.* 114:3795–3803.

Yang, L., Z. Cao, H. Yan, and W.C. Wood. 2003. Coexistence of high levels of apoptotic signaling and inhibitor of apoptosis proteins in human tumor cells: implication for cancer specific therapy. *Cancer Res.* 63:6815–6824.

Yu, W., A. Datta, P. Leroy, L.E. O'Brien, G. Mak, T.S. Jou, K.S. Matlin, K.E. Mostov, and M.M. Zegers. 2005. Beta1-integrin orients epithelial polarity via Rac1 and laminin. *Mol. Biol. Cell.* 16:433–445.

Published August 31, 2009

Supplemental material

JCB

Slattum et al., http://www.jcb.org/cgi/content/full/jcb.200903079/DC1

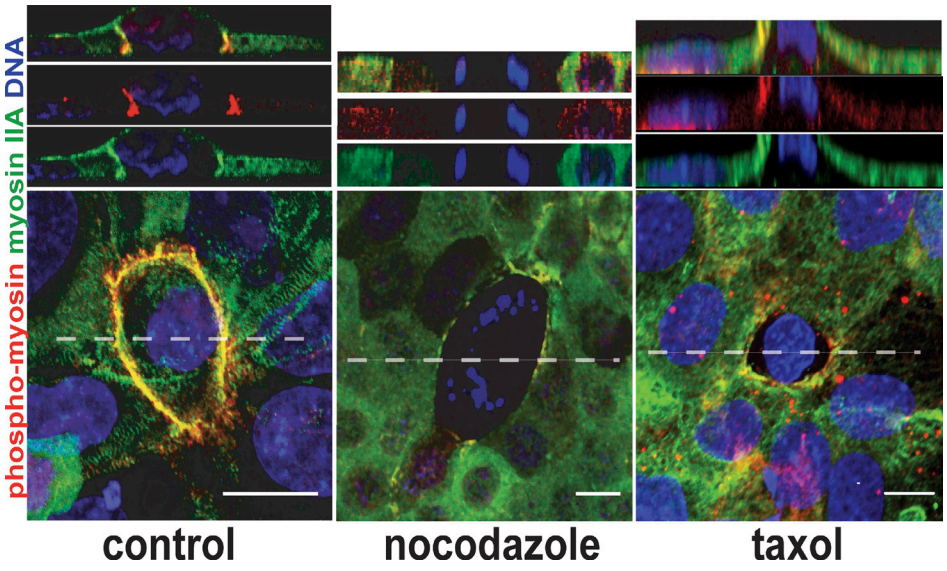

Figure S1. **Disruption of microtubules with nocodazole or taxol mislocalizes both myosin IIA and phospho-myosin II in 16-HBE-14o cell monolayers.** Both phospho-myosin II and myosin IIA localize throughout the extruding ring in control monolayers, but are absent in nocodazole and restricted to the apex in taxol-treated monolayers. Cross sections above are from the broken lines in the xy images. Bars, 10 µm.

Published August 31, 2009

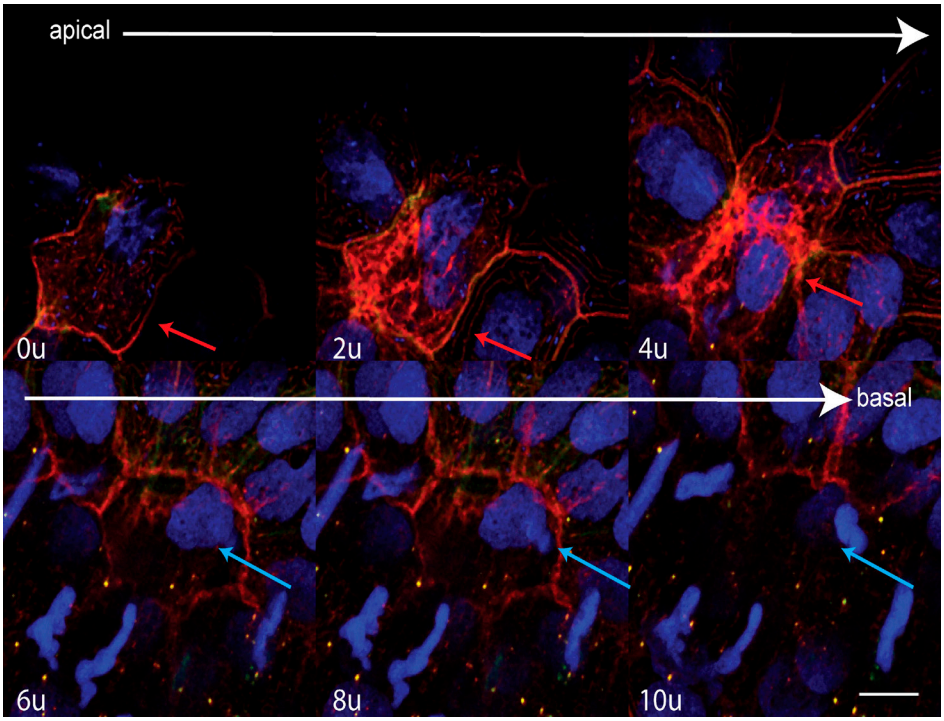

Figure S2. **Freezing microtubules with taxol drives extrusion basally in zebrafish larval epidermis.** Treatment of 4-d-old zebrafish larvae with G-418 to induce apoptosis and with taxol to stabilize microtubules drives extrusion basally. Note that the actin (red) ring is at the top (apex) of fish and the condensed DNA (blue) is basal, where numbers represent micrometers from the most apical part of ring. At this stage, active caspase-3 (green) is dim, but will become brighter later as the cell extrudes (as seen in Video 7). Bar, 10 µm

Published August 31, 2009

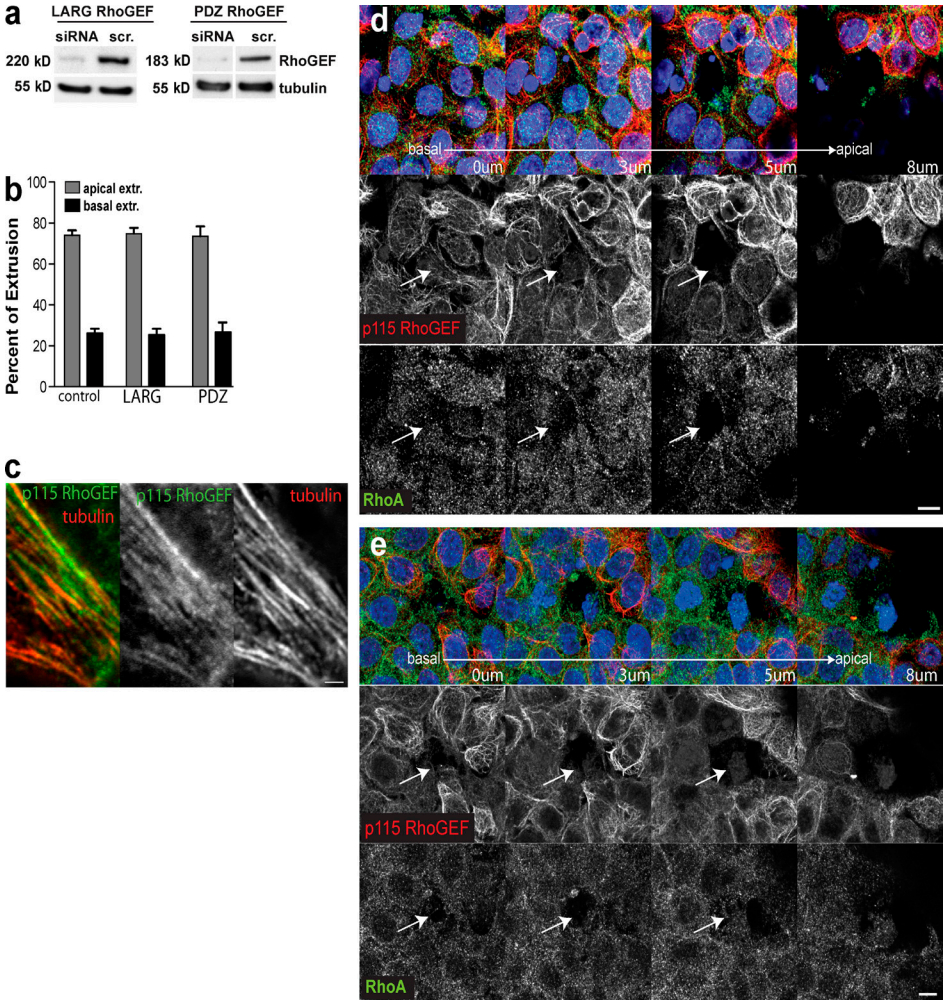

Figure S3. **siRNA-mediated knockdown of other RGS-RhoGEFs has no effect on the direction of extrusion.** (a) Immunoblots of LARG and PDZ RhoGEF knockdown (lanes from same blot). (b) Graphs representing the mean of five different experiments analyzing 1,000 extruding cells for their extrusion direction for each knockdown. (c) p115 RhoGEF and microtubules colocalize near the extrusion ring. Bar, 1 µm. (d and e) Treatment with taxol (d) or nocodazole (e) disrupts basolateral distribution of p115 RhoGEF (red; middle panels) and RhoA (green; bottom panels), where arrows point to the dying cell (DNA is blue). p115 RhoGEF localization with each treatment is quantified in Fig. 5. Bars, 10 µm.

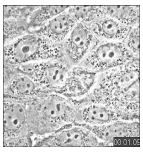

Video 1. **An apoptotic cell extruding apically from an MDCK cell monolayer.** The cell that will extrude is marked by a blue arrow in the beginning frame. Frames were taken every 60 s using a 40× 0.75 NA Nikon phase lens.

Published August 31, 2009

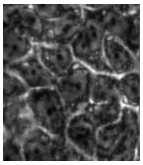

Video 2. **An apoptotic cell extruding basally from an MDCK cell monolayer.** Note that the cell that extrudes basally (arrow in the beginning frame) appears to migrate under the monolayer, and presumably is later engulfed. Frames were taken every 60 s using a 40× 0.75 NA Nikon phase lens.

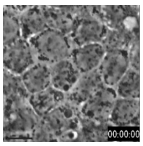

Video 3. **Another apoptotic cell extruding basally from an MDCK cell monolayer.** Note that the cell that extrudes basally (arrow in beginning frame) appears to migrate under the monolayer, and presumably is later engulfed. Frames were taken every 60 s using a 40× 0.75 NA Nikon phase lens.

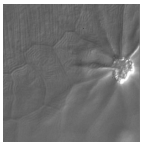

Video 4. **Apical extrusion of a dying cell from the epidermis of a 4-d-old zebrafish.** The dying cell extrudes apically out of the epidermis and is trapped between fish and cover glass when zebrafish 4-d-old larvae are treated with 450 µg/ml G-418 and 0.2% DMSO (as carrier control). Frames were taken every 60 s using a 40× 0.8 W Nikon water immersion DIC lens.

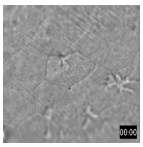

Video 5. **Basal extrusion of a dying cell in the epidermis of a 4-d-old zebrafish treated with taxol.** The dying cell extrudes basally into the epidermis and is trapped beneath the epidermis when zebrafish larvae are treated with 450 µg/ml G-418 and 20 µM taxol. Frames were taken every 60 s using a 40× 0.8W Nikon water immersion DIC lens.

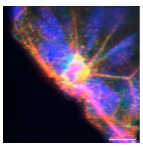

Video 6. **Apical extrusion of a dying cell from the epidermis of a 4-d-old zebrafish: 3D reconstruction.** An apoptotic cell (with active caspase-3 staining; green) is extruded out of the plane, where actin ring (red) is below the cell and its DNA (blue). Shown is a tilting reconstruction of confocal projections from a z series taken on a TCS SP5 confocal microscope (Leica) using a 63× oil lens at 1,024 × 1,024 resolution.

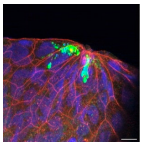

Video 7. **Basal extrusion of a dying cell into the epidermis of a 4-d-old zebrafish: 3D reconstruction.** An apoptotic cell (with active caspase-3 staining; green) is extruded out of the plane, where actin ring (red) is above the caspase-positive cell and its DNA (blue). Tilting reconstruction of confocal projections from a z series taken on a TCS SP5 confocal microscope (Leica) using a 63× oil lens at 1,024 × 1,024 resolution.

Published August 31, 2009

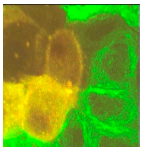

Video 8. **Apical extrusion in MDCKs expressing mApple-actin and GFP-tubulin.** Microtubules (green) target toward the extruding actin ring (red) early during the extrusion process and remain throughout until the ring has closed. Then, the microtubules retract from this point. The video was acquired with an inverted microscope (Nikon) with a 60× lens using a spinning disc system (Yokogawa) and a cooled CCD camera (Andor 1000). Four z-section planes were taken through 9 µm and projected together using 4D software from Andor. The entire video represents 1 h.

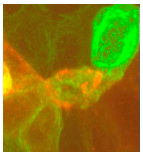

Video 9. **Basal extrusion in MDCKs expressing mApple-actin and GFP-tubulin.** Microtubules (green) target toward the top of the extruding actin ring (red) throughout the extrusion process. Note that far fewer microtubules target the actin/myosin ring than in the apical extrusion case (Video 8). The video was acquired with an inverted Nikon with a 60× lens using a spinning disc system (Yokogawa) and a cooled CCD camera (Andor 1000). Four z-section planes were taken through 9 µm and projected together using 4D software from Andor Technologies. The entire video represents 1 h.

CHAPTER 3

ONCOGENIC K-RAS PROMOTES BASAL EXTRUSION OF EPITHELIAL CELLS BY DEGRADING S1P THROUGH AUTOPHAGY

Reprinted with permission from Current Biology. Slattum, G., Gu, Y., Sabbadini, R., and Rosenblatt, J. (2014). Oncogenic K-Ras promotes basal extrusion of epithelial cells by degrading S1P through autophagy. Current Biology. Jan 6;24(1):19-28.

Chapter 3 is a published article.

Current Biology 24, 19–28, January 6, 2014 ©2014 Elsevier Ltd All rights reserved http://dx.doi.org/10.1016/j.cub.2013.11.029

Article

Autophagy in Oncogenic K-Ras Promotes Basal Extrusion of Epithelial Cells by Degrading S1P

Gloria Slattum,[1] Yapeng Gu,[1] Roger Sabbadini,[2] and Jody Rosenblatt[1,*]

[1]Huntsman Cancer Institute, University of Utah, 2000 Circle of Hope, Salt Lake City, UT 84112, USA

[2]Lpath, Inc., 4025 Sorrento Valley Boulevard, San Diego, CA 92121, USA

Summary

Background: To maintain a protective barrier, epithelia extrude cells destined to die by contracting a band of actin and myosin. Although extrusion can remove cells triggered to die by apoptotic stimuli, to maintain constant cell numbers, epithelia extrude live cells, which later die by anoikis. Because transformed cells may override anoikis and survive after extrusion, the direction of extrusion has important consequences for the extruded cell's fate. As most cells extrude apically, they are typically eliminated through the lumen; however, cells with upregulated survival signals that extrude basally could potentially invade the underlying tissue and migrate to other sites in the body.

Results: We found that oncogenic K-Ras cells predominantly extrude basally, rather than apically, in a cell-autonomous manner and can survive and proliferate after extrusion. Expression of K-Ras^{V12} downregulates the bioactive lipid sphingosine 1-phosphate (S1P) and its receptor $S1P_2$, both of which are required for apical extrusion. Surprisingly, the S1P biosynthetic pathway is not affected because the S1P precursor, sphingosine kinase, and the degradative enzymes S1P lyase and S1PP phosphatase are not significantly altered. Instead, we found that high levels of autophagy in extruding Ras^{V12} cells leads to S1P degradation. Disruption of autophagy chemically or genetically in K-Ras^{V12} cells rescues S1P localization and apical extrusion.

Conclusions: Oncogenic K-Ras cells downregulate both S1P and its receptor $S1P_2$ to promote basal extrusion. Because live basally extruding cells can survive and proliferate after extrusion, we propose that basal cell extrusion provides a novel mechanism for cells to exit the epithelium and initiate invasion into the surrounding tissues.

Introduction

Epithelia provide a protective barrier for the organs they encase, yet the cells comprising epithelia are constantly turning over via cell death and cell division. To maintain a functional barrier, cells destined to die are squeezed out of the epithelium by a mechanism that we have termed "cell extrusion" [1]. In previous work, we have shown that this process is mediated by the bioactive sphingolipid, sphingosine 1-phosphate (S1P), which is produced by the extruding cell and binds to a G protein-coupled receptor ($S1P_2$) in the neighboring cells to trigger the guanosine triphosphatase (GTPase) Rho to form and contract an intercellular actomyosin band [2]. This contraction squeezes the cell out of the epithelial sheet while simultaneously closing the gap that may have resulted from the cell's exit, thus preserving the epithelial barrier function.

Although extrusion is activated whenever cells are targeted to die by apoptotic stimuli, we have found that normally during homeostasis, extrusion drives cell death [3, 4]. To maintain cell number homeostasis, epithelia extrude live cells at sites where epithelial cells are most crowded both in vivo and in vitro. Live extruded cells generally die by anoikis, a type of cell death caused by the loss of survival signals from cell matrix [5]. Blocking extrusion leads to epithelial cell masses, supporting the idea that cell extrusion promotes death. On the other hand, metastatic tumor cells upregulate survival signaling, which can override anoikis and enable survival after extrusion [6–8].

Should cells survive after extrusion, the direction they extrude could have important consequences for their fate. Typically, epithelia extrude cells apically into the lumen, so that even transformed live cells would be eliminated into essentially dead space. Less frequently, however, cells can extrude basally into the tissue the epithelium encases. Should transformed cells that can no longer die extrude basally, they may have the potential to invade the underlying tissue and initiate metastasis. The direction a cell extrudes depends on if the actomyosin ring formed in its neighboring cells contracts along the basolateral cell surface or at the apex to push the cell out above or below the epithelium, respectively [9, 10]. Where the actomyosin ring contracts depends, at least in part, upon microtubule dynamics and the tumor suppressor adenomatous polyposis coli (APC), which target where the ring forms [9, 10].

To investigate the fate of extruded cells that upregulate survival signals and override anoikis, we expressed a commonly occurring oncogenic allele of K-Ras (K-Ras^{V12}), which renders it constitutively active, leading to downregulation of apoptosis and increased cell survival. Increased survival in K-Ras-transformed cells is thought to be from not only increased expression of survival signals but also enhanced protective autophagy [11–14]. The importance of mutations in the K-RAS proto-oncogene is well established in epithelial-based carcinogenesis, especially in lung, pancreatic, and colon carcinomas.

Here, we investigated if cells expressing oncogenic K-Ras could still extrude, and if so, could they survive after extrusion. We found that K-Ras^{V12} cells not only survive and proliferate after extrusion but, surprisingly, also preferentially extrude basally, beneath epithelia. Moreover, we found that K-Ras^{V12} cell basal extrusion is cell autonomous. Interestingly, we found that high levels of autophagy in extruding oncogenic K-Ras cells disrupt S1P production and signaling required for apical extrusion. S1P normally forms puncta at the interface between an apically extruding cell and its neighboring cells and is required only for apical but not basal extrusion. In extruding oncogenic K-Ras cells, however, S1P is greatly decreased despite the fact that the pathways required for its synthesis and degradation are unaltered. We found that markers of autophagy, typically upregulated in oncogenic K-Ras cells, are even more pronounced in extruding K-Ras cells. Blocking

*Correspondence: jody.rosenblatt@hci.utah.edu

Current Biology Vol 24 No 1
20

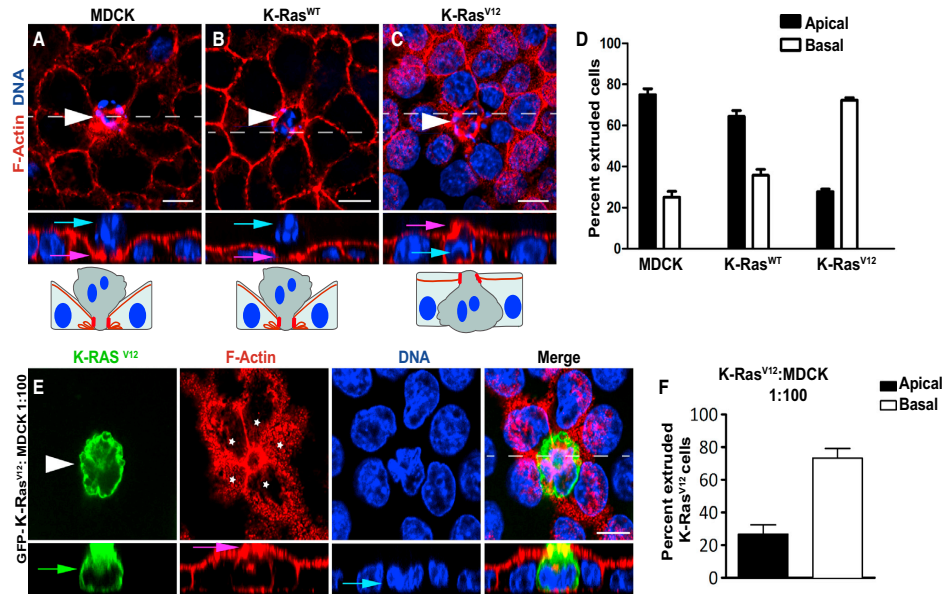

Figure 1. Epithelial Cells Expressing K-Ras^{V12} Extrude Basally in a Cell-Autonomous Manner

(A–C) Confocal projections and xz cross-sections (below) showing extruding cells (white arrowheads). Control MDCK cells (A) and those expressing YFP-K-Ras^{WT} (B) extrude apically (DNA of extruding cell is out of plane with neighboring cells), whereas those expressing GFP-K-Ras^{V12} (C) extrude basally (DNA of extruding cell is in same plane as neighboring cells).

(D) Quantification of cell extrusion events from five independent experiments with >1,000 extruding cells per cell line.

(E) MDCK GFP-K-Ras^{V12} cells mixed with WT MDCK cells 1:100 indicate that K-Ras^{V12} cells (green arrow) drive basal extrusion cell autonomously, where arrowhead indicates basally extruded K-Ras^{V12} cell, and asterisks show WT cells. Pink and blue arrows indicate actin ring and DNA, respectively, and dashed line where the xz section was taken.

(F) Quantification of three independent experiments, where n = 600 extruding cells.

Scale bars represent 10 μm. Error bars indicate the SEM. $p < 0.001$ by Student's t test comparing control to Ras^{V12}. See also Figure S1 and Movies S1 and S2.

autophagy rescues S1P localization and apical extrusion. Thus, K-Ras transformation can promote basal extrusion and enable cells with higher survival and proliferation potential to exit the epithelia and initiate invasion.

Results

Epithelial Cells Expressing K-Ras^{V12} Extrude Basally in a Cell-Autonomous Manner

Because we previously found that epithelia normally extrude cells that later die due to loss of survival signaling, or anoikis, we wondered if transformed cells that block anoikis could still extrude and survive after extrusion. To test this hypothesis, we expressed oncogenic K-Ras, which upregulates survival signals that override anoikis. To determine whether cells expressing oncogenic K-Ras can still extrude, we induced extrusion in Madin-Darby canine kidney (MDCK) II cell monolayers that stably express either yellow fluorescent protein (YFP)-tagged K-Ras^{WT} or GFP-tagged K-Ras^{V12} by irradiating with UV^{254} to induce apoptosis. Surprisingly, we found that GFP-K-Ras^{V12}-expressing cells extrude predominantly (~75%) basally rather than apically, the direction typically seen in wild-type (WT) MDCK monolayers or MDCK cells expressing WT K-Ras (Figures 1A–1C and quantified in Figure 1D). To demonstrate the direction a cell extrudes in a single picture, we overlaid the xy plane of the actin-extruding ring with the xy plane of the DNA of the extruded cell. Thus, during apical extrusion in WT and YFP-K-Ras^{WT}, the apoptotic nucleus lies above the plane of the actin ring so that the nuclei of the surrounding cells are not in focus (also see xz insets in Figures 1A and 1B and schematics below). GFP-K-Ras^{V12} basally extruding cells, conversely, contract an actin ring apically above the apoptotic nucleus, which lies in the same xy plane as the nuclei of the surrounding cells (Figure 1C, xz insets, schematic below; Movie S1 available online). Although these extruding cells did not survive such harsh apoptotic stimulus, we found that cells extruding without apoptotic stimulus from overgrown monolayers also did so predominantly basally (Figure S1).

To determine if K-Ras^{V12} expression controls basal extrusion within the extruding cell or the cells neighboring it, we induced extrusion by UV-irradiating monolayers comprised of a 1:100 ratio of GFP-K-Ras^{V12} to WT MDCK cells. GFP-K-Ras^{V12} expression in the extruding cell was sufficient to drive extrusion basally at rates similar to homogeneously expressed GFP-K-Ras^{V12} (Figure 1E, with quantification in Figure 1F; Movie S2). Thus, K-Ras^{V12} drives basal extrusion cell autonomously, suggesting that tumor cells in which this mutation arises could use basal extrusion to invade beneath the epithelium. Alternatively, cells could be induced to extrude and invade from a mosaic patch of K-Ras-transformed cells.

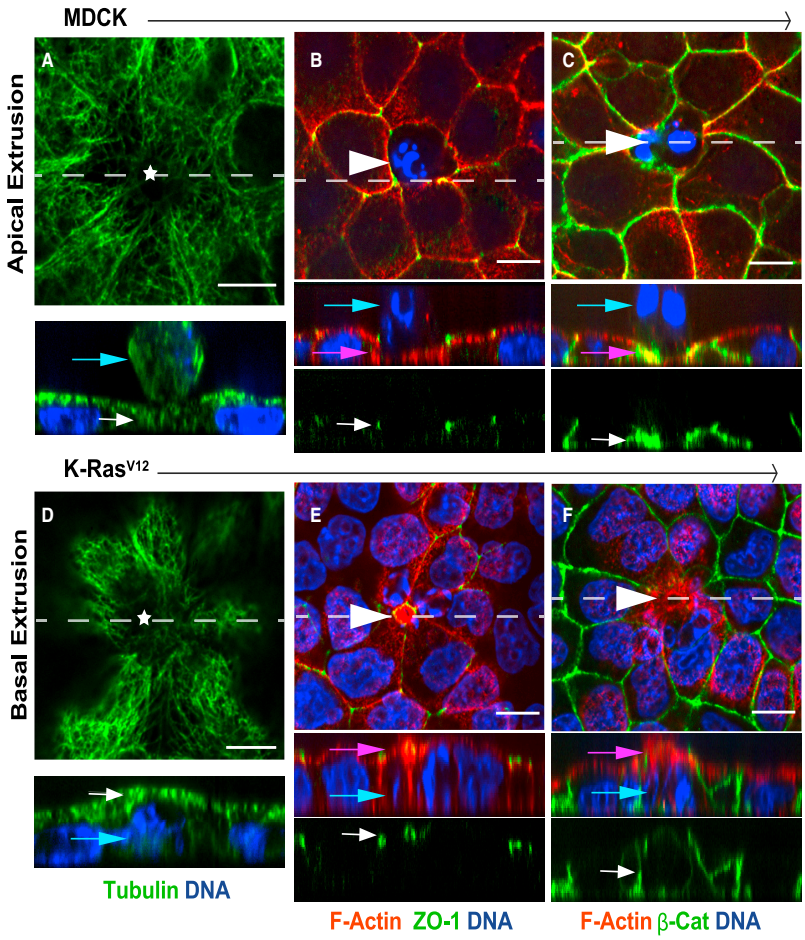

Figure 2. K-Ras^{V12} Does Not Affect Direction of Extrusion by Altering Microtubule Dynamics or Cell Intrinsic Polarity

Confocal projections and xz cross-sections (below) of control MDCK monolayers apically extruding (A–C) and K-Ras^{V12} monolayers basally extruding (D–F). White arrows point to the microtubules pointing basally during apical extrusion (A) and apically during basal extrusion (D), where asterisks indicate extruding cells location. White arrows show the apical marker ZO-1 (B and E) and the basal marker β-catenin (Cat) (E and F) are both localized correctly. White arrowhead indicates extruding cell, pink and blue arrows indicate actin ring and DNA, respectively, and dashed line where the xz section was taken. Scale bars represent 10 μm.

S1P Signals Apical but Not Basal Extrusion and Is Misregulated in K-Ras^{V12}-Expressing Cells

To determine how oncogenic K-Ras induces basal extrusion, we investigated if the cytoskeletal mechanism or the signaling controlling extrusion was altered in K-Ras^{V12}-expressing monolayers. We previously found that the direction a cell extrudes depends upon where the actin and myosin ring in the surrounding cells contracts [9, 10]. If it contracts at the bottom of the cell, the cell exits apically, whereas if it contracts apically, the cell extrudes basally. The site of actomyosin ring contraction depends on microtubules because altering microtubule dynamics with either taxol or nocodazole or disruption of a protein that regulates microtubules, APC, shifts the direction of extrusion from apical to basal [9, 10]. Therefore, we examined if microtubules were altered in K-Ras^{V12}-extruding cells. Unlike other situations where the direction of extrusion was linked to misregulation of microtubules, we found no obvious changes in microtubules in K-Ras^{V12}-extruding cells or cells surrounding them (Figures 2A and 2D). Next, we examined whether K-Ras^{V12} expression could alter the intrinsic polarity of cells to alter extrusion direction by immunostaining extruding monolayers for ZO-1, an apical marker, and β-catenin, a component of adherens-type junctions, used here as a basal marker. However, both of these polarity markers were also unaltered in Ras^{V12}-compared to WT-extruding cells, suggesting that K-Ras^{V12} expression does not affect the direction of extrusion by disrupting the intrinsic polarity (Figures 2B–2F). Therefore, we examined if K-Ras^{V12} acted cell autonomously to alter extrusion signaling.

Current Biology Vol 24 No 1
22

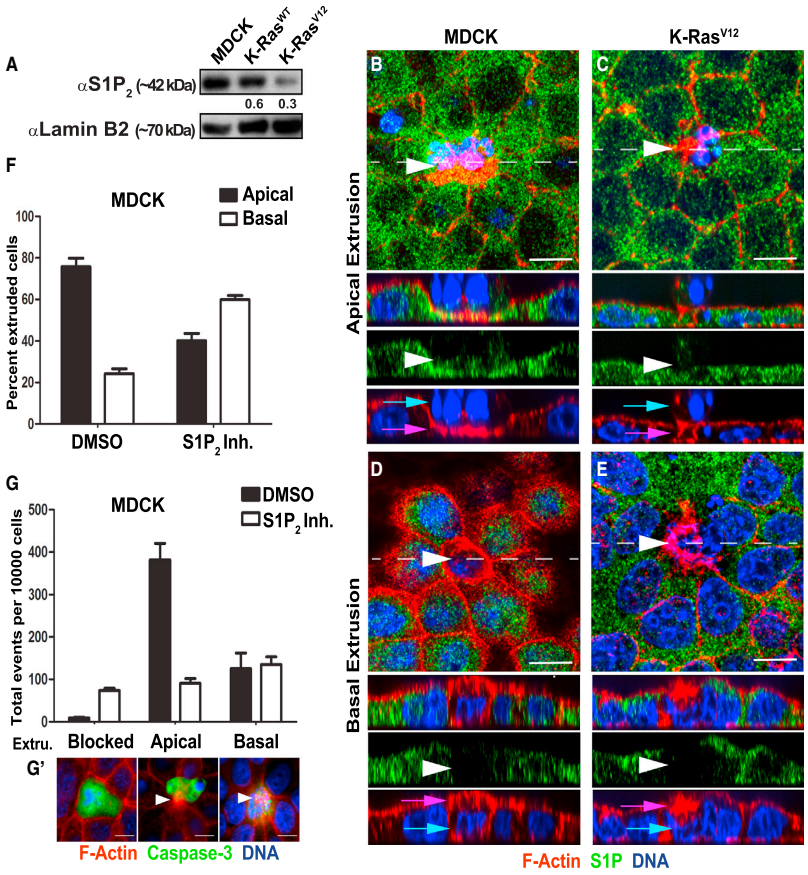

Figure 3. S1P and the S1P Receptor 2 Signal Apical but Not Basal Extrusion and Are Misregulated in K-Ras^{V12}-Expressing Cells

(A) Immunoblot analysis comparing the expression levels of S1P$_2$ in control MDCK cells, and MDCK cells expressing K-Ras^{WT} or K-Ras^{V12}, where lamin B2 serves as a loading control, and quantified ratio compared to control is below.

(B–E) Confocal projections and xz cross-sections (below) showing an apically extruding control MDCK produces high S1P levels (B), whereas an apically extruding K-Ras^{V12} cell does not (C). Basally extruding control (D) and K-Ras^{V12} (E) MDCK cells do not produce any S1P. White arrowheads point to dying, extruding cells at live-dead cell interfaces, pink arrows indicate actin ring, blue arrows show DNA, and dashed line where the xz section was taken. Scale bars represent 10 μm.

(F–G') Apical extrusion is disrupted in control MDCK cells treated with S1P$_2$ antagonist (JTE-013), where (F) shows comparative rates, and (G) shows total rates from three independent experiments analyzing 300 extrusion events for each experiment. Error bars indicate the SEM. $p < 0.001$ by Student's t test comparing control versus each treatment. (G') shows examples of blocked extrusion, scored by the presence of a faint actin ring that does not contract around a late-staged caspase-3-positive dying cell, apical extrusion, and basal extrusion. Arrowheads show extruding cell.

We next tested if extrusion signaling through S1P and the S1P$_2$ receptor were altered in oncogenic K-Ras-extruding cells. We previously found that a cell destined to extrude emits S1P, which binds the S1P$_2$ receptor in neighboring cells to activate Rho-mediated assembly and contraction of an intercellular actomyosin ring that squeezes it out [1, 2]. Because our previous data showed that disrupting S1P$_2$ disrupts extrusion, we assessed S1P$_2$ levels in K-Ras^{V12} cells and found that they had ~3-fold lower levels than WT MDCK cells by immunoblotting (Figure 3A). S1P is normally amplified only in extruding cells; therefore, we immunostained for this lipid using a specific monoclonal antibody to S1P [2, 15] in extruding monolayers. Whereas S1P forms prominent puncta at the interface of extruding/neighboring cells along the basolateral surface in control apically extruding cells (Figure 3B), S1P was completely absent in basally extruding K-Ras^{V12} cells induced to extrude with UV (Figure 3E) or under homeostatic conditions (Figure S1). By quantifying the number of extruding cells that have S1P, we found that 89% of apically extruding WT cells had S1P, whereas only 7% of K-Ras^{V12} basally extruding cells had S1P, where n = 100 for each cell type. In the minor populations of K-Ras^{V12} cells that extruded apically, S1P was diffuse and mislocalized (Figure 3C). Importantly, the minor population of control cells that basally extrudes also lacked S1P puncta, suggesting that the S1P-S1P$_2$ signaling pathway signals apical but not basal extrusion (Figure 3D).

To test if the S1P pathway controls only apical and not basal extrusion, we blocked extrusion in MDCK control cells with the

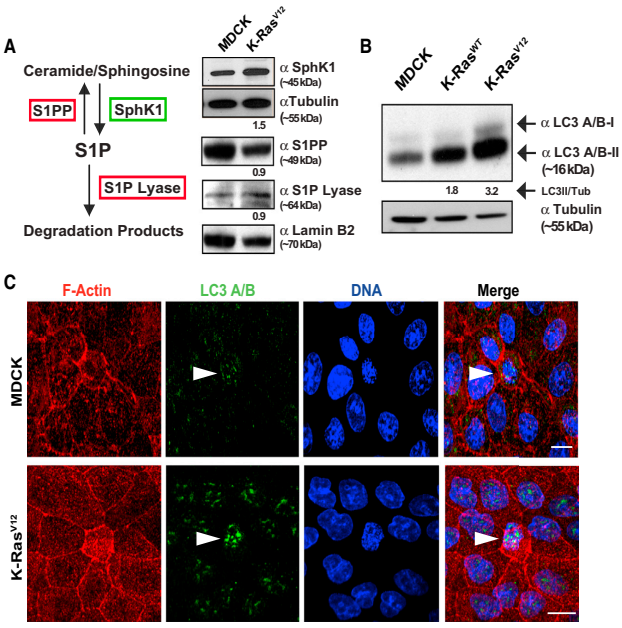

Figure 4. K-Ras^{V12}-Extruding Cells Express High Levels of the Autophagy Marker LC3A/LC3B

(A) SIP synthetic pathway and immunoblots comparing the expression levels of key regulators of S1P in control versus K-Ras^{V12} cell lysates where tubulin and lamin serve as loading controls.

(B) LC3A/LC3B immunoblots of MDCK, K-Ras^{WT}, and K-Ras^{V12} cells, where α-tubulin serves as a loading control, LC3A/LC3B-I is the cytosolic form, whereas LC3A/LC3B-II is associated with autophagosomes. Ratios compared to the control are below.

(C) Confocal projections of control MDCK cells and K-Ras^{V12} basal-extruding cell; white arrowheads show increased LC3 puncta in extruding cell. Scale bars represent 10 μm.

See also Figure S2 and Movies S3 and S4.

S1P$_2$ antagonist, JTE-013. JTE-013 increased the percentage of blocked extrusions, scored by the presence of a faint actin ring that does not contract around a late-staged caspase-3-positive dying cell, and seen previously in [2]. However, it increased the relative percentage of basal extrusions (Figure 3F). Although blocking S1P$_2$ signaling shifts the direction of extrusion from apical to basal, it actually does so by blocking apical extrusion without affecting basal extrusion, as indicated when total numbers of each type of extrusion were quantified (Figure 3G). When total rates of apical versus basal extrusion were similarly quantified in K-Ras^{V12}-extruding monolayers, instead of relative percentages, we found that they mirrored the effects of blocking S1P-S1P$_2$ signaling pathway on extrusion.

K-Ras^{V12}-Extruding Cells Express High Levels of the Autophagy Marker LC3A/LC3B

To determine how S1P is downregulated in K-Ras^{V12}-extruding cells, we analyzed the S1P synthetic pathway in WT versus oncogenic K-Ras monolayers induced to extrude with UV^{254}. We found that sphingosine kinase 1 (SphK1), the enzyme that converts sphingosine to S1P, was 1.5-fold upregulated in K-Ras^{V12}-expressing cells (Figure 4A). Furthermore, enzymes that downregulate S1P, by converting it back to sphingosine or degrading it into phosphoethanolamine and hexadecanal, S1P phosphatase 1 (S1PP), and S1P lyase, respectively, were not significantly altered in K-Ras^{V12} cells (Figure 4A, where both are 0.9-fold that of WT cells). Immunofluorescence also confirmed that S1P synthetic and degradative enzymes were not significantly altered in K-Ras^{V12}-extruding cells compared to WT-extruding MDCK cells (data not shown). Because neither S1P synthetic nor degradative pathways were significantly altered in K-Ras^{V12}-expressing cells, we next considered if S1P depletion in extruding K-Ras^{V12} cells was due to an alternative degradation pathway.

Because other studies have found that both oncogenic K-Ras expression [11–14] and SK1 levels [16] can promote autophagy, we investigated if autophagy may act to degrade S1P during K-Ras^{V12} cell extrusion. Autophagy is a process of cellular degradation where components of the cytoplasm and organelles are sequestered into autophagosomes, which then fuse with lysosomes to become degraded. Although cells use autophagy to conserve energy and resources during starvation, oncogenic Ras cells have been found to be addicted to autophagy to increase their survival rates [11–14]. Although autophagy has not been previously reported to degrade S1P, the fact that other membranous compartments of the cell can be degraded by autophagy suggests that S1P could also be degraded in this way. Additionally, because several sphingolipids have been found to promote autophagy [17, 18], it seemed possible that a sphingolipid also could be regulated by autophagy. Autophagosomes form by converting the autophagy marker Microtubule-Associated Protein 1-Light-Chain 3 (LC3) forms A and B from a cytosolic form (LC3-I) to a phosphatidylethanolamine-conjugated membrane-bound form (LC3-II). Thus, autophagic activity can be identified by LC3 puncta formation using immunofluorescence and LC3-II by a shift in its migration on immunoblots [19]. Using both methods, we found that compared to control cells, K-Ras^{V12} cells had elevated levels of the autophagy marker LC3-II (Figure 4B). LC3A/LC3B was even more enriched in K-Ras^{V12}-extruding cells compared to neighboring K-Ras^{V12} cells when viewed by immunofluorescence (Figure 4C). Quantification of LC3A/LC3B fluorescent intensity showed that K-Ras^{V12}-extruding cells had consistently higher numbers of puncta (~2,300 mean fluorescent intensity per 20 cells) compared to their non-extruding neighboring cells (~800 mean fluorescent intensity per 20 cells). The LC3A/LC3B increase in extruding cells may be similar to that seen in extruding cells in *Drosophila* amnioserosa prior to extrusion [20]. Extruding K-Ras^{V12} may have higher levels of autophagy than either WT-extruding or unextruding K-Ras^{V12} cells due to the fact that both K-Ras^{V12} signaling and extrusion signaling promote autophagy (as seen in Figure 4B). Our findings that autophagy is especially prominent in K-Ras^{V12} cells targeted to extrude suggests a mechanism for how these cells downregulate S1P to promote

Current Biology Vol 24 No 1
24

basal extrusion. To determine if inducing autophagy in control MDCK cells alone could switch the direction of extrusion from predominantly apical to basal, we treated MDCK monolayers with Torin-2 (a potent ATP-competitive inhibitor of mammalian target of rapamycin [mTOR]) that induces autophagy. We found that inducing autophagy in otherwise WT cells was sufficient to cause cells to extrude basally (Figure S2).

Blocking Autophagy in K-Ras^{V12} Cells Rescues S1P Localization and Apical Extrusion

To test if the increased autophagy in K-Ras^{V12} cells disrupts S1P-mediated apical extrusion, we blocked autophagy to assess if it would rescue both S1P and apical extrusion. We pretreated control and K-Ras^{V12} monolayers with commonly used small molecule inhibitors of autophagy, induced extrusion, and assayed for both S1P expression (Figures 5A and 5B) and the direction cells extrude (Figure 5C). By blocking autophagy with the phosphoinositide-3 kinase inhibitor wortmannin, which blocks autophagosome formation [21], or with bafilomycin A_1 [22] or chloroquine [23], which both block autophagosome degradation by preventing fusion with the lysosome, we found that inhibition of autophagy increased the percentage of cells undergoing apical extrusion compared to untreated K-Ras^{V12} cells (Figures 5A and 5B and quantified in Figure 5C). We expressed the tandem mCherry-EGFP-LC3B reporter in oncogenic K-Ras cells to confirm that autophagic flux to the lysosome was occurring in basally extruding cells. This reporter indicated that LC3 becomes targeted to lysosomes, inactivating GFP and turning red when a K-Ras^{V12} cell extrudes basally (Movie S3; Figure S3A) but stays yellow when fusion to the lysosome is blocked with chloroquine and the cell extrudes apically (Movie S4; Figure S3B). Moreover, the treatments rescued S1P expression in extruding K-Ras^{V12} cells (Figure 5B). On the other hand, blocking autophagy did not affect $S1P_2$ receptor levels, as measured by immunoblotting or immunostaining (Figure S4), suggesting that enough $S1P_2$ remains in the K-Ras^{V12} to rescue apical extrusion if S1P levels are increased.

Because these inhibitors can also affect other cellular functions, we confirmed if blocking autophagy could rescue S1P accumulation and apical extrusion in K-Ras^{V12} by knocking down two essential autophagy genes: Atg7 and Atg5. Similarly, Atg7 or Atg5 knockdown rescued both S1P puncta formation (Figure 5E) and apical extrusion (Figure 5F) in K-Ras^{V12}-extruding cells (Figure S5). The decrease in autophagy flux by diminished expression of LC3-II and accumulation of the p62/SQSTM1-scaffolding protein that is degraded by autophagy confirmed that Atg knockdown blocked autophagy (Figures 5D and S5). Therefore, K-Ras^{V12} cells drive cells to extrude basally by targeting the proextrusion signal S1P for degradation, and both S1P and apical extrusion can be rescued by simply blocking autophagy.

Although these experiments yielded the surprising finding that oncogenic K-Ras drives extrusion basally rather than apically, they were not able to assess whether basally extruded cells could survive and proliferate after extrusion for several reasons. First, to increase the rates of extrusion, we typically induce extrusion with the strong apoptotic stimulus, UV^{254}, which makes the extruding cells apoptotic. Although K-Ras^{V12} cells extruding during homeostasis (without UV treatment) extrude predominantly basally (Figure S1) and WT cells extrude predominantly apically at the same ratios as when apoptosis is induced, the extrusion rates are greatly reduced, making them harder to score. Second, if we allow cells to naturally extrude and accumulate over time, it is extremely hard to identify quantifiable numbers of live extruded cells in two-dimensional (2D) cultures: live apically extruded cells are lost within the medium, and live basally extruded cells may intercalate into the normal surrounding cells within the monolayer. Moreover, live basally extruded K-Ras^{V12} cells would be far more likely to die after basal extrusion in cell culture than in real tissue because they could become trapped between the cover glass and the monolayer, which would prevent their access to growth factors. In vivo, live basally extruded cells might still have access to growth factors in the matrix and underlying stroma. Therefore, we decided to investigate the fate of basally extruded cells in 3D cultures.

Basally Extruded K-Ras^{V12} Cells Survive and Proliferate in 3D Cultures

To test if GFP-K-Ras^{V12} cells can survive after extrusion, we grew control and K-Ras^{V12}-expressing MDCK cells as 3D cysts [24], where we would be able to score viability after extrusion. MDCK cells grown in Matrigel form a clonal acinar structure containing a hollow lumen that faces the apical surface (Figure 6A). Cysts comprised of oncogenic K-Ras MDCK cells, however, extruded live cells that persisted and often divided (Figure 6B). Eventually, these K-Ras^{V12} cells developed lumens filled with apoptotic cells, live cells, and smaller cysts, similar to results found with ErbB2 expression [25] (Figure S6). Additionally, approximately 20% of K-Ras^{V12} MDCK cysts also formed mini cysts attached to the outside of the main cyst (Figure 6C).

To determine the frequency of survival of the basally extruded K-Ras^{V12} compared to WT control cells, and those expressing WT K-Ras in 3D cultures, we immunostained cysts grown under homeostatic conditions for 3 days for the apoptotic marker antiactive caspase-3. We found that 67% of K-Ras^{V12} cells extrude live cells, whereas WT MDCK cells or MDCK cells expressing WT K-Ras only extrude 2% live cells, where the remainder are apoptotic (Figure S6). Attached basal mini cysts could arise either from other live migrating cells attaching to cysts or from proliferation of live basally extruded cells to form new smaller cysts. To test between these two models, we imaged live-cell extrusion by phase time-lapse video microscopy of control MDCK or GFP-K-Ras^{V12} cysts grown under homeostatic conditions. Whereas cells from MDCK cysts extruded into the lumen, underwent apoptosis, and were engulfed by neighboring cells (Figure 6D; Movie S5, left), apically extruded K-Ras^{V12} cells were not engulfed and instead filled the cyst's lumen. Furthermore, basally extruded K-Ras^{V12} cells either migrated away from the cyst or proliferated into a mini cyst (Figure 6E; Movie S5, right). Oncogenic K-Ras cells expressing fluorescently tagged myosin light chain (MLC) or actin clearly show that cells escaping the cyst do so by extrusion, as characterized by contraction of an actin and myosin II ring (Figure 6F; Movie S6). These data indicate that K-Ras^{V12} cells under homeostatic conditions extrude basally and, instead of dying, proliferate, suggesting that basal extrusion could provide a mechanism for invading matrix and tissue underlying epithelia.

Discussion

We have found that epithelial cells stably expressing oncogenic K-Ras extrude predominantly basally from both epithelial monolayers and 3D cysts in culture. Basal extrusion is cell autonomous because single K-Ras^{V12} cells surrounded

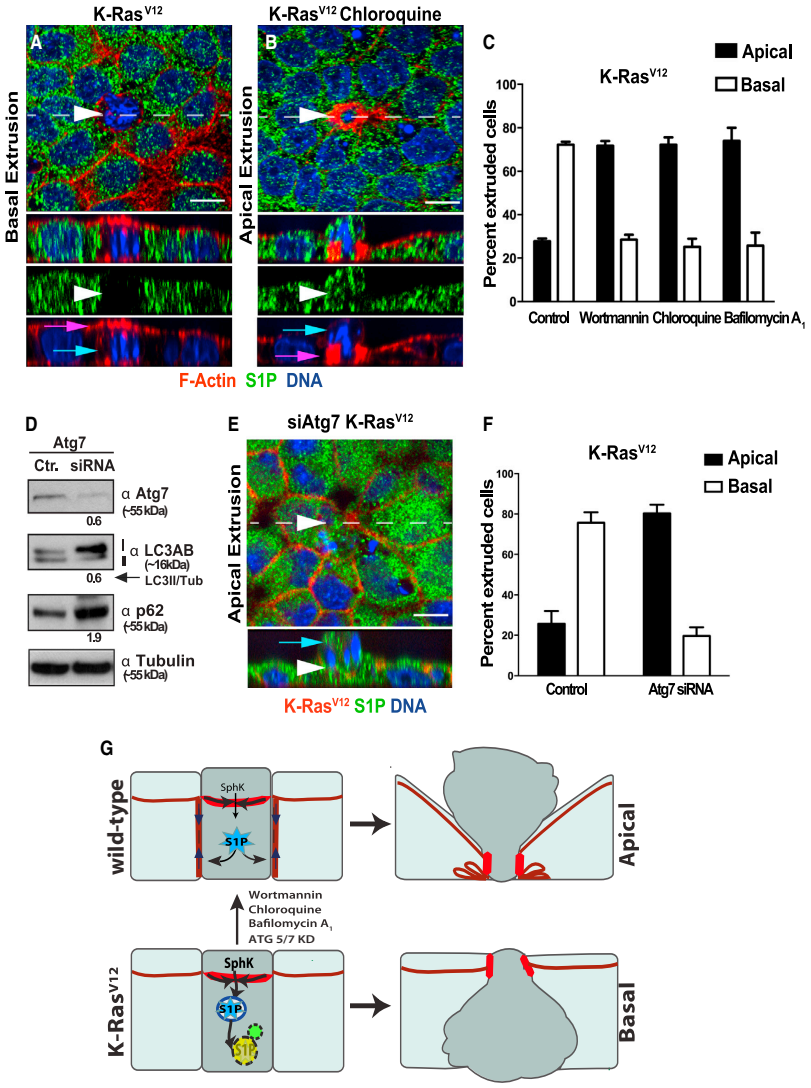

Figure 5. Blocking Autophagy in K-Ras^{V12} Cells Rescues S1P Localization and Apical Extrusion

(A and B) Confocal section and xz cross-sections (below) of a K-Ras^{V12} monolayer that extrudes primarily basally and lacks SIP (A) but extrudes apically and accumulates S1P puncta with 30 μM chloroquine, which blocks autophagy (B), where white arrowheads indicate extruding cells at the live-dead cell interfaces, pink arrows indicate actin ring, blue arrows show DNA, and dashed line the xz section. Scale bars represent 10 μm.

(C) Quantifications of cell extrusion direction with three autophagy inhibitors from four independent experiments where >1,000 extrusions were analyzed per treatment. Error bars indicate the SEM.

(D) Immunoblots show siRNA-mediated knockdown of Atg7 and LC3-II reduction and p62 upregulation. Ratios compared to the control (Ctr.) are below. Atg7 knockdown also rescues apical extrusion and S1P. Tub, tubulin.

(E and F) Quantification from <500 total extrusion events from three siRNA experiments. $p < 0.001$ by Student's t test comparing control versus each treatment. The scale bar represents 10 μm.

(G) Model for how apical extrusion is misregulated in K-Ras^{V12}-expressing cells. S1P normally binds S1P$_2$ in surrounding cells to contract basally and squeeze the cell out. However, in K-Ras^{V12}-extruding cells, S1P is targeted for degradation by increased autophagy. Without S1P, basolateral contraction in neighboring cells is not activated, and instead, only apical contraction of the dying cell occurs, driving extrusion basally. S1P (blue), autophagosome (yellow), lysosome (green), extruding cell actomyosin contraction (red), and neighboring cell actomyosin contraction (maroon). KD, knockdown.

See also Figures S3–S5.

Current Biology Vol 24 No 1
26

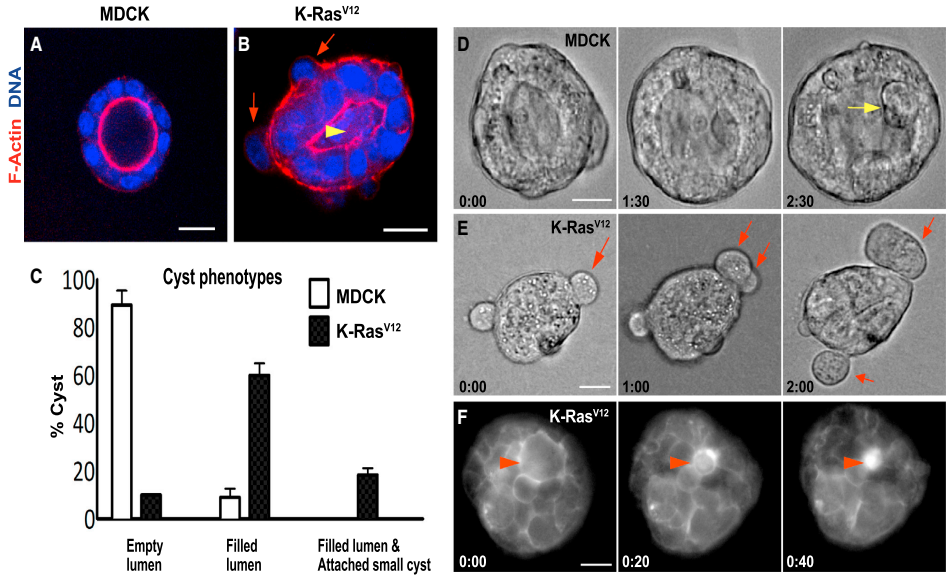

Figure 6. Basally Extruded K-Ras^{V12} Cells Survive and Proliferate in 3D Cultures

(A and B) Cysts from MDCK and K-Ras^{V12}-MDCK cells cultured in Matrigel for 3 days. Confocal sections show that WT MDCK cysts have clear lumens (A), whereas MDCK K-Ras^{V12} cysts extrude live cells basally (B). Yellow arrowhead, filled lumen; red arrows, live basal extruded cells.

(C) Quantification of phenotypes over time from three independent experiments ($n > 100$ cysts per experiment). Error bars indicate the SEM. $p < 0.001$ by Student's t test comparing control to Ras^{V12}.

(D and E) Stills from movies of cysts (in Movie S5) filmed at day 3 for 24 hr without UV treatment. A control MDCK cyst extrudes cells apically into the lumen (yellow arrow) (D), whereas a K-Ras^{V12} cyst extrudes cells basally into the matrix, which later proliferate (E) (red arrows).

(F) Stills from a movie of a UV-treated K-Ras^{V12} cyst expressing MLC-red fluorescent protein (RFP) (in Movie S6) show that basal extrusion of a cell occurs by contraction of a myosin ring.

Scale bars represent 20 μm. Time is indicated as hr:min. See also Figure S6 and Movies S5 and S6.

by WT cells also drive extrusion basally. Importantly, we found that although oncogenic K-Ras cells are typically autophagic, autophagy is even higher when these cells extrude, which disrupts S1P critical for apical extrusion. The normal S1P synthesis pathway is not altered in K-Ras^{V12} cells, however, because blocking autophagy either by knockdown of Atg5 or Atg7 or by chemical inhibitors rescues S1P puncta formation and apical extrusion. Together, our results suggest a model where K-Ras^{V12} cells targeted for normal extrusion produce S1P, which due to high levels of autophagy, becomes degraded in the lysosomes (Figure 5G). When S1P is absent, it can no longer signal neighboring cells to contract basally and extrude the cell apically. Instead, the basally extruding K-Ras^{V12} cell contracts at the apical junctions where actin and myosin II already exist, driving the cell out basally. In WT cells or when autophagy is blocked, S1P produced in the cell targeted for extrusion activates $S1P_2$ in the neighboring cells to contract basally and shove the cell out apically.

Although we previously identified that extrusion requires the S1P-$S1P_2$-Rho pathway, here, we find that this signaling axis controls only apical but not basal extrusion. This was not directly apparent because most cells extrude apically. Our finding that K-Ras^{V12} cells switch the extrusion direction from apical to basal by degrading S1P and downregulating $S1P_2$ also demonstrated that S1P signaling is only required for apical extrusion. Rescuing S1P by blocking autophagy rescues apical extrusion in K-Ras^{V12} cells. K-Ras^{V12} cells may affect extrusion also by downregulating the $S1P_2$ receptor by an autophagy-independent mechanism. However, the fact that blocking autophagy is sufficient to rescue apical extrusion suggests that there is enough $S1P_2$ present in K-Ras-transformed cells to enable apical extrusion when S1P levels are restored.

Our results showing that oncogenic K-Ras cells extrude basally contrast somewhat to those found by Hogan et al. that show H-Ras transformation causes apical extrusion [26]. We believe that the main difference in our results lies in the length of time K-Ras^{V12} is expressed. In experiments like ours where K-Ras^{V12} is expressed constitutively, Liu et al. found that a single oncogenic H-Ras cell within a cyst either extruded basally or migrated [27], suggesting that basal extrusion may be a common feature of expressing any form of oncogenic Ras long term. Hogan et al. [26], instead, use an inducible expression system to activate H-Ras^{V12} acutely. Acute H-Ras^{V12} causes cells that divide to segregate from their surrounding WT cells within the monolayer by what appears to be differential adhesion, rather than the extrusion process we have defined [26]. We have found similar results if we express K-Ras^{V12} acutely (data not shown), suggesting that expressing any isoform of activated Ras transiently will cause delamination apically. Although the ultimate effect is the same—that these cells delaminate from the epithelium—they do not do so through the canonical extrusion pathway that requires S1P-mediated activation of an intercellular actomyosin cable

that contracts in surrounding cells. Therefore, alternative downstream signaling may lead to apical delamination versus basal extrusion depending on the length of oncogenic K-Ras signaling.

Although we focused mainly on the mechanism that drives K-Ras^{V12} epithelial cells to extrude basally when targeted for cell death, it is important to note that live cells also extrude basally when no apoptotic stimulus is present. Because most cells extrude live prior to dying, the direction live cells extrude has important consequences for their later fate. Apically extruded cells will essentially be eliminated through the lumen or outside the body, even if transformed by K-Ras^{V12}, whereas basally extruded transformed cells could potentially invade and initiate metastasis. Thus, apical elimination of cells that become mutated with K-Ras^{V12} could act as a self-regulating mechanism to rid the body of transformed precancerous cells. On the other hand, oncogenic K-Ras-driven tumors, such as lung or pancreatic carcinomas, serve as testament to the fact that this mechanism sometimes fails. In these cases, shifting extrusion from apical to basal coupled with increased cell survival could act to promote tumor progression and metastasis. This newly defined potential mechanism for invasion, which is enhanced specifically in K-Ras-transformed cells, could explain why K-Ras-driven tumors are so metastatic and deadly. Our results suggest that simply blocking autophagy with chloroquine, a drug already in clinical use [28, 29], could prevent invasion of K-Ras^{V12}-driven tumors and better target them for apoptosis. Therefore, future studies will need to determine if basal extrusion of K-Ras cells can promote their invasion and metastasis in vivo and, if so, whether inhibition of autophagy can reverse this invasive phenotype.

Experimental Procedures

Cell Culture

Control MDCK II cells and cells expressing oncogenic K-Ras (gift from K. Matlin, University of Chicago, Chicago, IL) were cultured in Dulbecco's modified Eagle's medium (DMEM) high glucose with 5% FBS (all from HyClone) and 100 μg/ml penicillin/streptomycin (Invitrogen) at 5% CO_2, 37°C. MDCK II cells stably expressing GFP-oncogenic or YFP-WT K-Ras were generated by transfecting pEGFP C3 containing K-Ras^{V12} or pEYFP C1 containing K-Ras^{WT} (gift from Channing J. Der, University of North Carolina, Chapel Hill, NC), respectively, by using Lipofectamine 2000 (Invitrogen) according to manufacturer's instructions. To monitor autophagy flux in oncogenic K-Ras cells, we nucleofected cells (according to the manufacturer Lonza Biologics) with pBABE-puro mCherry-EGFP-LC3B tandem biosensor (Addgene plasmid 22418 deposited by Jayanta Debnath).

MDCK cysts were generated as previously described in [24] and the Supplemental Experimental Procedures. For live fluorescent imaging of MLC (gift from Thomas Marshall, University of Utah, Salt Lake City, UT) or mApple-actin-7 (a gift from Michael W. Davidson, Florida State University, Tallahassee, FL), oncogenic K-Ras cells were transduced or transfected, respectively, before culturing in Matrigel.

UV and Drug Treatment

MDCK II cells grown to confluence on glass coverslips were exposed to 1,200 uJ/cm^2 UV^{254} for 43 s using a Spectrolinker (Spectroline) to induce apoptotic extrusion and incubated for 2 hr before fixation. For complete cell drug treatment, please refer to the Supplemental Experimental Procedures.

Cell Staining

Cells were either fixed with ice-cold 100% methanol for 45 s or 4% paraformaldehyde in PBS at 37°C for 20 min. For protocols and antibodies, please refer to the Supplemental Experimental Procedures.

RNAi

siRNAs against the canine ATG7 and ATG5 sequences were synthesized at the University of Utah Oligo and Peptide Synthesis Core. For complete sequences, refer to the Supplemental Experimental Procedures.

Image, Video Acquisition, and Immunoblot Analysis

Microscopy and immunoblots were performed according to standard protocols. For details, please see the Supplemental Experimental Procedures.

Statistical Analysis

All statistical analyses were performed using Prism 5 (GraphPad) and employing unpaired t test.

Supplemental Information

Supplemental Information includes Supplemental Experimental Procedures, six figures, and six movies and can be found with this article online at http://dx.doi.org/10.1016/j.cub.2013.11.029.

Acknowledgments

We thank Katie Ullman and Thomas Marshall for helpful comments on our manuscript. We also thank Karl Matlin for his MDCK cell lines and Jayanta Debnath for first suggesting that we investigate autophagy. This work was supported by a National Institute of Health Innovator Award numbers DP2 OD002056-01 and 1R01GM102169-01 to J.R., a NIH Developmental Biology Training Grant 5T32 HDO7491 to G.S., and P30 CA042014 awarded to the Huntsman Cancer Institute for core facilities. R.A.S. has stock options in Lpath, Inc.

Received: January 11, 2013
Revised: October 11, 2013
Accepted: November 14, 2013
Published: December 19, 2013

References

1. Rosenblatt, J., Raff, M.C., and Cramer, L.P. (2001). An epithelial cell destined for apoptosis signals its neighbors to extrude it by an actin- and myosin-dependent mechanism. Curr. Biol. *11*, 1847–1857.
2. Gu, Y., Forostyan, T., Sabbadini, R., and Rosenblatt, J. (2011). Epithelial cell extrusion requires the sphingosine-1-phosphate receptor 2 pathway. J. Cell Biol. *193*, 667–676.
3. Eisenhoffer, G.T., Loftus, P.D., Yoshigi, M., Otsuna, H., Chien, C.B., Morcos, P.A., and Rosenblatt, J. (2012). Crowding induces live cell extrusion to maintain homeostatic cell numbers in epithelia. Nature *484*, 546–549.
4. Marinari, E., Mehonic, A., Curran, S., Gale, J., Duke, T., and Baum, B. (2012). Live-cell delamination counterbalances epithelial growth to limit tissue overcrowding. Nature *484*, 542–545.
5. Frisch, S.M., Vuori, K., Ruoslahti, E., and Chan-Hui, P.Y. (1996). Control of adhesion-dependent cell survival by focal adhesion kinase. J. Cell Biol. *134*, 793–799.
6. Douma, S., Van Laar, T., Zevenhoven, J., Meuwissen, R., Van Garderen, E., and Peeper, D.S. (2004). Suppression of anoikis and induction of metastasis by the neurotrophic receptor TrkB. Nature *430*, 1034–1039.
7. Horbinski, C., Mojesky, C., and Kyprianou, N. (2010). Live free or die: tales of homeless (cells) in cancer. Am. J. Pathol. *177*, 1044–1052.
8. Taddei, M.L., Giannoni, E., Fiaschi, T., and Chiarugi, P. (2012). Anoikis: an emerging hallmark in health and diseases. J. Pathol. *226*, 380–393.
9. Marshall, T.W., Lloyd, I.E., Delalande, J.M., Näthke, I., and Rosenblatt, J. (2011). The tumor suppressor adenomatous polyposis coli controls the direction in which a cell extrudes from an epithelium. Mol. Biol. Cell *22*, 3962–3970.
10. Slattum, G., McGee, K.M., and Rosenblatt, J. (2009). P115 RhoGEF and microtubules decide the direction apoptotic cells extrude from an epithelium. J. Cell Biol. *186*, 693–702.
11. Mathew, R., and White, E. (2011). Autophagy, stress, and cancer metabolism: what doesn't kill you makes you stronger. Cold Spring Harb. Symp. Quant. Biol. *76*, 389–396.
12. Guo, J.Y., Chen, H.Y., Mathew, R., Fan, J., Strohecker, A.M., Karsli-Uzunbas, G., Kamphorst, J.J., Chen, G., Lemons, J.M., Karantza, V., et al. (2011). Activated Ras requires autophagy to maintain oxidative metabolism and tumorigenesis. Genes Dev. *25*, 460–470.
13. Mirzoeva, O.K., Hann, B., Hom, Y.K., Debnath, J., Aftab, D., Shokat, K., and Korn, W.M. (2011). Autophagy suppression promotes apoptotic cell death in response to inhibition of the PI3K-mTOR pathway in pancreatic adenocarcinoma. J. Mol. Med. *89*, 877–889.

Current Biology Vol 24 No 1
28

14. Lock, R., and Debnath, J. (2011). Ras, autophagy and glycolysis. Cell Cycle *10*, 1516–1517.
15. Swaney, J.S., Moreno, K.M., Gentile, A.M., Sabbadini, R.A., and Stoller, G.L. (2008). Sphingosine-1-phosphate (S1P) is a novel fibrotic mediator in the eye. Exp. Eye Res. *87*, 367–375.
16. Lavieu, G., Scarlatti, F., Sala, G., Carpentier, S., Levade, T., Ghidoni, R., Botti, J., and Codogno, P. (2006). Regulation of autophagy by sphingosine kinase 1 and its role in cell survival during nutrient starvation. J. Biol. Chem. *281*, 8518–8527.
17. Young, M.M., Kester, M., and Wang, H.G. (2013). Sphingolipids: regulators of crosstalk between apoptosis and autophagy. J. Lipid Res. *54*, 5–19.
18. Bedia, C., Levade, T., and Codogno, P. (2011). Regulation of autophagy by sphingolipids. Anticancer. Agents Med. Chem. *11*, 844–853.
19. Tanida, I., Ueno, T., and Kominami, E. (2008). LC3 and autophagy. Methods Mol. Biol. *445*, 77–88.
20. Cormier, O., Mohseni, N., Voytyuk, I., and Reed, B.H. (2012). Autophagy can promote but is not required for epithelial cell extrusion in the amnioserosa of the *Drosophila* embryo. Autophagy *8*, 252–264.
21. Blommaart, E.F., Krause, U., Schellens, J.P., Vreeling-Sindelárová, H., and Meijer, A.J. (1997). The phosphatidylinositol 3-kinase inhibitors wortmannin and LY294002 inhibit autophagy in isolated rat hepatocytes. Eur. J. Biochem. *243*, 240–246.
22. Yoshimori, T., Yamamoto, A., Moriyama, Y., Futai, M., and Tashiro, Y. (1991). Bafilomycin A1, a specific inhibitor of vacuolar-type H(+)-ATPase, inhibits acidification and protein degradation in lysosomes of cultured cells. J. Biol. Chem. *266*, 17707–17712.
23. Paludan, C., Schmid, D., Landthaler, M., Vockerodt, M., Kube, D., Tuschl, T., and Münz, C. (2005). Endogenous MHC class II processing of a viral nuclear antigen after autophagy. Science *307*, 593–596.
24. Zegers, M.M., O'Brien, L.E., Yu, W., Datta, A., and Mostov, K.E. (2003). Epithelial polarity and tubulogenesis in vitro. Trends Cell Biol. *13*, 169–176.
25. Leung, C.T., and Brugge, J.S. (2012). Outgrowth of single oncogene-expressing cells from suppressive epithelial environments. Nature *482*, 410–413.
26. Hogan, C., Dupré-Crochet, S., Norman, M., Kajita, M., Zimmermann, C., Pelling, A.E., Piddini, E., Baena-López, L.A., Vincent, J.P., Itoh, Y., et al. (2009). Characterization of the interface between normal and transformed epithelial cells. Nat. Cell Biol. *11*, 460–467.
27. Liu, J.S., Farlow, J.T., Paulson, A.K., Labarge, M.A., and Gartner, Z.J. (2012). Programmed cell-to-cell variability in Ras activity triggers emergent behaviors during mammary epithelial morphogenesis. Cell Rep *2*, 1461–1470.
28. Krishna, S., and White, N.J. (1996). Pharmacokinetics of quinine, chloroquine and amodiaquine. Clinical implications. Clin. Pharmacokinet. *30*, 263–299.
29. Solomon, V.R., and Lee, H. (2009). Chloroquine and its analogs: a new promise of an old drug for effective and safe cancer therapies. Eur. J. Pharmacol. *625*, 220–233.

Current Biology, Volume *24*

Supplemental Information

Autophagy in Oncogenic K-Ras Promotes Basal Extrusion of Epithelial Cells by Degrading S1P

Gloria Slattum, Yapeng Gu, Roger Sabbadini, and Jody Rosenblatt

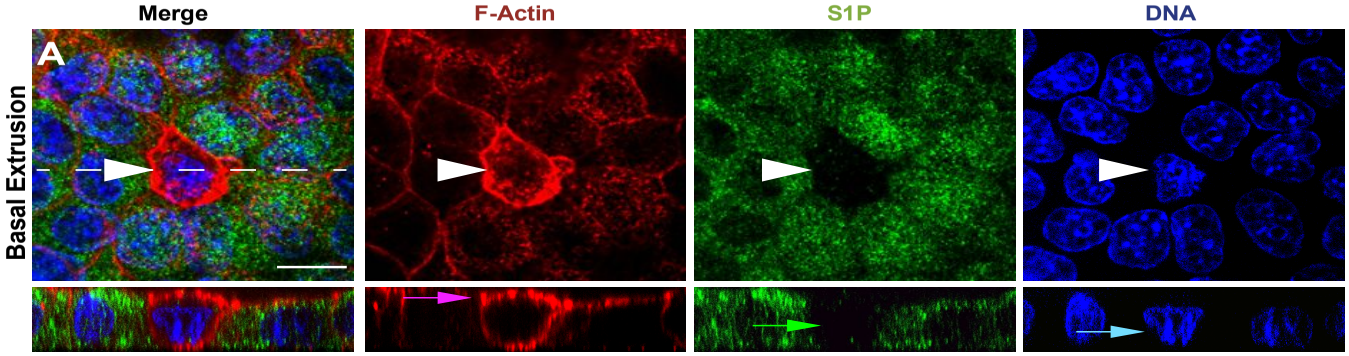

Figure S1. Extruding K-Ras^{V12} cells lack S1P and extrude basally under homeostatic conditions. Confocal projections and XZ cross-sections (below) showing a basally extruded K-Ras^{V12} cell, where white arrowheads point to a basally extruded cell, pink arrows indicate actin ring, blue arrows indicate DNA, green arrows point lack of S1P, and dashed line where XZ section was taken. Scale Bar=10 μm. (Related to Figure 1)

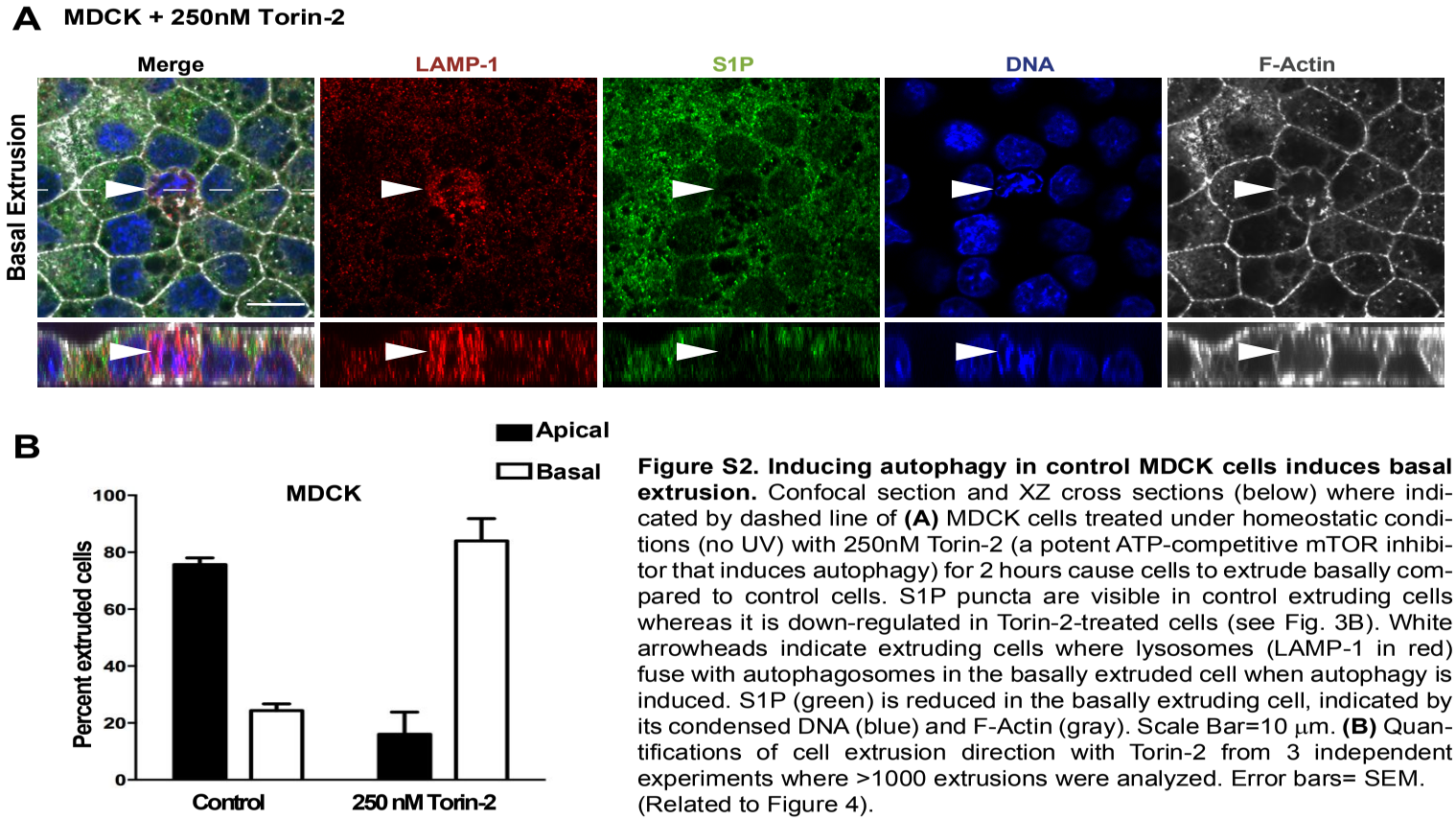

Figure S2. Inducing autophagy in control MDCK cells induces basal extrusion. Confocal section and XZ cross sections (below) where indicated by dashed line of **(A)** MDCK cells treated under homeostatic conditions (no UV) with 250nM Torin-2 (a potent ATP-competitive mTOR inhibitor that induces autophagy) for 2 hours cause cells to extrude basally compared to control cells. S1P puncta are visible in control extruding cells whereas it is down-regulated in Torin-2-treated cells (see Fig. 3B). White arrowheads indicate extruding cells where lysosomes (LAMP-1 in red) fuse with autophagosomes in the basally extruded cell when autophagy is induced. S1P (green) is reduced in the basally extruding cell, indicated by its condensed DNA (blue) and F-Actin (gray). Scale Bar=10 μm. **(B)** Quantifications of cell extrusion direction with Torin-2 from 3 independent experiments where >1000 extrusions were analyzed. Error bars= SEM. (Related to Figure 4).

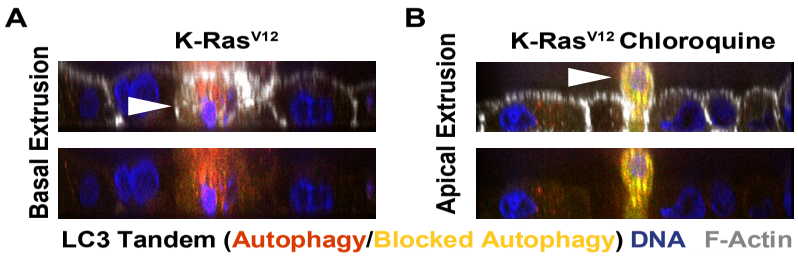

Figure S3. Chloroquine blocks autophagic flux and drives extrusion apically. A mCherry-EGFP-LC3B-expressing KRas^{V12} cell becomes red as LC3 fuses with lysosomes and the cell extrudes basally **(A)**, whereas a mCherry-EGFP-LC3B-expressing KRas^{V12} cell treated with Chloroquine remains yellow (from tandem mCherry-EGFP expression) when autophagosome fusion to the lysosome is blocked and apical extrusion is rescued **(B)**. Arrowheads indicate extruding cells. (Related to Figure 5).

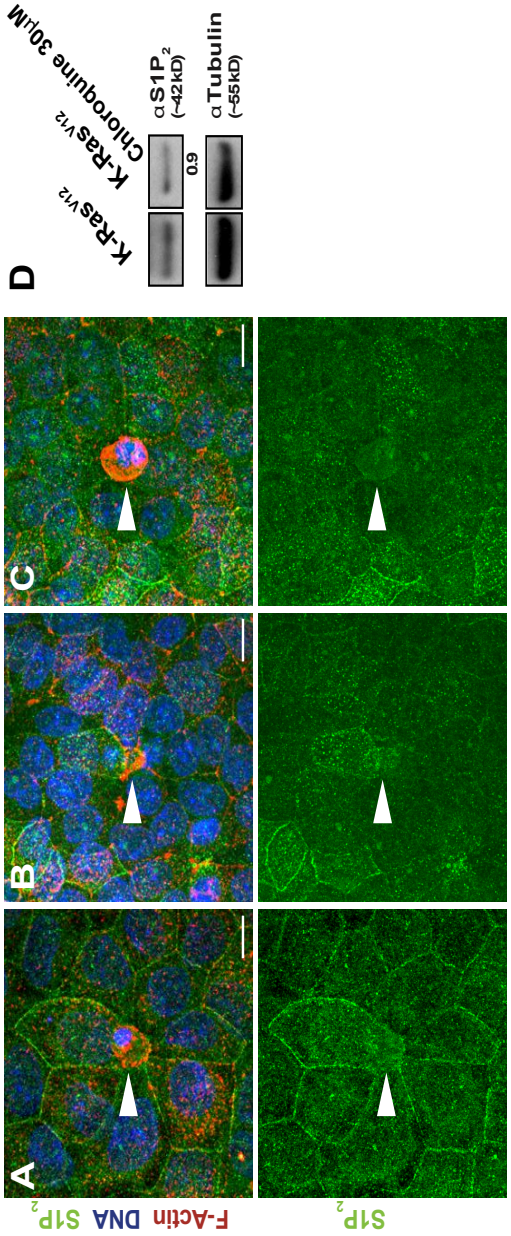

Figure S4. Chloroquine-mediated inhibition of autophagy does not rescue S1P2 levels in K-Ras^{V12} cells. Confocal projections showing S1P$_2$ expression levels in a control extruding cell **(A)** and K-Ras^{V12} extruding cells with and without chloroquine **(B-C)**, where white arrowheads indicate extruding cells. S1P$_2$ is down regulated in K-Ras^{V12} cells **(B)** compared to MDCK control **(A)** but not rescued by chloroquine treatment **(C)**. Scale Bar=10 μm. **(D)** S1P$_2$ immunoblots of MDCK-K-Ras^{V12} with and without chloroquine. Ratios compared to the control K-Ras^{V12} cells are below where tubulin serves as a loading control. (Related to Figure 5).

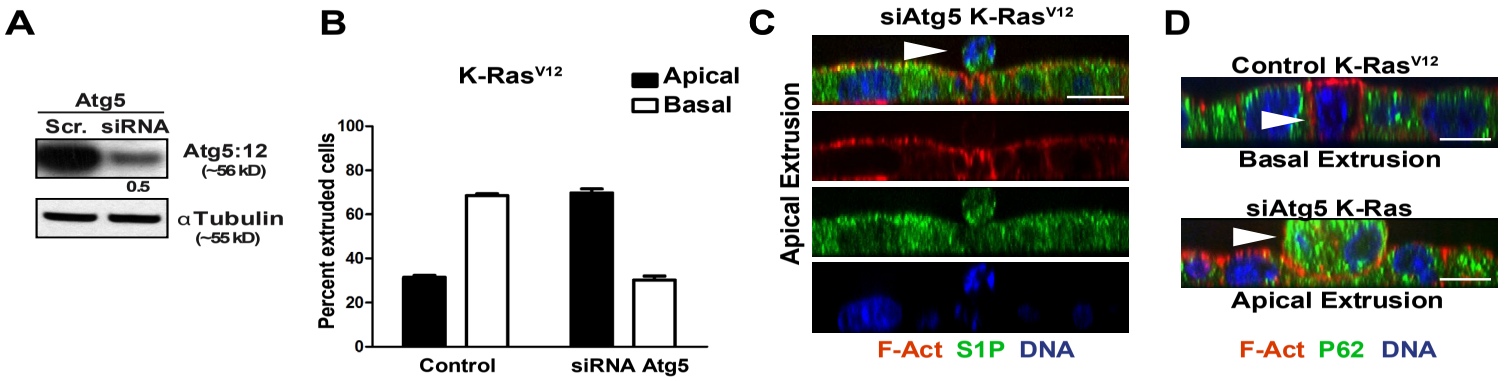

Figure S5. siRNA-mediated knockdown of ATG5 in K-Ras^{V12} cells rescues apical extrusion. (A) Immunoblot showing MDCK-K-Ras^{V12} cells transfected with siRNA oligonucleotides targeting ATG5. Ratios compared to the control are below. Quantification showing that Atg5 knockdown rescues apical extrusion, where n=200 extrusions from 3 siRNAs experiments **(B)**. P<0.001 by student's t test comparing control versus siRNA. **(C)** Confocal XZ cross-sections of siRNA-mediated knockdown of Atg5 from K-Ras^{V12} cells showing rescue of S1P and apical extrusion. **(D)** Autophagic flux and apical extrusion is restored by Atg5 knockdown, as the autophagic cargo p62 protein accumulates in siAtg5 treated but not control K-Ras^{V12} cells. White arrowheads indicate extruding cells. (Related to Figure 5).

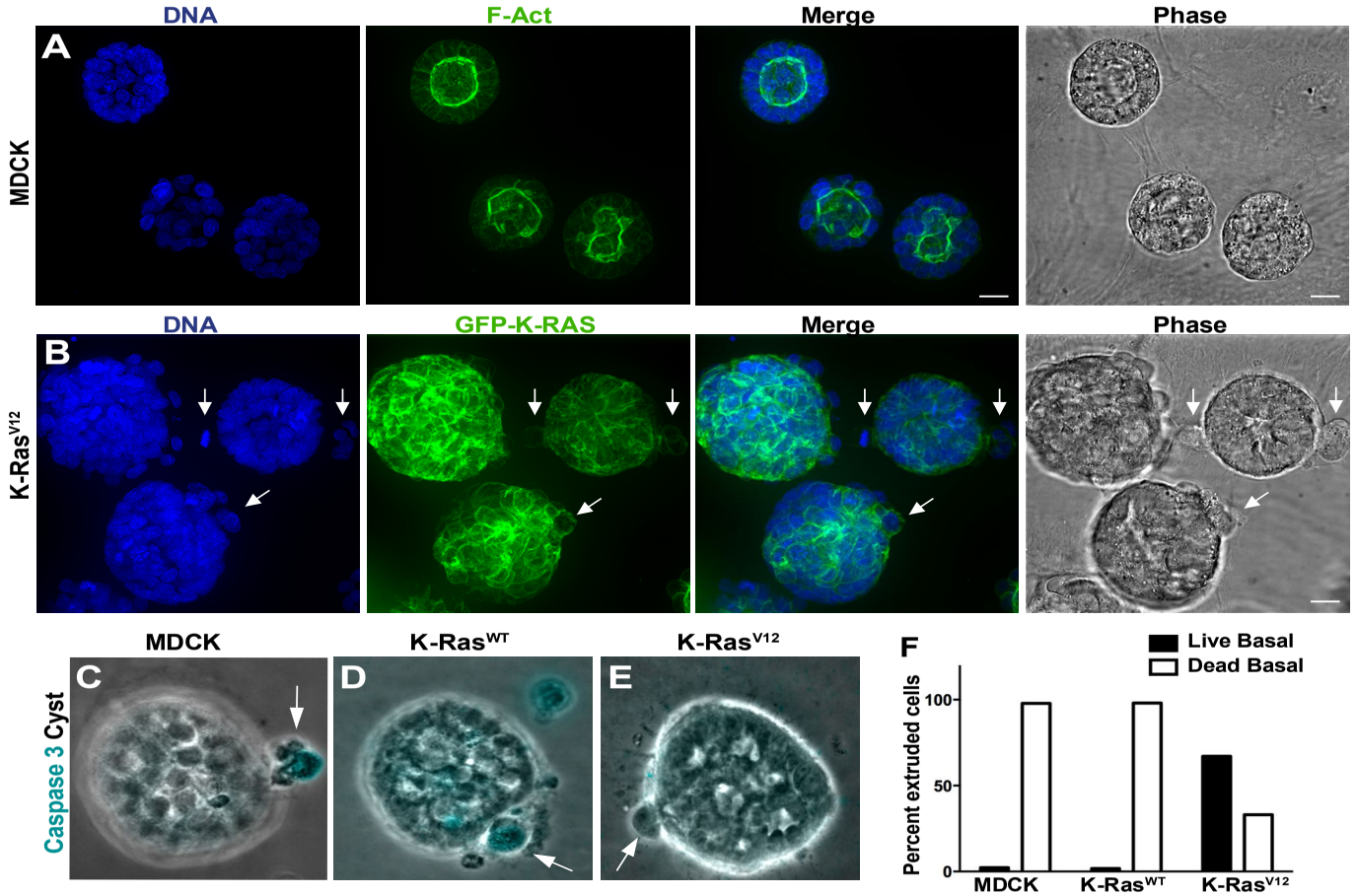

Figure S6. K-Ras^{V12} cells grown in 3-D form mini-cysts by extruding live cells basally. Confocal projections of cysts grown in matrigel for five days showing that wild type MDCK cysts have clear lumens **(A)** whereas MDCK K-Ras^{V12} cysts have filled lumens and attached small cysts (arrows)**(B)**. Approximately 2% of cells extruding basally from control MDCK **(C)** or K-Ras^{WT} **(D)** cysts are live, whereas ~67% of basally extruding cells from K-Ras^{V12} cysts are live **(E)**. The remaining extruding cells we scored as apoptotic by the presence of active caspase-3 immunostaining (turquoise), quantified in **(F)**. White arrows indicate extruding cell. n=188, 461, 217 cysts for C,D, and E respectively. Scale bar=20 μm. (Related to Figure 6).

Supplemental Experimental Procedures

Cell Culture

MDCKs cysts were generated by a single cell suspension of MDCK II cells resuspended in Growth Factor Reduced Matrigel (BD Biosciences) to a final concentration 4% and placed in 8 well coverglass chambers (Nalge Nunc) coated with a thin polymerized layer of Matrigel. For live imaging cells were placed on 24 well glass-bottom culture dishes (MatTeK Corporation). After 20 min incubation at 37°C, cell-growth medium was added on top. Cysts were allowed to grow for the indicated duration and analyzed by time-lapse imaging or fixed with 4% paraformaldehyde.

UV and Drug treatment

To prevent photobleaching over the long time periods require to catch a live basal extrusion in 3D, for fluorescent live imaging, we treated cyst with 1200 uJ/cm^2 UV^{254} using a Spectrolinker (Spectroline) for 43 seconds to induce apoptotic extrusion. For 2D cultures, MDCK II cells grown to confluence on glass coverslips were exposed to 1200 uJ/cm^2 UV^{254} for 43 seconds to induce apoptotic extrusion and incubated for 2 h before fixation.

Cells were treated with 10 μM JTE-013, 250nM of Torin-2 (Tocris Bioscience), 1 μM Wortmannin, 10 nM Bafilomycin A_1, and 30 μM Chloroquine (all from Sigma-Aldrich) or 1% DMSO as a control for 10 min before UV treatment.

RNA Interference

siRNAs against the canine ATG7 and ATG5 sequences were synthesized at the University of Utah Oligo and Peptide Synthesis Core to the following sequences: ATG7 #1 AGAGAAAGCUGAAUGAGUA and ATG7#2 (GACCAAAGGACAAAGAUAA). ATG5 #1 (5'-CAUUAGUGAGAUAUGGUUUGA-3') and ATG5 #2 (5'-AAACCAUAUCUCACUAAUGUC-3') annealed in 100 mM potassium acetate, 30 mM Hepes-KOH, 2 mM magnesium acetate, pH 7.4, for 1 min at 90°C and 37°C for 1 h. 30 pMol siRNAs were transfected by RNAimax reverse transfection according to the manufacturer's instructions (Invitrogen).

Cell staining

Cells grown in 2-D, were either fixed with ice-cold 100% methanol for 45 sec (for LC3AB staining) or 4% paraformaldehyde in phosphate-buffered saline (PBS) at 37°C for 20 min. Cells were then permeabilized with 0.5% Triton X-100 in PBS (PBS-T) for 5 min and blocked in AbDil (PBS with 0.1% Triton X-100 and 2% BSA) for 30 min. Primary antibodies: anti-active caspase-3 1:200 (BD Pharmingen), anti-S1P 50 μg/ml (LPath Inc.), anti-actin 1:200 clone AC-74, anti-tubulin 1:200 (all from Sigma-Aldrich), anti-LC3AB 1:100, anti-β-Catenin 1:100, anti-ZO-1 1:100 and anti LAMP1 1:200 (all from Cell Signaling) were applied in AbDil for 1 h or overnight (for 3-D cultures). After washing coverslips three times with PBS-T 0.1%, secondary antibodies Alexa Fluor-conjugated 1:200, Alexa Fluor–conjugated phalloidin 1:500 (all from Invitrogen), and DAPI 1 μg/ml (Sigma-Aldrich) to detect DNA were applied for 45 min. Following 3 washes with PBS-T 0.1%, coverslips were mounted onto slides with Prolong Gold mounting media (Invitrogen).

Image and video acquisition

Imaging (confocal and live) was performed in a Nikon Eclipse TE300 inverted microscope converted for spinning disc confocal microscopy (Andor Technologies) using

a 60X (for fixed samples) or 20X (for live imaging) Nikon Plan Apochromat lenses. Images were acquired with an electron-multiplied cooled charge-coupled device camera (DV887 1004X1002; Andor Technologies) driven by Andor IQ2 imaging software. For live imaging, temperature and CO_2 were controlled by a Live Cell module (Pathology Devices) connected to the microscope. NIS Elements software (Nikon) and Image J were also used to analyze intensity of fluorescent for LC3AB and to quantify cell numbers. For quantification of extrusion, extruding cells were manually scored based on the presence of an actin ring and the apoptotic body localization with respect to the neighboring cells. Apoptotic cells that came out of the plane of the monolayer with strong actin staining around and/or underneath the cells were defined as apical extruded cells. Apoptotic cells remaining in the monolayer and underneath an apical ring were considered basally extruded cells. Cell survival following basal extrusion from cysts was defined by its lack of staining with active caspase-3 antibody. All images were processed further using Photoshop and Illustrator (Adobe), and QuickTime Pro (Apple) software.

Immunoblot Analysis

Whole-cell extracts were prepared by resuspending cells in NP40 Cell Lysis Buffer (Invitrogen) plus protease inhibitor cocktail (Roche). Proteins were resolved by SDS-PAGE using NuPage gels (Invitrogen), and transferred to polyvinylidene difluoride membrane (Thermo). Membranes were probed with the following primary antibodies: anti-tubulin 1:1000 (Sigma- Aldrich), anti-LC3AB 1:1000, anti ATG5, and ATG7 1:1000 (All from Cell Signaling), anti-sphingosine-1-phosphate phosphatase-1 1:500, anti p62 (SQMT1) 1:500, anti Lamin B2 1:200 (All from Abcam), anti $S1P_2$ 1:500 (Imgenex), anti Sphingosine-1-phosphate Lyase-1 1:500 (Bioss), anti Sphingosine Kinase-1 1:1000 (Cayman Chemical), and identified using horseradish peroxidase conjugated secondary antibodies and enhanced chemiluminescense. Blots were quantified using Photoshop (Adobe).

CHAPTER 4

DEFECTIVE APICAL EXTRUSION SIGNALING CONTRIBUTES TO AGGRESIVE TUMOR HALLMARKS

Reprinted with permission from eLife. Gu Y, Shea J, Slattum G, Firpo MA, Alexander M, Mulvihill SJ, Golubovskaya VM, and Rosenblatt J. (2015). Defective apical extrusion signaling contributes to aggressive tumor hallmarks. eLife Jan 26;4:e04069.

Chapter 4 is a published article. Here, I contributed with data on Rac inhibitor, made S1P2 morphant fish and filmed them. Revised manuscript, acquisition of data, analysis and interpretation of data, drafting and revising the article.

eLIFE elifesciences.org

RESEARCH ARTICLE

Defective apical extrusion signaling contributes to aggressive tumor hallmarks

Yapeng Gu[1]*, Jill Shea[2], Gloria Slattum[1], Matthew A Firpo[2], Margaret Alexander[1], Sean J Mulvihill[2], Vita M Golubovskaya[3], Jody Rosenblatt[1]*

[1]Huntsman Cancer Institute, University of Utah, Salt Lake City, United States; [2]Department of Surgery, University of Utah, Salt Lake City, United States; [3]Department of Surgical Oncology, Roswell Park Cancer Institute, Buffalo, United States

Abstract When epithelia become too crowded, some cells are extruded that later die. To extrude, a cell produces the lipid, Sphingosine 1-Phosphate (S1P), which activates $S1P_2$ receptors in neighboring cells that seamlessly squeeze the cell out of the epithelium. Here, we find that extrusion defects can contribute to carcinogenesis and tumor progression. Tumors or epithelia lacking $S1P_2$ cannot extrude cells apically and instead form apoptotic-resistant masses, possess poor barrier function, and shift extrusion basally beneath the epithelium, providing a potential mechanism for cell invasion. Exogenous $S1P_2$ expression is sufficient to rescue apical extrusion, cell death, and reduce orthotopic pancreatic tumors and their metastases. Focal Adhesion Kinase (FAK) inhibitor can bypass extrusion defects and could, therefore, target pancreatic, lung, and colon tumors that lack $S1P_2$ without affecting wild-type tissue.
DOI: 10.7554/eLife.04069.001

***For correspondence:** yapeng.gu@hci.utah.edu (YG); jody.rosenblatt@hci.utah.edu (JR)

Competing interests: The authors declare that no competing interests exist.

Funding: See page 15

Received: 17 July 2014
Accepted: 22 January 2015
Published: 26 January 2015

Reviewing editor: Ewa Paluch, University College London, United Kingdom

Introduction

Epithelial cells must act collectively to provide a protective barrier for the organs they encase even though they continuously turn over through cell death and division. The link between cell division and death is critical: if the relative death rate is too high, barrier function diseases may result whereas if division outpaces cell death, epithelia could become neoplastic. We previously identified a process critical for promoting cell death when cells within epithelia become overcrowded termed epithelial extrusion (***Rosenblatt et al., 2001***; ***Eisenhoffer et al., 2012***). The stretch-activated channel Piezo-1 senses cell crowding and enables some cells to produce the bioactive sphingolipid, Sphingosine 1-phosphate (S1P), which binds G-protein coupled receptors ($S1P_2$) in neighboring cells to activate Rho-mediated assembly and contraction of an intercellular actomyosin ring (***Gu et al., 2011***). This contraction squeezes live cells apically out of the epithelial sheet while simultaneously closing the gap that might have resulted from the cell's exit, thus preserving epithelial barrier function. Because live extruded cells become stripped from the underlying matrix and its associated survival signaling, they later die by anoikis (***Frisch and Francis, 1994***).

Advanced tumors typically have increased survival signaling that overrides anoikis, suggesting that cells could survive following extrusion. In this case, the direction a cell extrudes can impact its later fate. Typically, epithelia extrude cells apically into the lumen of the tissue (***Slattum et al., 2009***), which would act to essentially eliminate tumor cells with upregulated survival signaling. However, some cells are extruded basally into the tissue encased by the epithelium (***Slattum et al., 2009***). If basally extruded cells survive following extrusion, they might be able to invade into the underlying tissue (***Slattum and Rosenblatt, 2014***). Interestingly, we have found that oncogenic mutations in either adenomatous polyposis coli or K-Ras misregulate apical extrusion and drive extrusion basally (***Marshall et al., 2011***; ***Slattum et al., 2014***).

eLife digest Epithelial cells cover the surface of our bodies, line our lungs, stomach and intestines and serve as a protective layer around other organs. If too many epithelial cells die and are not replaced, this protective layer may erode and lead to organ damage. However, if too many new cells grow, tumors can form.

One process that helps to maintain the right number of epithelial cells is called extrusion. When too many epithelial cells are present, the resulting overcrowding triggers this process to squeeze excess cells out of the layer and away from the organ. Usually, these cells quickly die. However, if the pathway that regulates this process—which involves a receptor protein called $S1P_2$—is disturbed, the cells may instead be pushed into the space between the epithelial layer and the organ. When this happens, the cells are more likely to survive and may then form a tumor that invades the organ.

Gu et al. interfered with extrusion by reducing the levels of the $S1P_2$ receptor in layers of human epithelial cells grown in the laboratory. Fewer epithelial cells were squeezed out of these cell layers, making the layers up to three times as thick in places. Moreover, mutant zebrafish lacking the $S1P_2$ receptor also accumulated epithelial masses throughout their bodies.

Gu et al. found that disrupting the extrusion process made the cells resistant to chemotherapy, and that certain hard-to-treat human pancreatic, lung, and colon cancers had lower levels of the $S1P_2$ receptors. Boosting the activity of $S1P_2$ receptors helped to restore normal extrusion and reduced the size of pancreatic tumors in mice.

Gu et al. then focused on an enzyme called Focal Adhesion Kinase that helps cells to survive. Treating zebrafish with a drug to block the activity of this enzyme left normal fish unharmed. However, in mutant fish with malfunctioning extrusion pathways, the drug rescued the number of cells that died, reduced the size and number of masses, and cured their leaky skin barrier. If further studies confirm the results, the drug may offer a new, less toxic, treatment for certain cancers that do not respond to currently available treatments.

DOI: 10.7554/eLife.04069.002

Here, we examined the long-term effects of disrupting the S1P-$S1P_2$ epithelia extrusion-signaling pathway. We found that inhibition of $S1P_2$ leads to large epithelial masses in both zebrafish epidermis and cultured epithelia and increased rates of basal extrusion. Moreover, disrupting extrusion by a variety of methods leads to chemotherapy resistance. Inhibition of Focal Adhesion Kinase (FAK), a key survival signal generated from cell-matrix adhesion, selectively promotes apoptosis in cells where extrusion is defective and eliminates epidermal cell masses formed in zebrafish $S1P_2$ mutants without affecting epithelial morphology and function. Pancreatic Ductal Adenocarcinomas (PDACs) have little to no $S1P_2$, which could explain why these tumors are typically more invasive and chemo-resistant. HPAF II human pancreatic cancer cells cannot extrude apically and instead extrude basally, survive, and proliferate following extrusion. Ectopically expressing $S1P_2$ in HPAF II cells rescues apical extrusion and apoptosis and reduces orthotopic mouse tumors and their metastases. Together, our results suggest that defective extrusion may be a new mechanism for how PDACs and other carcinomas lacking $S1P_2$ initiate and invade. Furthermore, FAK inhibitors, which are currently in clinical trials for other tumors, may provide an effective therapeutic opportunity to treat pancreatic cancer without destroying nearby normal tissue.

Results

Disruption of extrusion signaling reduces epithelial apoptosis rates

To test if the S1P-$S1P_2$-Rho signaling pathway that controls extrusion (***Gu et al., 2011***) was critical for preventing neoplastic growth over time, we knocked down $S1P_2$ in Human Bronchial Epithelial (HBE) cells (***Figure 1A***) and grew them for up to 3 weeks after they formed an intact monolayer. $S1P_2$-depleted HBE epithelia, which are extrusion-deficient (***Gu et al., 2011***), accumulated into masses over three layers thick whereas control-knockdown monolayers retained a single layer (***Figure 1B***). Because cell extrusion typically promotes epithelial cell death (***Eisenhoffer et al., 2012***; ***Marinari et al., 2012***) and because $S1P_2$ depletion did not affect the proliferation rate in a yellow tetrazolium MTT (3-(4, 5-dimethylthiazolyl-2)-2, 5-diphenyltetrazolium bromide) assay (***Figure 1C***), masses were likely to

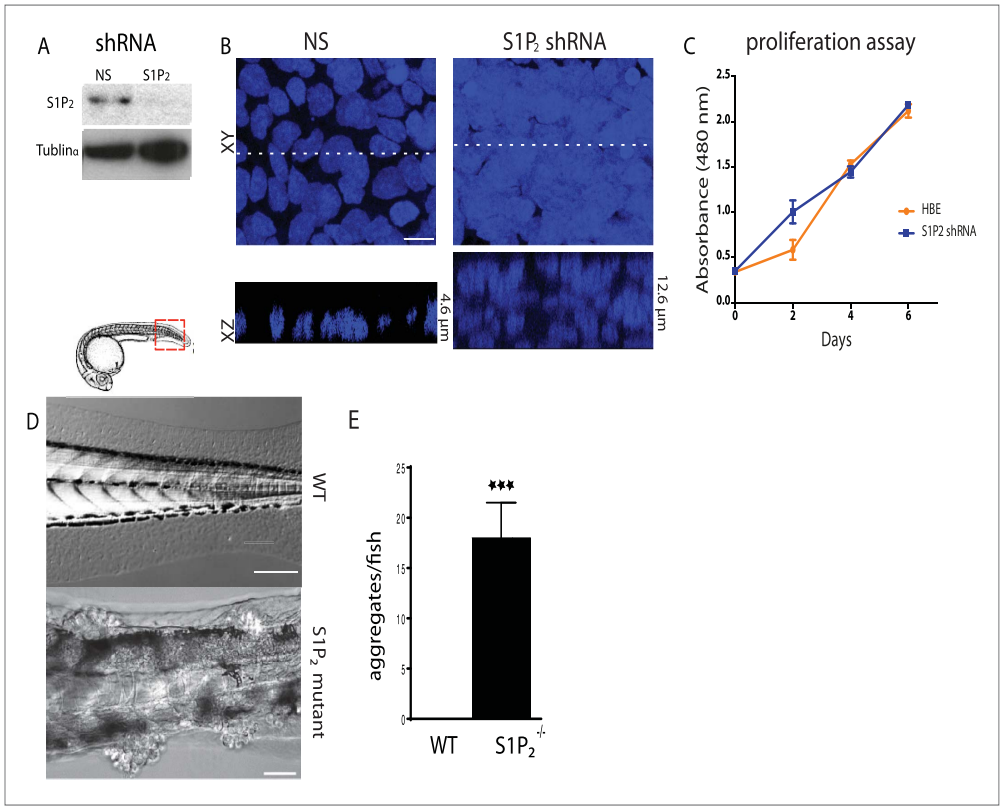

Figure 1. Loss of $S1P_2$ and extrusion leads to accumulation of epithelial cell masses. (**A**) $S1P_2$ immunoblot of HBE cells expressing control (left) or $S1P_2$-specific shRNA (right) with α-tubulin as loading control. (**B**) Representative images of HBE cells (DNA only) expressing control (left) or $S1P_2$-specific shRNA (right) grown for 3 weeks. Scale bar, 10 µm. (**C**) Proliferation assay indicates that $S1P_2$-knockdown cells proliferate at the same rate as wild type controls cells. (**D**) Representative DIC micrographs of 5-dpf WT (top) and Mil ($S1P_2$ mutant) (bottom) zebrafish larvae, where cartoon shows region where fish was imaged. Scale bars, 100 µm where red box indicates region imaged. (**E**) Quantification of epidermal clumps of 22 zebrafish larvae.
DOI: 10.7554/eLife.04069.003

arise due to reduced apoptosis. Additionally, zebrafish larvae carrying a loss-of-function mutation in $S1P_2$ (Miles apart [*Mil*]) cannot extrude apoptotic epidermal cells (***Gu et al., 2011***), and similarly accumulated numerous epidermal cell aggregates throughout the body (18 ± 3.5 aggregates/fish, n = 22) by only 5 days post fertilization (dpf) (***Figure 1D,E***). By contrast, masses were undetectable in heterozygote *Mil* or WT siblings of the same age (***Figure 1D,E***).

We next wondered if extrusion-deficient cells were also more resistant to cell death in response to apoptotic stimuli. While extrusion promotes apoptosis during normal homeostasis by extruding live cells that later die from loss of contact to matrix-derived survival signaling (***Eisenhoffer et al., 2012***), treating epithelia with apoptotic stimuli causes cells to simultaneously die and extrude (***Rosenblatt et al., 2001***; ***Andrade and Rosenblatt, 2011***). Because extrusion normally drives cell death, could it also help promote apoptosis in response to apoptotic stimuli by eliminating competing survival signaling associated with the underlying matrix? We find that disrupting extrusion signaling also disrupted apoptosis in response to a variety of apoptotic stimuli. HBE monolayers lacking $S1P_2$ (***Figure 2A***) or treated with a selective $S1P_2$ receptor antagonist, JTE-013 (***Figure 2B***) had greatly reduced rates of apoptosis in response to a strong apoptotic stimulus, UV-C, compared to controls. Madin–Darby Canine Kidney (MDCK) monolayers treated with $S1P_2$ antagonist were similarly resistant to several common chemotherapy drugs that cause apoptosis (***Figure 2B,C***).

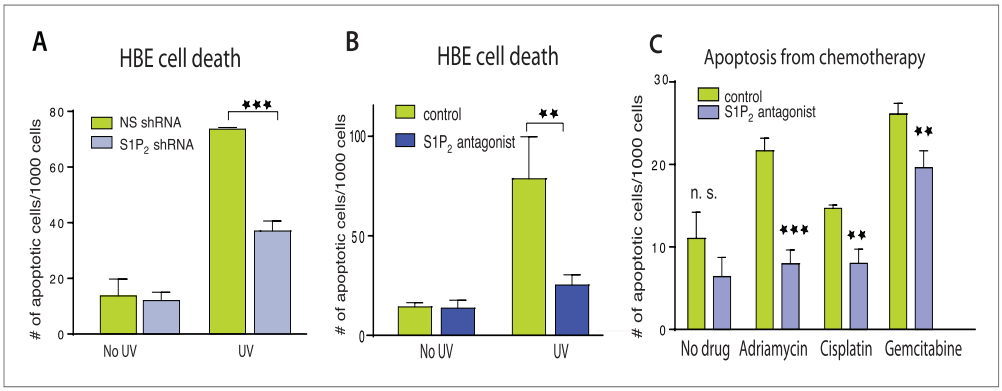

Figure 2. Disruption of $S1P_2$-extrusion signaling reduces apoptotic response. (**A**) Quantification of UV-induced apoptotic cells in HBE monolayers expressing control or $S1P_2$-specific shRNA. (**B**) Quantification of UV-induced apoptosis of HBE monolayers in the presence or absence of the $S1P_2$ antagonist JTE-013. (**C**) Quantification of indicated chemotherapy-induced apoptotic MDCK cells in the presence or absence of JTE-013, where all error bars are STD (**p < 0.01, and ***p < 0.001).

DOI: 10.7554/eLife.04069.004

The reduced cell death rates in epithelia lacking $S1P_2$ were due to disruption of extrusion rather than altered S1P signaling, since other inhibitors of extrusion, Rho kinase inhibitor (Y-27632), myosin II inhibitor (Blebbistatin), or Rac inhibitor (EHT1864) all decreased cell death rates to the extent that they inhibit extrusion (***Figure 3A***). In each case, the ratio of cell death to extrusion inhibition is ~1:1 (***Figure 3C***). Inhibition of apoptosis was not due to increasing levels of S1P, which can act as a pro-survival signal, as S1P levels in apoptotic cells varied independently of extrusion inhibition (***Figure 3B***). Since freshly plated single MDCK cells are resistant to apoptotic stimuli, we tested if these same compounds reduced apoptosis in similarly aged single MDCKs by treating with EGTA to disrupt cadherin-dependent cell–cell contacts. Inhibitors that blocked apoptosis by blocking extrusion in an intact monolayer do not impact the apoptosis rates of single cells that are incapable of extrusion (***Figure 3D***). Similarly, UV-induced apoptosis was unaltered in single HBE cells lacking $S1P_2$ when HBE monolayers where treated with EGTA (***Figure 3D***). Additionally, inhibiting $S1P_2$ with JTE-013 in a cell line that cannot extrude but expresses this receptor (***Clair et al., 2003***; ***Pham et al., 2013***), NIH 3T3 fibroblasts, does not affect the cell death rate in response to UV-C (***Figure 3E***). These data together suggest that increased cell survival is linked with the inability to extrude rather than to any intrinsic block of the apoptosis pathway.

Pancreatic cancer cells lack the $S1P_2$ receptor and extrude basally rather than apically

Since disruption of $S1P_2$ in epithelia results in reduced apoptosis and cellular masses both in vitro and in vivo, we wondered if this receptor might be deficient in carcinomas. Our analysis of published tumor microarray data found $S1P_2$ mRNA to be significantly reduced in PDAC (***Buchholz et al., 2005***; ***Segara et al., 2005***; ***Badea et al., 2008***), and some lung and colon tumors (***Bhattacharjee et al., 2001***), compared to their corresponding normal tissues. To investigate if cancer cells lacking $S1P_2$ also have extrusion and apoptosis defects, we analyzed a pancreatic adenocarcinoma cell line, HPAF II, that has reduced $S1P_2$ levels (***Figure 4A***) and forms epithelial monolayers necessary for assaying extrusion. We used MDCK and HBE cells as controls, which are well characterized in several extrusion studies (***Rosenblatt et al., 2001***; ***Slattum et al., 2009***; ***Gu et al., 2011***), as the only immortalized normal pancreatic cells, HPDEs, cannot form a confluent monolayer (data not shown).

Our experiments show that the reduced $S1P_2$ levels in HPAF II cells disrupted apical extrusion, leading to reduced apoptosis rates and enhanced basal extrusion. Similar to HBE monolayers lacking $S1P_2$, HPAF II cells formed masses within a week of culture and displayed extrusion defects and reduced rates of UV-C-induce apoptosis (***Figure 4A–D***). While ~50% of cells did not extrude, most of the remaining cells extruded in the opposite direction—basally, underneath the layer (***Figure 4D,E***) at

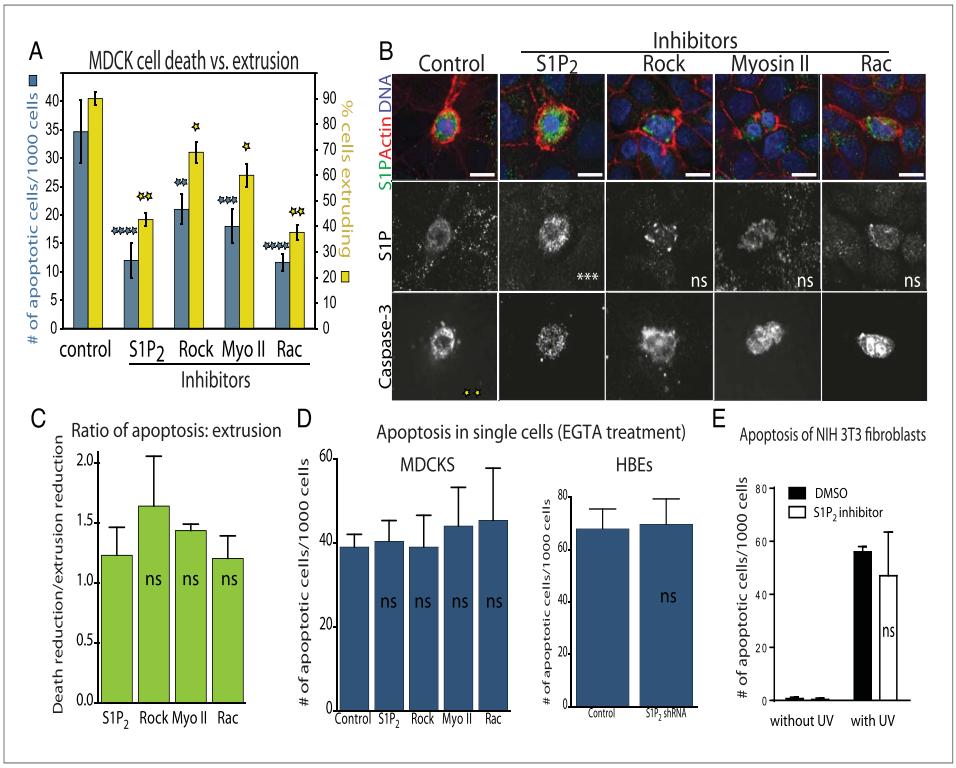

Figure 3. Decreased apoptosis is due to blocked extrusion rather than S1P signaling. (**A**) Rates of MDCK cell death (left Y-axis, blue) correspond with cell extrusion rates (right Y-axis, yellow) in response to UV-C when treated with extrusion inhibitors. (**B**) Representative images of apoptotic cells with and without compounds that block extrusion. When extrusion occurs, the dying cell DNA lies above (out of plane from) the neighboring cells with a contracted actin ring but when it fails, it lies in the same plane as surrounding cells with an uncontracted actin ring. Only the $S1P_2$ antagonist JTE013 causes significant S1P accumulation in the dying cell (second column), whereas blocking extrusion with the other compounds does not impact S1P levels, where p values of each drug treatment compared to control are listed on each S1P panel as asterisks (n = 4). Bar = 10 μm. (**C**) Ratio of reduction of extrusion to reduction of apoptosis shows nearly a 1:1 correlation throughout, where p-values compared to $S1P_2$ are not significant. (**D**) Compounds used to block extrusion do not affect apoptosis rates in single MDCK cells treated with EGTA in response to UV. (**E**) Quantification of UV-induced apoptotic NIH 3T3 cells in the presence of vehicle or JTE-013; All results are expressed as mean values ± STD of three separate experiments (*p < 0.01, **p < 0.005, ***p < 0.005, and ****p < 0.0001), and NS in graphs **B**, **D**, and **E** indicate that p values of a unpaired T-test are not significant.

DOI: 10.7554/eLife.04069.005

rates similar to when MDCK monolayers are treated with $S1P_2$ antagonist (***Slattum et al., 2014***). Basal extrusion of cells with upregulated survival signaling could potentially enable their invasion beneath the epithelium (***Slattum and Rosenblatt, 2014***). To investigate if basally extruded cells can survive following extrusion (***Slattum and Rosenblatt, 2014***), we analyzed extrusion from three-dimensional cysts, where the fate of basally extruded cells can be followed outside the cyst, rather than beneath a monolayer. MDCKs were used as controls, which, like HPAF II cells, form cysts with hollow apical lumens of 34 μm ± 5 μm in diameter when grown in Matrigel (***Figure 5B***). Approximately 30% of HPAF II cysts extrude cells basally that survive, compared to only ~3% of MDCK cysts (***Figure 5C,D***). Live imaging confirmed that 28.6% of basally extruded cells remained alive throughout a 12-hr video, whereas those from MDCK cysts died during this time (***Video 1***, n = 5 videos of each). Importantly, $S1P_2$-GFP expression is sufficient to rescue apical extrusion (***Figure 5C***), decrease the frequency of live cells that basally extrude (***Figure 5D***), and increase the percentage of cysts with dead cells in their lumens (***Figure 5E***). These data suggest that the S1P-$S1P_2$ signaling required for extrusion is critical not only for promoting cell death but also for preventing basal extrusion, which could enable cells to invade.

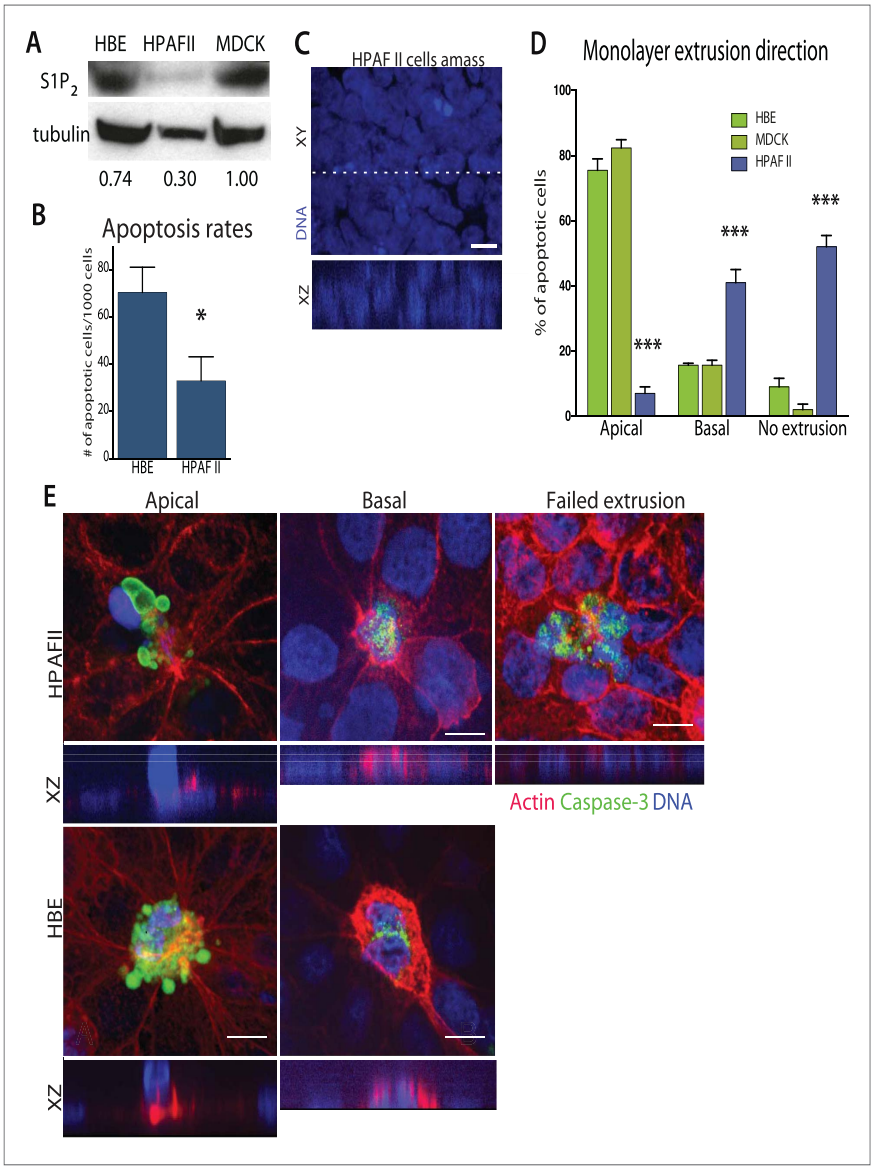

Figure 4. Pancreatic cancer cell line HPAF II accumulates into masses and extrudes basally. (**A**) $S1P_2$ immunoblot of HBE (left), HPAF II (middle), and MDCK (left) cells with α-tubulin as loading control. (**B**) Cell death rates in response to UV-C. (**C**) Quantification of cell extrusion events from three independent experiments; n = 300 apoptotic cells per cell line, error bars are STD where *<0.01 and ***<0.0001. (**D**) Representative confocal projection and XZ cross-section (from region in dashed line above) of HPAF II cells that grew into masses rather than monolayers. (**E**) Representative confocal projections of HPAF II (upper panel) and HBE (lower panel) cells undergoing apical (left) or basal (middle) extrusion, with XZ sections below. Basal extrusion was scored when an actin ring contracted above the dying cell (marked by DNA and caspase-3 staining) and the DNA of the dying cell lies in the same plane as the neighboring cells. Scale bars, 10 μm.

DOI: 10.7554/eLife.04069.006

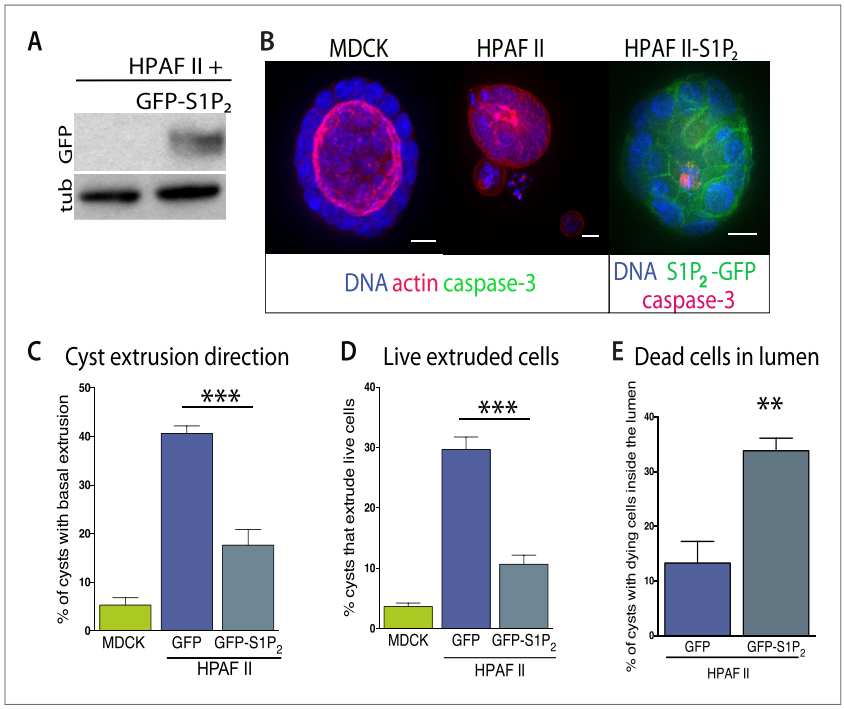

Figure 5. Exogenous expression of $S1P_2$ rescues apical extrusion and cell death. (**A**) GFP immunoblot of HPAF II cells expressing $S1P_2$ GFP. (**B**) Representative confocal projections of MDCK, HPAF II, and HPAF II-$S1P_2$ cysts, where scale bar = 10 μm. (**C**) Percentages of MDCK, HPAF II GFP, and HPAF II $S1P_2$ cysts with basal extrusion; n = 300 cysts per cell line. (**D**) Quantification of MDCK, HPAF II GFP, and HPAF II $S1P_2$ cysts extruding live cells basally; n = 300 cysts per cell line. (**E**) Frequency of HPAF II GFP and HPAF II $S1P_2$ cysts with dying cells inside the lumen; n = 300 cysts per cell line. All results are expressed as mean values ± STD of three separate experiments (**p < 0.01, and ***p < 0.001).

DOI: 10.7554/eLife.04069.007

Inhibiting FAK rescues cell death rates in epithelia defective in extrusion

Because extrusion promotes cell death in response to apoptotic stimuli (***Rosenblatt et al., 2001***; ***Andrade and Rosenblatt, 2011***) and during normal homeostasis (***Eisenhoffer et al., 2012***; ***Marinari et al., 2012***), we hypothesized that it does so by eliminating the competing survival signaling associated with cell-matrix attachment. If so, increased cell survival when extrusion is blocked would derive from prolonged cell attachment to the underlying matrix. Since Focal Adhesion Kinase (FAK) is critical for matrix-dependent survival (***Frisch et al., 1996***), we investigated if FAK were increased in cells targeted for death when extrusion was blocked. Surprisingly, we found that control MDCK cells in early stages of extrusion have far higher levels of active FAK, by immunostaining with a phospho-FAK antibody, than surrounding live cells but that these levels decrease during later stages of extrusion (***Figure 6A***). This increase in pro-survival phospho-FAK in cells targeted to die mimics the increased levels of S1P, another pro-survival signal, in cells triggered to extrude and die that also decrease once cells extrude (***Figure 3C*** and [***Gu et al., 2011***]). However, late-staged apoptotic cells (detected by piknotic DNA) still have high levels of active FAK when extrusion is blocked with $S1P_2$ antagonist (***Figure 6A***). This paradoxical survival signaling increase in cells targeted to die may reflect cell-intrinsic compensatory signals to apoptotic signaling that eventually decrease as cells commit to apoptosis. The fact that these survival signals stay high when cell extrusion is blocked suggests that this increased survival signaling derives from inability to detach from matrix.

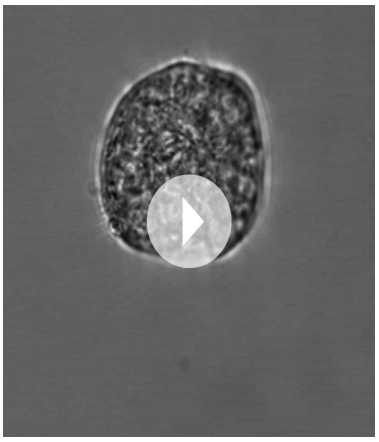

Video 1. An HPAF II cyst growing without apoptotic stimuli extrudes live cells basally. Note that some cells extrude and die while others survive and/or migrate away.
DOI: 10.7554/eLife.04069.008

Because FAK activity remains high in cells where extrusion is blocked, we wondered if chemically blocking FAK activation would rescue the apoptosis rates of monolayers lacking functional $S1P_2$ signaling. The specific FAK inhibitor PF 573228 had no effect on untreated or UV-treated wild type monolayers (***Figure 6B*** and [***Slack-Davis et al., 2007***]), likely because cells not targeted to extrude have quite low levels of active FAK (***Figure 6A***). However, this same FAK inhibitor rescued the cell death rates of monolayers where extrusion is blocked with $S1P_2$ antagonist JTE013 or Rac inhibitor to those seen in wild type monolayers (***Figure 6B***). FAK inhibitor dramatically decreased phospho-FAK staining in cells where JTE013 blocks extrusion (***Figure 6A***). Over-expression of a dominant negative FAK isoform (FRNK) (***Park et al., 2004***) acted similarly to FAK inhibitor (***Figure 6C***). Importantly, FAK inhibitor alone induced apoptosis of HPAF II cells in monolayers (***Figure 6D***) and even those basally extruding from HPAF II cysts (***Figure 6E,F***). Additionally, treatment with FAK inhibitor to cysts that had already accumulated live basally extruded cells was sufficient to nearly double apoptosis rates of basally extruded cells (from 15 ± 2% to 28 ± 3%) when added for only 2 hr.

FAK inhibitor eliminates $S1P_2$ mutant zebrafish embryo epidermal masses and improves epidermal barrier function

Because inhibition of FAK appears to promote cell death of only extrusion-defective epithelial cells without affecting normal epithelia, we wondered if FAK inhibition could eliminate the epidermal masses of Mil zebrafish embryos as they formed without adversely impacting the animal. While FAK inhibitor had no visible effect on wild-type zebrafish at 5 dpf, it greatly decreased the number and size of epidermal cell masses in $S1P_2$-mutant embryos of the same age (***Figure 7A–C***). While FAK inhibitor treatment sloughed off many of the epidermal cells, which could be found at the bottom of the dish, it also increased the apoptosis rate within the masses (***Figure 7D***). To test if FAK inhibitor could eliminate epidermal masses *after* they form, we needed to inducibly knockdown $S1P_2$ later in development, since Mil zebrafish mutants die due to heart defects around the time cell masses form (~5 dpf; [***Kupperman et al., 2000***]). To do so, we used we photo-activated $S1P_2$ morpholino at 24 hpf (see [***Eisenhoffer et al., 2012***] for characterization of this method) to knockdown $S1P_2$ after heart development occurred. $S1P_2$ morphants had 0.18-fold lower $S1P_2$ protein levels (***Figure 7E***) and phenocopied the epidermal masses seen in Mil mutants (***Figure 7F***). Addition of FAK inhibitor to an $S1P_2$ morphant at 5 dpf with epidermal masses caused the masses to slough off within 19 hr (***Figure 7F***, where n = 6 videos total). Remarkably, we found that while *Mil* embryos had poor epidermal barrier function, as assayed by Texas Red-Dextran^{MW70} permeability, epidermal permeability was significantly reduced with FAK inhibitor (***Figure 7A***). These results suggest that FAK inhibitor alone may selectively target masses resulting from cells defective in extrusion and improve overall epithelial integrity without affecting the normal surrounding tissue.

Expression of $S1P_2$ is sufficient to reduce orthotopic pancreatic tumors and their metastases

We have shown that disrupting S1P/$S1P_2$ signaling inhibits epithelial cell death, causes masses, and promotes a potential mechanism for invasion—basal extrusion, which together could promote tumor formation and progression. Yet, it was not clear if this signaling pathway plays a role in malignancy. To test the role of $S1P_2$ in tumorigenesis, we orthotopically transplanted HPAF II tumor cells expressing either GFP or $S1P_2$-GFP into nude mice and found that $S1P_2$ expression was sufficient to markedly reduce both tumor size and metastatic frequency (***Figure 8A,B***).

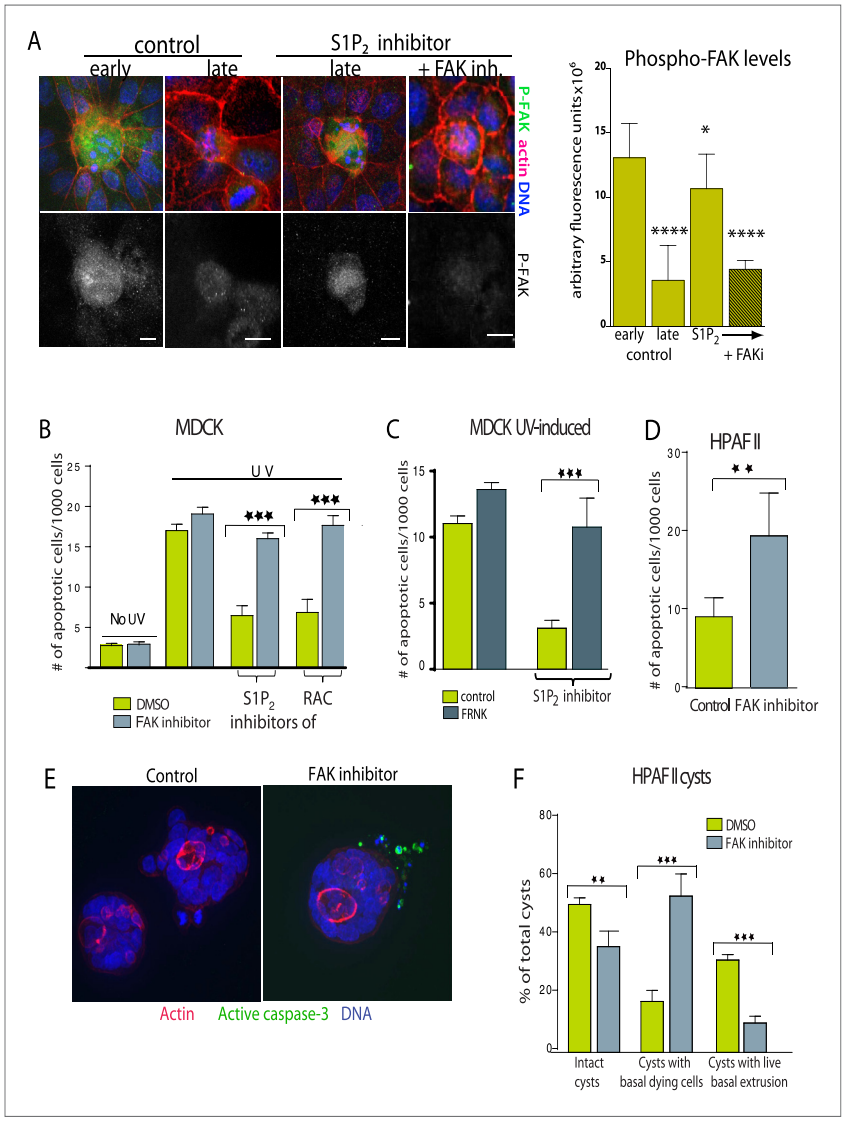

Figure 6. Inhibition of FAK activity specifically increases cell death in epithelial cells lacking $S1P_2$. (**A**) Immunostaining of active phospho-FAK in early and late control extrusions and in a JTE-013 ($S1P_2$ antagonist)-inhibited extrusion with late apoptotic cell or one with the FAK inhibitor PF573228, with averaged arbitrary fluorescence units and their p-values compared to early extruding cells in graph on right (n = 10 measurements each over three separate experiments). (**B**) Quantification of UV-induced MDCK apoptosis in the presence of control, JTE-013, or EHT1864 with or without treatment of the FAK inhibitor PF573228, where n = 3000. (**C**) Quantification of UV-induced apoptosis of MDCK cells and those expressing FRNK, where n = 3000. (**D**) Quantification of PF573228-induced apoptosis of HPAF II cells, where n = 3000. (**E**) Representative confocal projections of HPAF II cysts treated with control or PF573228. Scale bars = 10 μm. (**F**) Frequencies of HPAF II cysts with dying cells, live extruding cells, or neither, where n = 300. All quantification results are expressed as mean values ± STD of three separate experiments (*$p < 0.05$, **$p < 0.01$, ***$p < 0.001$, and ****$p < 0.0001$).

DOI: 10.7554/eLife.04069.009

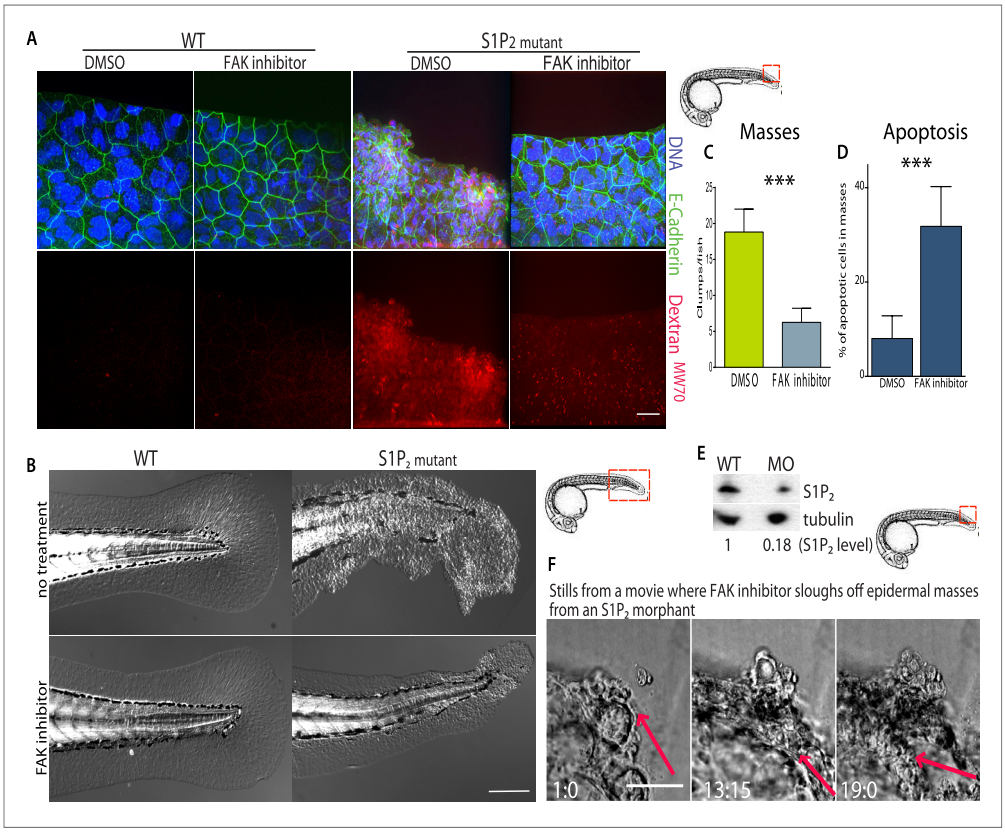

Figure 7. FAK inhibitors eliminate epidermal cell masses in $S1P_2$ zebrafish mutants and improve epidermal barrier function without affecting wild type zebrafish. (**A**) Representative confocal projections of 5-dpf WT (left) and *Mil* ($S1P_2$ mutant) (right) zebrafish larvae treated with DMSO or FAK inhibitor PF573228, where high Texas-Red Dextran indicates poor permeability in *Mil* but is greatly reduced when barrier function is improved with FAK inhibitor treatment. Scale bar = 10 μm and red box indicates region of fish imaged. (**B**) 5 dpf *Mil* and wild type zebrafish treated with and without FAK inhibitor. Note that while FAK inhibitor-treated *Mil* have other developmental defects (heart and circulation), there are no obvious clumps as seen in the untreated fish. Scale bar = 100 μm and red box indicates region of fish imaged. Note FAK inhibitor does not affect WT zebrafish. (**C**) Quantification of epidermal masses in 5 dpf *Mil* zebrafish larvae with and without PF573228. (**D**) Quantification of apoptotic cells within epidermal masses with and without PF573228. For both, error bars are SD and p values are ***<0.0001. (**E**) Immunoblot showing knockdown of $S1P_2$ by photo-activatable morpholinos. (**F**) Stills from a video where PF573228 was added to $S1P_2$ morphant at 5 dpf, where red arrows show the edge of the epidermis over time, scale bar = 50 μm and red box indicates region of fish imaged. Time is hours:minutes following FAK inhibitor addition. Note: epidermal cells that are sloughed off become embedded in the agarose where fish is mounted.

DOI: 10.7554/eLife.04069.010

Human pancreatic ductal carcinomas lack $S1P_2$ receptor

Further, we found that human pancreatic carcinomas have strikingly down-regulated $S1P_2$ protein levels. Because tumors typically have different stromal to epithelial ratios compared to uninvolved pancreatic tissue that can confound microarray data, we immunostained fixed tissue slices for both $S1P_2$ and cytokeratin to highlight epithelial cells so that we could compare $S1P_2$ protein levels in the epithelia alone (***Figure 9A***). We found that $S1P_2$ was significantly lower in pancreatic cancer (PDAC) cells compared to epithelial acini from uninvolved neck margins, from which PDACs may arise, or to pancreatic intraepithelial neoplasia (PanIN) precursor lesions (***Figure 9A–C***). Importantly, lower $S1P_2$ expression correlates with later tumor stages in both averaged (***Figure 9B***) and five patient-matched samples (***Figure 9C***). Loss of $S1P_2$ expression in pancreatic cancers suggests that defective extrusion may contribute to human PDAC development.

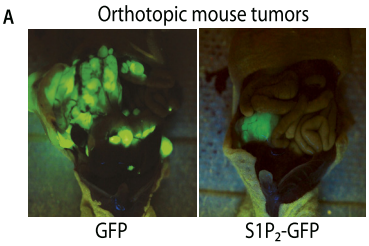

B

HPAF II tumors	GFP	GFP-$S1P_2$
Tumor weight (g)	2.35 ±0.95	1.14 ±0.33
# of metastases	4/9	1/10

Figure 8. Exogenous $S1P_2$ expression reduces orthotopic pancreatic tumors and rates of metastasis in mice. (**A**) Representative images of HPAF II GFP and HPAF II $S1P_2$ orthotopic xenograft tumors in nude mice. (**B**) Summary of tumor weights and metastatic frequency.

DOI: 10.7554/eLife.04069.011

Discussion

Our work presents a new paradigm for how an aggressive class of carcinomas may form and progress: failed extrusion (***Figure 10***). Normal epithelial cells produce S1P to trigger their extrusion and death once they become too crowded, simultaneously maintaining correct cell density and barrier function. Epithelia with defective S1P/$S1P_2$ signaling cannot extrude apically. Extrusion-defective epithelia retain cells, which can result in resistance to homeostatic and chemotherapy-induced cell death and neoplastic masses. Further, a small number of cells also die without getting extruded, which can disrupt barrier function. Aside from allowing access of inappropriate signals, poor epithelia barrier function could cause chronic inflammation—an important factor for tumor progression (***Coussens and Werb, 2002***). Additionally, defective apical extrusion signaling shifts extrusion basally, which could allow transformed cells to invade the underlying tissue (***Slattum and Rosenblatt, 2014***).

Basal extrusion may be a common hallmark of invasive tumor types. We have recently discovered that oncogenic $KRas^{V12}$ expression degrades S1P through autophagy and causes cell masses and basal extrusion, similar to the extrusion defects observed when $S1P_2$ is absent (***Slattum et al., 2014***). $KRas^{V12}$ is an important driver for the same cancers that lack $S1P_2$—pancreatic, lung, and colon carcinomas—and its expression alone reduces $S1P_2$ (***Slattum et al., 2014***), which may explain why PanIN precursors have reduced $S1P_2$ expression. Further, we have found that another oncogenic mutation, truncation of the adenomatous polyposis coli gene, also results in increased basal extrusion. While it is not clear what mechanisms drive tumor cell invasion, our work showing that exogenous expression of $S1P_2$ can dramatically reduce basal extrusion rates and orthotopic tumor metastasis rates in tumor cells that lack this receptor suggests that $S1P_2$-mediated extrusion may play an important role in metastatic cell invasion.

Because cancer cells lacking $S1P_2$ have increased survival signaling due to an inability to detach from the matrix and its associated survival signaling through increased active FAK, we found that FAK inhibitor on its own could rescue cell death rates to those seen in wild type cells (***Figure 7D***). Surprisingly, FAK inhibitor could also reverse other extrusion defects, such as poor barrier function and survival of basally extruded cells, factors that together could contribute to tumor progression. The fact that adding FAK inhibitor can rescue these defects when added after they form further supports the notion that anoikis results from extrusion and also suggests that FAK inhibitors may be particularly good at treating pancreatic and other carcinomas defective in extrusion. Moreover, we expect a specific FAK inhibitor to not cause the common toxicities associated with standard chemotherapies, as it does not affect normal epithelial tissue. Another FAK inhibitor, PF-00562271, reduces tumor growth, metastases, and ameliorates tumor microenvironment when used in an orthotopic mouse model for pancreatic cancer (***Stokes et al., 2011***), suggesting this drug could be promising for pancreatic cancer patients. However, it is important to note that PF-00562271 also inhibits a FAK-related kinase Pyk-2, which promotes non-specific cell death (***Schultze and Fiedler, 2011***). The phase I clinical trial for PF-00562271 showed that while this drug was tolerated fairly well, it did cause nausea, vomiting, and diarrhea (***Infante et al., 2012***), symptoms indicative of poor gut barrier function, likely due to

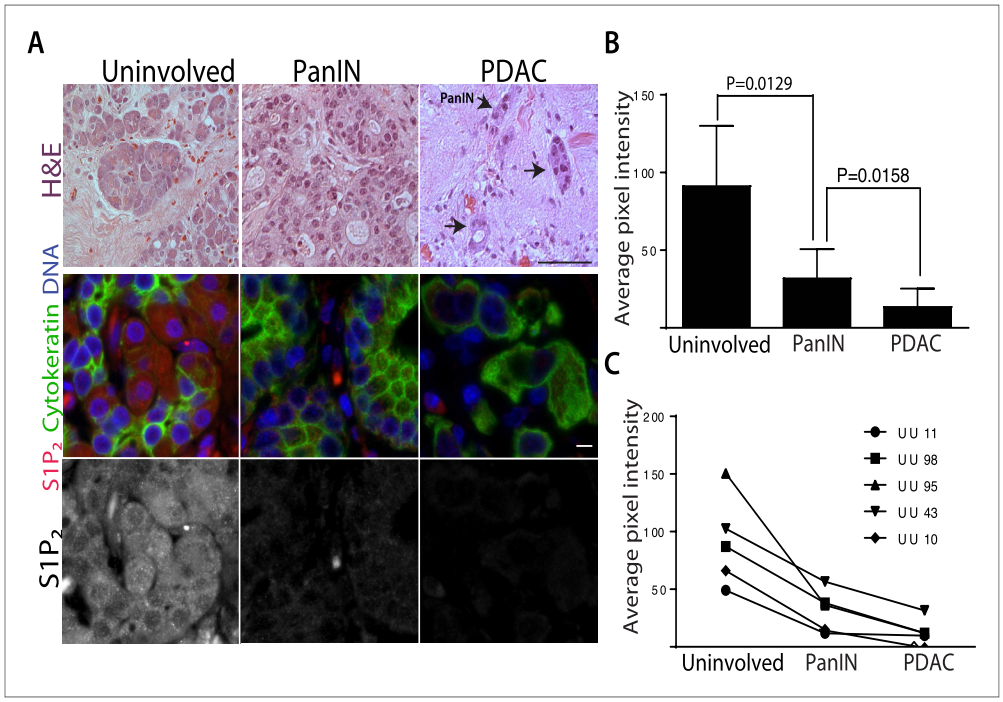

Figure 9. Human pancreatic tumors have reduced $S1P_2$ expression. (**A**) H&E (top panel) and confocal fluorescence images (middle and bottom panel) of normal acinar cells from uninvolved neck margin, PanIN, and invasive cancer cells. Scale bars, 100 and 10 μm, respectively. (**B**) Quantification of $S1P_2$ fluorescence intensity in acinar cells, PanIN, and invasive cancer cells from five individual patients. p values were calculated with a paired t test. (**C**) Changes of $S1P_2$ fluorescence intensity from normal acinar cells to invasive cancer cells in each individual patient.

DOI: 10.7554/eLife.04069.012

excessive non-specific apoptosis. Our results suggest that a newer more specific FAK inhibitor, such as VS-4718 (***Shapiro et al., 2014***), may provide a more targeted therapy for patients with pancreatic and lung carcinomas that have aberrant extrusion signaling without the common toxicities associated with older chemotherapies.

Based on our previous findings that extrusion drives normal epithelial cell turnover, we have found that disruption of extrusion may contribute to a class of cancers with poor prognosis. We find that cancer cells that lack the extrusion-signaling axis not only have reduced cell death rates but also have poor barrier function and a propensity to extrude cells basally, properties that could lead to higher invasion and metastatic rates. Therefore, aberrant extrusion signaling in pancreatic and lung carcinomas could not only contribute to tumor initiation but also progression. Importantly, specific inhibition of FAK, which does not disrupt normal epithelial tissue, is sufficient to reverse all of the effects of disrupted extrusion and could provide a better, less toxic therapy for this aggressive class of tumors.

Materials and methods

Cell culture

MDCK II cells were cultured in Dulbecco's minimum essential medium (DMEM) high glucose with 5% FBS (all from HyClone, Logan, UT) and 100 μg/ml penicillin/streptomycin (Invitrogen, Grand Island, NY) at 5% CO_2, 37°C. HBE cells were cultured in MEM supplemented with 10% FBS and l-glutamine in a flask coated with human fibronectin type I (BD, Franklin Lakes, New Jersey), bovine collagen I (Advanced BioMatrix, San Diego, CA), and BSA (Invitrogen). HPAF II cells were cultured in MEM (HyClone) supplemented with 10% FBS.

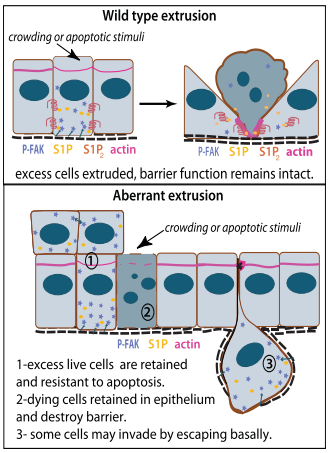

Figure 10. Model for how extrusion can promote cell death and suppress tumor formation. Apical extrusion promotes death of grey-blue cell (top panel). Here, pro-survival signals phospho-FAK and S1P (which also promotes extrusion) increase in an early extruding cell but decrease once a cell is extruded and targeted to die (right, cell with piknotic nucleus). However, when apical extrusion is blocked due to lack of $S1P_2$ receptor (bottom panel), epithelial cells do not die and can accumulate (left cell and those accumulating above) from increased matrix-derived survival signaling (arrows from matrix neighboring cells signaling to P-FAK). Additionally, cells can still basally extrude, which could potentially enable their invasion beneath the layer (right cell). Basally extruded cells may also have high P-FAK, since they are sensitive to FAK inhibitor when extruded into matrix in vitro, yet this point will be critical to test in vivo in disseminating tumors. Other cells may still die but not extrude (grey-blue cell with piknotic nucleus), leading to poor barrier function and inflammation, which could also promote tumor progression.

DOI: 10.7554/eLife.04069.013

Culturing HPAF II and MDCK cells in Matrigel generated HPAF II and MDCK cysts, respectively. Briefly, a single cell suspension of HPAF II cells was resuspended in Growth Factor Reduced Matrigel (BD Biosciences) final concentration 4% and placed in eight well coverglass chambers (Nalge Nunc, Rochester, NY) coated with a thin polymerized layer of Matrigel. For live imaging, cells were placed on 24 well glass-bottom culture dishes (MatTeK Corporation, Ashland, MA). After 20 min incubation at 37°C, cell-growth medium was added on top. Cysts were allowed to grow for the indicated duration and analyzed by time-lapse imaging or fixed with 4% paraformaldehyde for immunostaining.

Generation of stable Doxycyclin-inducible MDCK II cells over-expressing dominant negative FAK

We first transfected MDCK II cells with neomycin-resistant pTet-ON regulator plasmid, encoding rtTA protein (reverse tTA, tetracycline-controlled transactivator). The stable transfected MDCK II cells were selected by cultivation in media containing 500 μg/ml G418. We then transfected Tet-ON MDCK II cells with FAK-CD-TRE-2-hyg plasmids (***Golubovskaya et al., 2009***) and selected for stably transfected cells with 0.1 mg/ml hygromycin. Expression of FAK-CD was induced with 2 μg/ml doxycycline for 4 days.

UV and drug treatment

MDCK II, HBE, or HPAF II cells grown to confluence on glass coverslips were exposed to 1200 $\mu J/cm^2$ UV^{254} using a Spectrolinker (Spectroline, Westbury, NY) to induce apoptotic extrusion and incubated for 2 hr before fixation. Cells were treated with 10 μM JTE-013 (Tocris Bioscience, United Kingdom), 10 μM Y-27632, 10 μM Blebbistatin, 10 μM EHT 1864 (all from Sigma–Aldrich, Saint Louis, MO), 10 μM PF 573228 (Tocris Bioscience) or 1% DMSO as a control for 10 min before UV treatment. To induce apoptosis with chemotherapy drugs, cells were treated with 20 μg/ml Cisplatin, 1 μM Gemcitabine, or 20 μg/ml 5-Fluorouracil (all from Sigma–Aldrich) for 24 hr.

Cell staining

Cells were fixed with 4% formaldehyde in PBS at 37°C for 20 min, permeabilized for 10 min with 0.5% Triton in PBS, blocked with AbDil (PBS with 0.1% Triton X-100 and 2% BSA) for 10 min, and incubated with primary antibody for 1 hr. Antibody concentrations used for immunostaining were: 1:200 rabbit anti-active caspase-3 (BD), 1:100 rabbit anti-phospho FAK (Tyr 397) (Cell Signaling, Danvers, Massachusetts), and 50 μg/ml anti-S1P mAb (LPath Inc., San Diego, CA). Alexa Fluor 488 goat anti–rabbit IgG and Alexa Fluor 488 goat anti–mouse IgG were used as secondary antibodies to detect active caspase-3 and S1P, respectively. Actin was detected with Alexa Fluor 568–phalloidin (Invitrogen). DNA was detected with 1 μg/ml Hoechst 33,342 (Sigma–Aldrich).

Human pancreatic sections

Pancreatic tissue sections (3 μm) were generated from formalin-fixed, paraffin-embedded tissue collected from PDAC patient resections at the University of Utah Hospital. The sections were deparaffinised and rehydrated by incubating in citrus clearing solvent (CCS; Richard Allen Scientific, Kalamazoo, MI), 100%, 95%, 80%, 70% ethanol, and PBS. For immunofluorescence, antigens were retrieved by heating the slides in boiling 10 mM sodium citrate for 20 min, then rinsed three times with PBS, blocked with 5% BSA/0.5% Tween-20 in PBS for 4 hr, and incubated overnight with anti-$S1P_2$ (Imgenex, San Diego, CA) and anti-pan cytokeratin (Sigma–Aldrich) at 4°C, rinsed five times with PBS, incubated in Alexa-488 anti-mouse antibody, 1 μg ml^{-1} Hoechst, and Alexa-568 anti-rabbit antibody for 2 hr, rinsed three times in PBS, and mounted in Prolong Gold (Invitrogen). Fluorescence micrographs of stained slides were obtained using a Leica DM 6000B microscope and captured using a Micromax charge-coupled device camera (Roper Scientific, Sarasota, Florida). IPlab Software was used to control the camera and to process images. Pixel intensity interested area was measured with ImageJ. The University of Utah Institutional Review Board approved the use of human tissue in this study. Tissue sections were obtained from excess clinical pathology tissue from patients, deidentified, resected for pancreatic adenocarcinoma at the University of Utah Huntsman Cancer Institute with appropriate informed consent for use of samples for research purposes (IRB_00010924).

Zebrafish treatment and staining

We sorted *Mil* zebrafish embryos from their WT homozygous and heterozygous siblings at 2 days post-fertilization (dpf) by the presence or absence of tail blisters. We then treated half of *Mil* mutants and half of the wild type siblings with FAK inhibitor (10 μM PF 573228) for 3 days and added Texas Red-$Dextran^{MW70}$ 30 min before fixation. Embryos were then fixed in PBS with 4% formaldehyde and 0.1% Triton X-100 overnight, blocked with 2 mg/ml BSA for 2 hr, and stained for anti-E Cadherin (Gentex, Zeeland: MI) for 4 hr followed by incubation with Alexa Fluor 488 anti–rabbit IgG Ab. DNA was visualized using 1 μg/ml DAPI.

Zebrafish morpholino

The antisense morpholino oligonucleotides and photo-morpholino oligonucleotides were acquired from Gene Tools, LLC (Philomath, OR). For the photo-morpholino experiments, the translation blocking antisense morpholino (4 ng/embryo of each) was mixed at a 1:1 molar ratio with a 25 bp sense photo-morpholino and injected into 1–2-cell-stage wild-type AB zebrafish embryos. At 28–32 hpf, embryos were exposed to 350 nm light for 20 s to release the caging sense morpholino, then treated with 10 μM PF 573228 (FAK inhibitor), and filmed by timelapse video microscopy on a spinning disc confocal.

Image and video acquisition

Confocal Imaging was performed in a Nikon Eclipse TE300 inverted microscope converted for spinning disc confocal microscopy (Andor Technologies, United Kingdom) using a 40× Nikon Apo LWD lenses. Images were acquired with an electron-multiplied cooled charge-coupled device camera (DV887 1004X1002; Andor Technologies) driven by Andor IQ2 imaging software. All images were processed further using Photoshop and Illustrator (Adobe, San Jose, CA), and QuickTime Pro (Apple, San Jose, CA) software.

Live imaging of HPAF II cysts was taken with an OLYMPUS 1X71 inverted microscope using a 20× lens. The images were taken every 5 min for 12 hr. Temperature was controlled by a Weather station connected to the microscope.

For live imaging, FAK inhibitor treated $S1P_2$ morpholino fish were anesthetized with 0.02% Tricaine in E3, mounted in 1% low melt agarose and imaged on a spinning disc confocal at 20×, capturing a z-series every 2 min (***Eisenhoffer and Rosenblatt, in press***) for 3–6 hr.

Quantification of apoptosis and cell extrusion

To quantify the frequency of apoptosis within a monolayer, we counted the number of active caspase-3 positive cells still in contact with the monolayer per 1000 cells. We excluded round cells with strong caspase-3 staining that were not associated with monolayers, which were likely extruded well before experimental treatments could have impacted them.

To quantify extrusion, extruding cells were manually scored based on the presence of an actin ring compared to where apoptotic cell localized with respect to its neighboring cells. Apoptotic cells above

the plane of the monolayer with strong actin staining around and below them were defined as apically extruded cells. Apoptotic cells remaining in the monolayer and underneath an apical actin ring were considered basally extruded cells. Active caspase-3-positive cells that were not surrounded by a distinguishable actin ring were defined as non-extruded apoptotic cells.

Immunoblot analysis

Whole-cell extracts were prepared by resuspending cells in NP40 Cell Lysis Buffer (Invitrogen) plus protease inhibitor cocktail and PMSF (Roche, Switzerland). Proteins were resolved by SDS-PAGE using NuPage gels (Invitrogen), and transferred to polyvinylidene difluoride membrane (Thermo, Waltham, MA). Membranes were blocked with 5% dry milk and probed with anti-tubulin 1:1000 (Sigma–Aldrich) and anti-GFP 1:10,000 (Clontech, Mountain View, CA) or anti $S1P_2$ 1:500 (Santa Cruz, Santa Cruz, CA) and identified using horseradish peroxidase conjugated secondary antibodies and enhanced chemiluminescense.

Molecular cloning

pLL5.0 is a lentiviral expression plasmid containing a U6 promoter to drive expression of the shRNA sequence and a 5′-long terminal repeat to drive the expression of GFP. Designing and cloning of $S1P_2$-specific shRNA were performed as previously described (***Gu et al., 2011***). The full length of human $S1P_2$ was PCR amplified and ligated into the *EcoR*I/*Bam*HI sites of pLL5.0.

Lentiviral production and transduction

Retroviral production and infections were as described (***Gu et al., 2011***). Infected HPAF II or HBE cells were sorted for GFP by using a BD FACSAria Cell Sorter.

Surgical orthotopic pancreatic cancer xenograft mouse model

Animals were handled according to protocols approved by the University of Utah Institutional Animal Care and Use Committee. Mice were anesthetized under isoflurane gas; the abdominal skin and muscle were incised just off the midline and directly above the pancreas to allow visualization of the pancreatic lobes; the pancreas was gently retracted and positioned to allow for direct injection of a 100 µl bolus of 1×10^6 HPAF II cells expressing GFP or $S1P_2$ GFP using a 1 cc syringe with a 30 gauge needle; the pancreas was placed back within the abdominal cavity; and both the muscle and skin layers were closed. 8 weeks later, mice were sacrificed and xenograft tumors were resected and weighed. Metastatic tumors within abdominal wall, liver, and mesentery were also examined and resected.

Quantifications

P-FAK was quantified using Nikon Elements as the 'ROI Sum Intensity' on ROI statistics using the same ROI size for each projection micrograph measured, subtracting background average fluorescence. Lumen sizes were also measured using Nikon Elements using 'Radius size' using the largest diameter in the 'Annotations and Measurements' analysis package. The statistical analysis was performed using an unpaired or paired *t* test. Values of $p < 0.05$ were considered significant.

Acknowledgements

We thank Dr George Eisenhoffer, Alexandra Locke, and Richard Dawson for help on zebrafish experiments, and Drs Katie Ullman, Kim Schuske, and Trudy Oliver for helpful comments on our manuscript and LPath for S1P antibody. This work was supported by a National Institute of Health Director's New Innovator Award 1DP2OD002056-01, an R01 R01GM102169 and University of Utah Funding Incentive Seed Grant to JR and P30 CA042014 awarded to The Huntsman Cancer Institute for core facilities.

Additional information

Funding

Funder	Grant reference number	Author
National Institute of General Medical Sciences	NIH Director's New Innovator Award 1DP2OD002056-	Jody Rosenblatt
National Cancer Institute	Cancer Center Support Grant P30 CA042014	Yapeng Gu, Jody Rosenblatt

Funder	Grant reference number	Author
National Institute of General Medical Sciences	R01GM102169	Jody Rosenblatt

The funders had no role in study design, data collection and interpretation, or the decision to submit the work for publication.

Author contributions

YG, Identified the S1P extrusion pathway and that it was defective in tumors, did nearly all of the experiments, and wrote the paper, Conception and design, Acquisition of data, Analysis and interpretation of data, Drafting or revising the article; JS, Did mouse orthotopic tumor studies, Helped analyze data, Revised manuscript, Acquisition of data, Analysis and interpretation of data, Drafting or revising the article; GS, Contributed data on Rac inhibitor, Made S1P2 morphant fish and filmed them, Revised manuscript, Acquisition of data, Analysis and interpretation of data, Drafting or revising the article, Contributed unpublished essential data or reagents; MAF, Analyzed and obtained pancreatic cancer tissue samples, Helped interpret slides, Commented on manuscript, Analysis and interpretation of data, Drafting or revising the article, Contributed unpublished essential data or reagents; MA, Did experiments on chemotherapies with cell lines, Analyzed data, Had helpful comments on the paper, Acquisition of data, Analysis and interpretation of data, Drafting or revising the article; SJM, Did surgery on pancreatic cancer patients, Consulted on data, Reviewed the paper, Acquisition of data, Analysis and interpretation of data, Drafting or revising the article, Contributed unpublished essential data or reagents; VMG, Provided FAK reagents and consulting, Revised paper, Conception and design, Analysis and interpretation of data, Drafting or revising the article, Contributed unpublished essential data or reagents; JR, Conceived of many experiments, did some fish experiments, helped analyze data, helped write and edit manuscript drafts, Conception and design, Acquisition of data, Analysis and interpretation of data, Drafting or revising the article

Ethics

Human subjects: The use of human tissue in this study was approved by the University of Utah Institutional Review Board. Tissue sections were obtained from excess clinical pathology tissue from patients resected for pancreatic adenocarcinoma at the University of Utah Huntsman Cancer Institute with appropriate informed consent for use of samples for research purposes (IRB_00010924). Human tissue sample were deidentified and informed consent was obtained from all study participants. The protocol was approved and monitored by the University of Utah Institutional Review Board.

Animal experimentation: This study was performed in strict accordance with the recommendations in the Guide for the Care and Use of Laboratory Animals of the National Institutes of Health. All of the animals were handled according to approved institutional animal care and use committee (IACUC) protocols (#13-06006) of the University of Utah. The protocol was approved by the University of Utah IACUC board.

References

Andrade D, Rosenblatt J. 2011. Apoptotic regulation of epithelial cellular extrusion. *Apoptosis* **16**:491–501. doi: 10.1007/s10495-011-0587-z.

Badea L, Herlea V, Dima SO, Dumitrascu T, Popescu I. 2008. Combined gene expression analysis of whole-tissue and microdissected pancreatic ductal adenocarcinoma identifies genes specifically overexpressed in tumor epithelia. *Hepato-gastroenterology* **55**:2016–2027.

Bhattacharjee A, Richards WG, Staunton J, Li C, Monti S, Vasa P, Ladd C, Beheshti J, Bueno R, Gillette M, Loda M, Weber G, Mark EJ, Lander ES, Wong W, Johnson BE, Golub TR, Sugarbaker DJ, Meyerson M. 2001. Classification of human lung carcinomas by mRNA expression profiling reveals distinct adenocarcinoma subclasses. *Proceedings of the National Academy of Sciences of USA* **98**:13790–13795. doi: 10.1073/pnas.191502998.

Buchholz M, Braun M, Heidenblut A, Kestler HA, Kloppel G, Schmiegel W, Hahn SA, Luttges J, Gress TM. 2005. Transcriptome analysis of microdissected pancreatic intraepithelial neoplastic lesions. *Oncogene* **24**:6626–6636. doi: 10.1038/sj.onc.1208804.

Clair T, Aoki J, Koh E, Bandle RW, Nam SW, Ptaszynska MM, Mills GB, Schiffmann E, Liotta LA, Stracke ML. 2003. Autotaxin hydrolyzes sphingosylphosphorylcholine to produce the regulator of migration, sphingosine-1-phosphate. *Cancer Research* **63**:5446–5453.

Coussens LM, Werb Z. 2002. Inflammation and cancer. *Nature* **420**:860–867. doi: 10.1038/nature01322.

Eisenhoffer GT, Loftus PD, Yoshigi M, Otsuna H, Chien CB, Morcos PA, Rosenblatt J. 2012. Crowding induces live cell extrusion to maintain homeostatic cell numbers in epithelia. *Nature* **484**:546–549. doi: 10.1038/nature10999.

Eisenhoffer GT, Rosenblatt J. Live imaging of cell extrusion from the epidermis of developing zebrafish. *Journal of Visualized Experiments*. doi: 10.3791/2689. (in press).
Frisch SM, Francis H. 1994. Disruption of epithelial cell-matrix interactions induces apoptosis. *The Journal of Cell Biology* **124**:619–626. doi: 10.1083/jcb.124.4.619.
Frisch SM, Vuori K, Ruoslahti E, Chan-Hui PY. 1996. Control of adhesion-dependent cell survival by focal adhesion kinase. *The Journal of Cell Biology* **134**:793–799. doi: 10.1083/jcb.134.3.793.
Golubovskaya VM, Zheng M, Zhang L, Li JL, Cance WG. 2009. The direct effect of focal adhesion kinase (FAK), dominant-negative FAK, FAK-CD and FAK siRNA on gene expression and human MCF-7 breast cancer cell tumorigenesis. *BMC Cancer* **9**:280. doi: 10.1186/1471-2407-9-280.
Gu Y, Forostyan T, Sabbadini R, Rosenblatt J. 2011. Epithelial cell extrusion requires the sphingosine-1-phosphate receptor 2 pathway. *The Journal of Cell Biology* **193**:667–676. doi: 10.1083/jcb.201010075.
Infante JR, Camidge DR, Mileshkin LR, Chen EX, Hicks RJ, Rischin D, Fingert H, Pierce KJ, Xu H, Roberts WG, Shreeve SM, Burris HA, Siu LL. 2012. Safety, pharmacokinetic, and pharmacodynamic phase I dose-escalation trial of PF-00562271, an inhibitor of focal adhesion kinase, in advanced solid tumors. *Journal of Clinical Oncology* **30**:1527–1533. doi: 10.1200/JCO.2011.38.9346.
Kupperman E, An S, Osborne N, Waldron S, Stainier DY. 2000. A sphingosine-1-phosphate receptor regulates cell migration during vertebrate heart development. *Nature* **406**:192–195. doi: 10.1038/35018092.
Marinari E, Mehonic A, Curran S, Gale J, Duke T, Baum B. 2012. Live-cell delamination counterbalances epithelial growth to limit tissue overcrowding. *Nature* **484**:542–545. doi: 10.1038/nature10984.
Marshall TW, Lloyd IE, Delalande JM, Nathke I, Rosenblatt J. 2011. The tumor suppressor adenomatous polyposis coli controls the direction in which a cell extrudes from an epithelium. *Molecular Biology of the Cell* **22**:3962–3970. doi: 10.1091/mbc.E11-05-0469.
Park HB, Golubovskaya V, Xu L, Yang X, Lee JW, Scully S II, Craven RJ, Cance WG. 2004. Activated Src increases adhesion, survival and alpha2-integrin expression in human breast cancer cells. *The Biochemical Journal* **378**:559–567. doi: 10.1042/BJ20031392.
Pham DH, Powell JA, Gliddon BL, Moretti PA, Tsykin A, Van der Hoek M, Kenyon R, Goodall GJ, Pitson SM. 2013. Enhanced expression of transferrin receptor 1 contributes to oncogenic signalling by sphingosine kinase 1. *Oncogene* **33**:5559–5568. doi: 10.1038/onc.2013.502.
Rosenblatt J, Raff MC, Cramer LP. 2001. An epithelial cell destined for apoptosis signals its neighbors to extrude it by an actin- and myosin-dependent mechanism. *Current Biology* **11**:1847–1857. doi: 10.1016/S0960-9822(01)00587-5.
Schultze A, Fiedler W. 2011. Clinical importance and potential use of small molecule inhibitors of focal adhesion kinase. *Anti-cancer Agents in Medicinal Chemistry* **11**:593–599. doi: 10.2174/187152011796817727.
Segara D, Biankin AV, Kench JG, Langusch CC, Dawson AC, Skalicky DA, Gotley DC, Coleman MJ, Sutherland RL, Henshall SM. 2005. Expression of HOXB2, a retinoic acid signaling target in pancreatic cancer and pancreatic intraepithelial neoplasia. *Clinical Cancer Research* **11**:3587–3596. doi: 10.1158/1078-0432.CCR-04-1813.
Shapiro IM, Kolev VN, Vidal CM, Kadariya Y, Ring JE, Wright Q, Weaver DT, Menges C, Padval M, McClatchey AI, Xu Q, Testa JR, Pachter JA. 2014. Merlin deficiency predicts FAK inhibitor sensitivity: a synthetic lethal relationship. *Science Translational Medicine* **6**:237ra268. doi: 10.1126/scitranslmed.3008639.
Slack-Davis JK, Martin KH, Tilghman RW, Iwanicki M, Ung EJ, Autry C, Luzzio MJ, Cooper B, Kath JC, Roberts WG, Parsons JT. 2007. Cellular characterization of a novel focal adhesion kinase inhibitor. *The Journal of Biological Chemistry* **282**:14845–14852. doi: 10.1074/jbc.M606695200.
Slattum G, Gu Y, Sabbadini R, Rosenblatt J. 2014. Autophagy in oncogenic K-Ras promotes basal extrusion of epithelial cells by degrading S1P. *Current Biology* **24**:19–28. doi: 10.1016/j.cub.2013.11.029.
Slattum G, McGee KM, Rosenblatt J. 2009. P115 RhoGEF and microtubules decide the direction apoptotic cells extrude from an epithelium. *The Journal of Cell Biology* **186**:693–702. doi: 10.1083/jcb.200903079.
Slattum G, Rosenblatt J. 2014. Tumour cell invasion: an emerging role for basal epithelial cell extrusion. *Nature Reviews Cancer* **14**:495–501. doi: 10.1038/nrc3767.
Stokes JB, Adair SJ, Slack-Davis JK, Walters DM, Tilghman RW, Hershey ED, Lowrey B, Thomas KS, Bouton AH, Hwang RF, Stelow EB, Parsons JT, Bauer TW. 2011. Inhibition of focal adhesion kinase by PF-562,271 inhibits the growth and metastasis of pancreatic cancer concomitant with altering the tumor microenvironment. *Molecular Cancer Therapeutics* **10**:2135–2145. doi: 10.1158/1535-7163.MCT-11-0261.

CHAPTER 5

CONCLUSIONS AND FUTURE DIRECTIONS

In Chapter 1, I reviewed recent progress in the field of epithelial cell extrusion. While apical extrusion normally promotes cell death during homeostasis, I discussed how misregulation of apical extrusion and elevated survival signals might enable basally extruded cells to invade the underlying tissues. This review allowed me to speculate about how basal cell extrusion may relate to other known models for cell invasion: epithelial to mesenchymal transition (EMT), and collective or single cell invasion [1]. Following this review covering the rationale for my thesis project, in Chapter 2, I presented work on the cytoskeletal mechanism I found to be critical for controlling the direction a cell extrudes. In this work, I showed that microtubules target P115 RhoGEF to control basolateral contraction of actin/myosin at the interphase between extruding and neighboring cells that is necessary for driving apical extrusion. Blocking this mechanism by microtubule disrupters causes cells to instead contract apically and extrude basally [2]. This work led to a study showing that oncogenic mutation of Adenomatous Polyposis Coli also misregulates microtubules to drive extrusion basally [3]. Given this knowledge, I next asked whether cells expressing other oncogenic mutations could also alter extrusion. In Chapter 3, I found that high levels of autophagy in cells expressing oncogenic K-Ras disrupts the normal S1P-$S1P_2$ signaling required for apical extrusion. In addition, blocking autophagy with different chemical inhibitors or genetically is sufficient to rescue S1P localization and apical extrusion [4]. An essential part of training to become an independent scientist involves collaborating with other investigators. Chapter 4 highlighted my collaboration with Yapeng Gu, a postdoc in the Rosenblatt lab. In this work, we found that extrusion-deficient epithelia lacking $S1P_2$ form cell masses that are refractory to chemotherapy. Poor chemotherapy response derives from prolonged attachment of cells to the matrix and its associated survival signaling, which can be reversed by inhibiting Focal Adhesion Kinase (FAK).

While my graduate work provided answers to many of the questions that existed at the time I joined the lab, important questions still remain: What is the fate of live extruded cells in vivo? Is basal extrusion of cells expressing oncogenic K-Ras sufficient to invade the stroma? We are developing several tools to answer these questions in vivo using the zebrafish animal model. Here, I will highlight the tools we are developing and summarize our ongoing studies while suggesting future studies that could teach us how misregulated cell extrusion could promote cancer cell invasion.

Our finding that cells expressing oncogenic K-Ras can extrude basally into the matrix, survive, and proliferate when grown in a 3-dimensional system in vitro [4] made us wonder if cells expressing this mutation could invade in vivo. To address this, I developed a method to express K-Ras in the epidermis of the transparent zebrafish where cell extrusion and migration can be followed live without invasive techniques [5]. The developing zebrafish epidermis is very similar in structure and cell type composition to the epithelium coating mammalian organs such as lung, prostate, and breast [6, 7]. During development, zebrafish epidermis is a epithelial bilayer comprised of a basal p63 positive-layer of progenitor cells [8] and an outer cytokeratin 4 positive-layer [9, 10]. Because we can readily film cells extruding and invading live by studying zebrafish epidermis, we believe that the knowledge we gain from these studies will serve as an excellent model to understand if basal extrusion can drive invasion in carcinomas. Additionally, zebrafish will allow us to rapidly test and screen for small molecules that block basal extrusion and target invasive cells to die.

5.1 Expression of Oncogenic K-Ras in the Developing Zebrafish Epidermis

To test if extrusion of cells expressing oncogenic K-Ras is sufficient to enable invasion into the tissue underlying the epidermis of zebrafish, I expressed oncogenic EGFP-K-Ras (K-Ras^{V12}) or wild type EYFP-K-Ras (K-Ras^{WT}) in the developing outer cytokeratin positive layer. To do this, we used the Tol2 system [11] to drive human K-RAS (V12 or WT) with a zebrafish cytokeratin 4 promoter. Injection of either DNA plasmid into one-cell stage wild type embryos drives mosaic expression of either K-Ras isoform. I then follow the fate of the GFP-labeled cells once they become expressed at 12 hours by either time-lapse microscopy or by immunostaining. I find that embryos expressing GFP-K-Ras^{V12} form cell masses containing live and dying cells throughout the whole epidermis covering the body by 24 hpf (Figure 5.1).

5.2 Do Cells Expressing K-Ras^{V12} Extrude from the Developing Zebrafish Epidermis?

Because EGFP-K-Ras is membrane bound, we can readily view the cell cortex to detect cell extrusion by contracting rosettes before the cell extrudes out. Alternatively, we can detect actin ring formation by co-injecting mRNA an F-actin binding protein (RFP-UtrCH) that encodes red fluorescent protein fused to the calponin homology domain of utrophin [5].

I find that while cells expressing K-Ras^{WT} are stationary in the epidermis, those expressing K-Ras^{V12} basally extrude (Figure 5.2). Most of these basally extruded cells die shortly following extrusion, suggesting that K-Ras^{V12} alone is not sufficient for cell survival. To test if a small percentage of K-Ras^{V12} cells can survive after extrusion, we are currently working with the Cell Imaging Core Facility to film all the extrusion events in numerous embryos with high resolution. Typically,

however, transformation by a single oncogene results in cell death and oncogenic transformation requires collaborating mutations [12-15]. Therefore, I am currently (in the next section) testing if other mutations cooperate with K-Ras^{V12} to promote their survival following basal extrusion.

5.3 Is Invasion and Survival of K-Ras^{V12} Cells Enhanced by Loss of p53?

Because K-Ras^{V12} expressing cells basally extruded from the epidermis but then died, I decided to test if other collaborating mutations could enable extruded cells to live. Lung and pancreatic cancers typically contain mutations that activate K-Ras and disrupt the tumor suppressor p53 [16-18]. When I injected K-Ras constructs in a p53 mutant fish or in wild type fish co-injected with p53 morpholino, each 24 hpf embryo survived better than wild type fish and contained higher numbers of K-Ras^{V12} positive cells and larger and more cell masses per embryo. Furthermore, while some K-Ras^{V12} cells still die, some can be seen migrating below the periderm and within blood vessels (Figure 5.3). I am currently developing ways to film more embryos simultaneously using the Nikon A1R confocal microscope at the core facility, which enables fast and high resolution imaging to capture more events and be able to follow all cell movements from the beginning of extrusion to later migration. While visualizing EGFP-K-RasV12 cells in the vasculature suggests that these cells may be intravasating after they basally extrude, it is important to note that they may be able to enter before the blood vessels have formed, a process that ends at approximately 24hpf. To prevent extrusion until after blood vessels form so we can test how far these cells may transit, I will drive KRAS after 24 hpf in specific epithelial cell types after blood vessels formation. Additionally, these GFP-positive cells may result from clearance by inflammatory macrophages, which more readily migrate to and engulf oncogenic cells [19]. To investigate this possibility,

I will test if GFP positive cells within the vasculature are corpses of transformed cells, assessing if neutrophils and macrophages are associated with K-Ras cells and if these K-Ras cells are dead with apoptotic markers.

5.4 Developing Tools to Spatially and Temporally Control K-Ras Expression

We have characterized several GAL4 enhancer trap lines expressed in different epithelial cell types of the developing zebrafish (Eisenhoffer, G., Slattum, G., et al., in preparation & Otsuna, H., et al., under revision). To drive K-Ras in different epidermal cells using the Gal4-UAS system, I generated a UAS-K-Ras human line. We tested these constructs in transient transgenesis assay by injecting UAS:EGFP-K-RAS^{V12} or UAS:EYFP-K-RAS^{WT} plasmid DNA without Tol2 transposase mRNA in one-cell stage periderm Et(zc1044:Gal4);Tg(UAS:nfs-B-mCherry) embryos (hereafter called Periderm-Gal4). In preliminary results, I find the phenotypes from these embryos phenocopy those driven from the Krt4 promoter: K-Ras^{V12} cells extrude basally from the epidermis and form cells masses.

To delay the onset of K-Ras expression in the developing periderm, I am taking two approaches: 1) testing an antisense photo-cleavable morpholino against GAL4 (gal4-AS-photo-MO), which is destroyed by UV exposure, and 2) using an antisense morpholino against human K-Ras^{V12} (K-Ras^{V12}-MO) to delay its expression. I have preliminary results showing that co-injecting 0.2 mM gal4-AS-photo-MO and 25 pg UAS:KRAS^{V12} followed by 1-minute exposure to 365nm wavelength at 24 hpf enables the control of EGFP-K-Ras^{V12} expression in the Periderm-Gal4-mCherry line. Without photo-activation, 70% of the embryos co-injected with gal4-AS-photo-MO and UAS:KRAS^{V12} showed no expression of mCherry or EGFP fluorescence at 24hpf. However, in 2-day-old photo-activated embryos (24 hours after photoactivation), only 30% of embryos express mCherry

in the periderm in the tail and gill epithelium and GFP cells were undetectable. By day 5, EGFP-K-Ras cells start to appear in the epidermis. Because K-Ras expression occurs so slowly and at low frequency, I am further testing for the optimal concentrations of AS-photo-morpholinos and time to photoactivate; however, there is some concern that by 5dpf, much of the original plasmid will have degraded. To circumvent this problem, I am trying to stabilize the DNA expression by co-injecting with Tol2 transposase mRNA to promote DNA integration.

While trouble-shooting this method, I am currently trying to delay KRAS expression in the periderm by co-injecting with a K-RAS^{V12}-AS-morpholino, which should become diluted or degraded over time. I find that EGFP-K-RAS becomes expressed within the first 3 days of development. In a pilot study, injected wild type or Periderm-Gal4 embryos with K-RAS^{V12}-AS-MO alone had no detectable phenotypes. When I co-inject this morpholino with CK- or UAS-driven K-Ras^{V12} constructs, 90% of injected embryos undergo normal development for the first two days but express EGFP positive cells through out the periderm and form cells masses by 4 dpf. These recent data are very compelling and suggest that we will now be able to quickly test if driving KRAS expression later in development after vasculature is fully formed still allows basally extruded cells to invade the underlying stroma and intravasate into blood vessels.

5.5 Future Perspectives to Spatially and Temporally Control K-Ras Expression

New techniques are being developed to generate inducible systems that precisely control the timing of transgene expression both in space and time [20]. One approach, the ERT2-Gal4 system, where Gal4 expression can be driven reversibly by 4-OHT addition could be useful for our studies. Because it uses Gal4, these can also be crossed to effector UAS lines to drive genes of interest with temporal

control. ERT2-Gal4 has been successfully fused to tissue specific drivers to drive gene expression in the skin and a subset of migrating lateral line primordium with a Claudin B tight junction protein promoter [21]. We may use reported Keratin 5 or 4 similarly to express K-Ras in the skin epithelia [22] [23]. Importantly, these lines can be crossed to our already developed UAS-bearing transgenic lines and constructs that includes reporters or filamentous actin.

5.6 Expressing K-Ras in Other Cell Types

Cells expressing $KRas^{V12}$ even with p53 loss may become trapped between two epithelial layers following basal extrusion. Therefore, we would like to drive $KRas^{V12}$ in other cells within the epidermis where they may be more likely to invade from, such as ionocytes or basal cells. To this end, I have injected the UAS:EGFP-$K\text{-}RAS^{V12}$ in a Gal4 enhancer trap line marking ionocytes (Eisenhoffer, G., Slattum, G., et al., in preparation). The ionocytes are imbedded between the two layers of the epidermis and are equivalent to Clara cells of the lung. Interestingly, some lung tumors are thought to originate from Clara cells [24] and their transformation with K-RAS may make these cells more invasive that differentiated superficial epidermal cells. Similarly, I will express $KRas^{V12}$ in a p63 basal progenitor line, as they may have more survival and proliferative potential than the periderm cells.

5.7 Can Small Molecule Inhibitors Selectively Target K-Ras Expressing Cell to Extrude and Die?

Because we found that disrupting autophagy in $K\text{-}Ras^{V12}$ cells either chemically or genetically rescued S1P accumulation and apical extrusion [4], I will test if autophagy inhibitors can reverse invasion. Once I better establish if basal extrusion drives invasion, in collaboration with Adam Gardner, another student in

the lab, I will test if chloroquine, an autophagy inhibitor currently in clinical trials for tumors driven by oncogenic K-Ras, can target K-Ras expressing cells to apically extrude and die in vivo. Importantly, we will be able to also monitor the toxicity of surrounding wild type cells. Similarly, we will test other small molecules such as FAK inhibitors and other drugs alone or in combination with traditional chemotherapies to test their ability to reverse invasion or to target invasive cells to die. These experiments will help us develop novel therapies for tumors that have shown poor response to standard chemotherapies.

In this dissertation, I have presented work identifying novel insights into the mechanisms that govern epithelial cell extrusion both under physiological and pathological conditions. Additionally, I discussed the rationale for continuing our studies addressing other ways extrusion may become misregulated. So far, all the oncogenic mutations we have examined alter the direction of extrusion, suggesting basal extrusion may provide a conserved mechanism for tumor cells to initiate invasion.

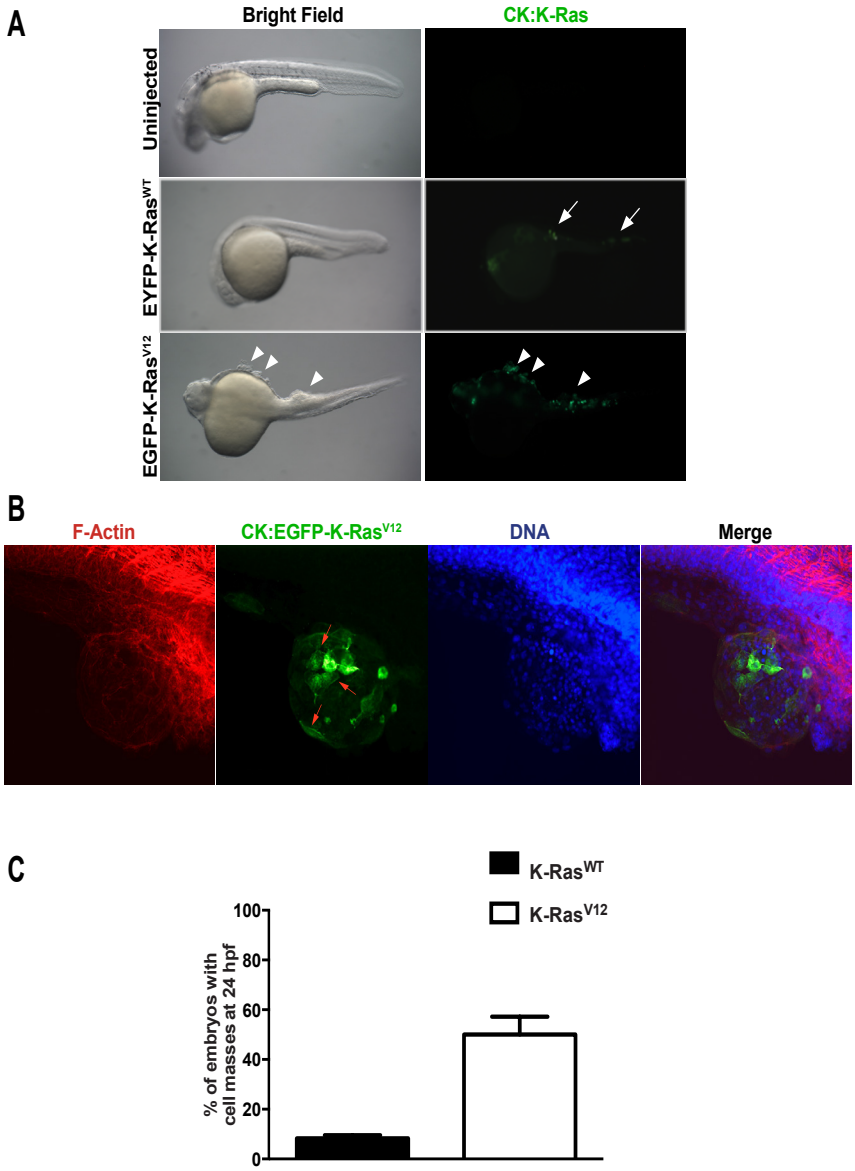

Figure 5.1. Expressing oncogenic K-Ras in the developing zebrafish epidermis results in the formation of cell masses. (A) 24hpf wild type embryo un-injected (top), Injected with CK-EYFP-K-RasWT (middle) or CK:EGFP-K-RasV12 (bottom) showing positive fluorescent cells (white arrows) and cell masses (white arrow head) trough out the epidermis. (B) Confocal projections of a fixed and stained cell mass showing EGFP-K-RasV12 positive cells (red arrows). (C) Quantification of cell masses in injected embryos where n= 209 embryos for K-RasV12 and 187 embryos for K-RasWT from 3 independent experiments.

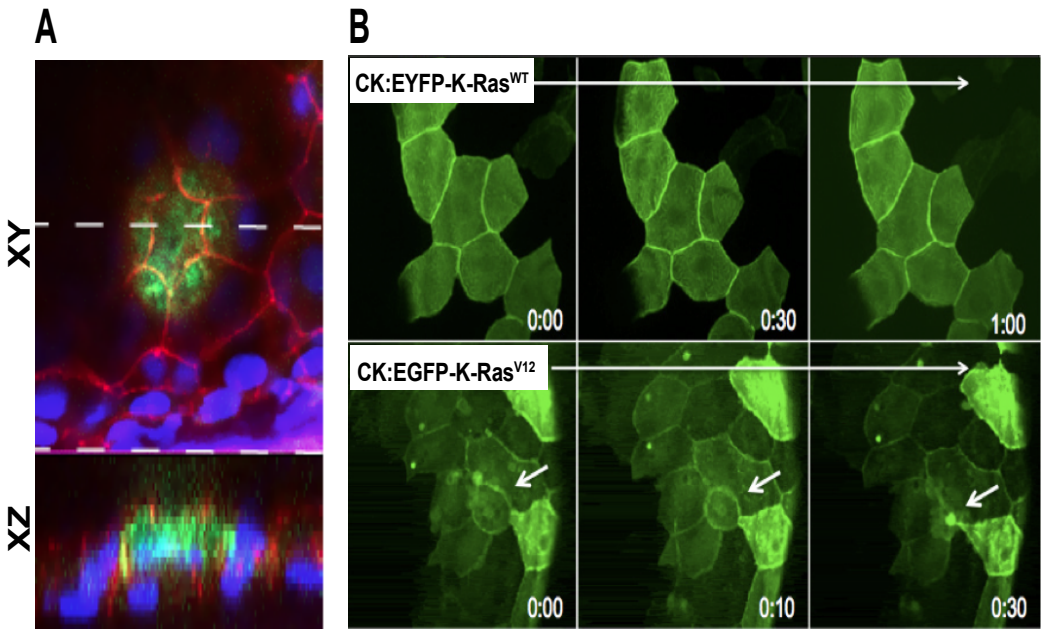

Figure 5.2. Expression of CK:EGFP-K-RasV12 causes cells to extrude basally. (A) Confocal projection and XZ cross-sections (below) of an early basal extrusion, whereas E-Cadherin (red), K-Ras (green), DNA (blue). (B) Stills from a movie showing that K-RasWT expressing cells are stationary in the epidermis (top), but those expressing K-RasV12 extrude basally and die (bottom and arrow).

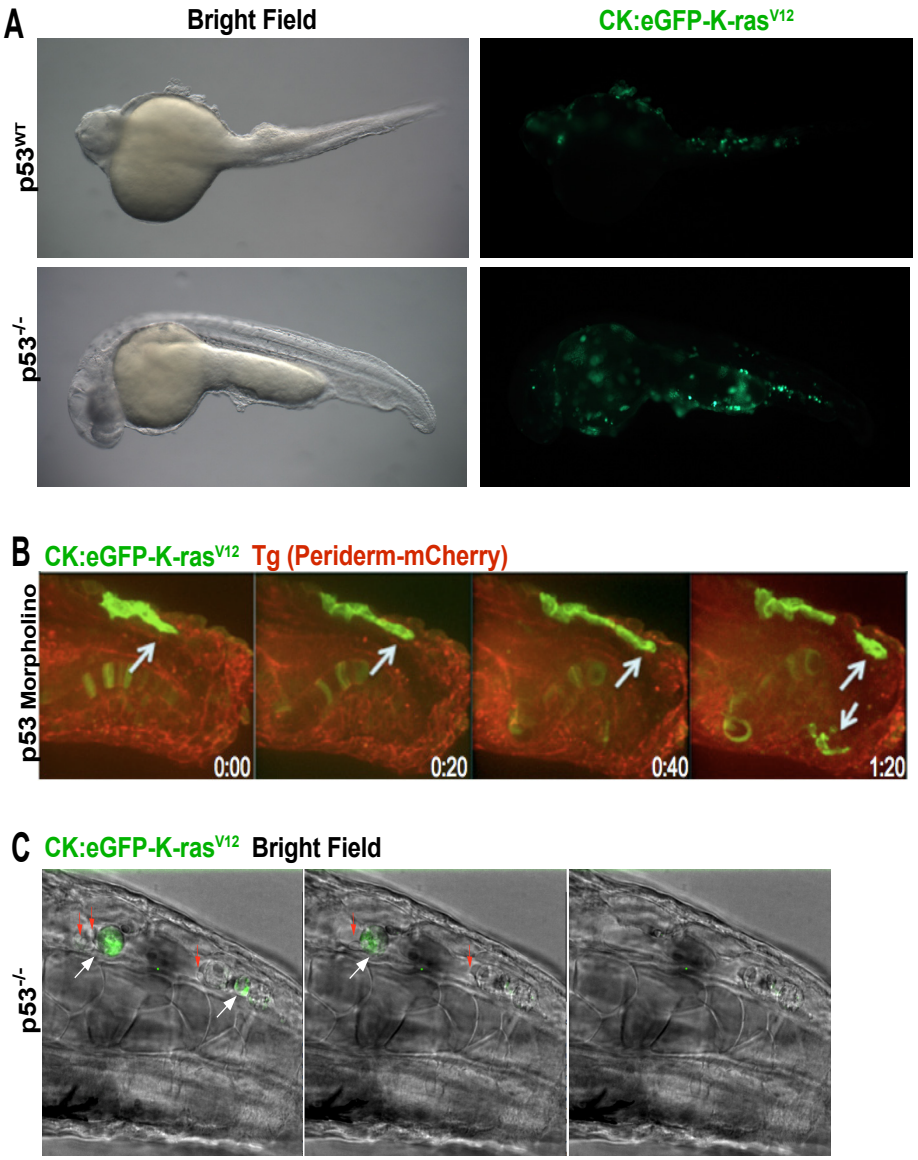

Figure 5.3. Loss of p53 enhanced survival and Invasion of CK:EGFP-K-RasV12 cells. (A) K-RasV12 cells (green) expressed in a p53 mutant fish survived better and contained higher numbers cells at 24hpf. (B) Stills from a movie showing that CK:EGFP-K-RasV12 coinjected with a p53 morpholino appears to migrate from the top and basal layer of the epidermis whereas (red) is Tg line marking the zebrafish periderm. (C) Stills from a movie showing GFP positive cells (arrows) traveling and being cleared out from the circulatory system of a 48 hpf p53 mutant embryo, red blood cells (red arrows).

5.8 References

1. Slattum, G.M. & Rosenblatt, J. Tumour cell invasion: an emerging role for basal epithelial cell extrusion. *Nat Rev Cancer* **14**, 495-501 (2014).

2. Slattum, G., McGee, K.M. & Rosenblatt, J. P115 RhoGEF and microtubules decide the direction apoptotic cells extrude from an epithelium. *J Cell Biol* **186**, 693-702 (2009).

3. Marshall, T.W., Lloyd, I.E., Delalande, J.M., Nathke, I. & Rosenblatt, J. The tumor suppressor adenomatous polyposis coli controls the direction in which a cell extrudes from an epithelium. *Mol Bio Cell* **22**, 3962-3970 (2011).

4. Slattum, G., Gu, Y., Sabbadini, R. & Rosenblatt, J. Autophagy in oncogenic K-Ras promotes basal extrusion of epithelial cells by degrading S1P. *Curr Biol* **24**, 19-28 (2014).

5. Eisenhoffer, G.T. & Rosenblatt, J. Live Imaging of Cell Extrusion from the Epidermis of Developing Zebrafish. *J Vis Exp* ***57*** (2011).

6. Le Guellec, D., Morvan-Dubois, G. & Sire, J.Y. Skin development in bony fish with particular emphasis on collagen deposition in the dermis of the zebrafish (Danio rerio). *Int J Dev Biol* **48**, 217-31 (2004).

7. Kimmel, C.B., Ballard, W.W., Kimmel, S.R., Ullmann, B. & Schilling, T.F. Stages of embryonic development of the zebrafish. *Dev Dyn* **203**, 253-310 (1995).

8. Lee, H. & Kimelman, D. A dominant-negative form of p63 is required for epidermal proliferation in zebrafish. *Dev Cell* **2**, 607-16 (2002).

9. Gong, Z. et al. Green fluorescent protein expression in germ-line transmitted transgenic zebrafish under a stratified epithelial promoter from keratin8. *Dev Dyn* **223**, 204-15 (2002).

10. Wang, Y.H., Chen, Y.H., Lin, Y.J. & Tsai, H.J. Spatiotemporal expression of zebrafish keratin 18 during early embryogenesis and the establishment of a keratin 18:RFP transgenic line. *Gene Expr Patterns* **6**, 335-9 (2006).

11. Kwan, K.M. et al. The Tol2kit: a multisite gateway-based construction kit for Tol2 transposon transgenesis constructs. *Dev Dyn* **236**, 3088-99 (2007).

12. Serrano, M., Lin, A.W., McCurrach, M.E., Beach, D. & Lowe, S.W. Oncogenic ras provokes premature cell senescence associated with accumulation of p53 and p16INK4a. *Cell* **88**, 593-602 (1997).

13. Downward, J. Ras signalling and apoptosis. *Curr Opin Genet Dev* **8**, 49-54 (1998).

14. Podsypanina, K., Politi, K., Beverly, L.J. & Varmus, H.E. Oncogene cooperation in tumor maintenance and tumor recurrence in mouse mammary tumors induced by Myc and mutant Kras. *Proc Natl Acad Sci U S A* **105**, 5242-7 (2008).

15. McMurray, H.R. et al. Synergistic response to oncogenic mutations defines gene class critical to cancer phenotype. *Nature* **453**, 1112-6 (2008).

16. Morton, J.P. et al. Mutant p53 drives metastasis and overcomes growth arrest/senescence in pancreatic cancer. *Proc Natl Acad Sci U S A* **107**, 246-51 (2010).

17. Scarpa, A. et al. Pancreatic adenocarcinomas frequently show p53 gene mutations. *Am J Pathol* **142**, 1534-43 (1993).

18. Feldser, D.M. et al. Stage-specific sensitivity to p53 restoration during lung cancer progression. *Nature* **468**, 572-5 (2010).

19. Feng, Y., Renshaw, S. & Martin, P. Live imaging of tumor initiation in zebrafish larvae reveals a trophic role for leukocyte-derived PGE(2). *Curr Biol* **22**, 1253-9 (2012).

20. Weber, T. & Koster, R. Genetic tools for multicolor imaging in zebrafish larvae. *Methods* **62**, 279-91 (2013).

21. Gerety, S.S. et al. An inducible transgene expression system for zebrafish and chick. *Development* **140**, 2235-43 (2013).

22. Akerberg, A.A., Stewart, S. & Stankunas, K. Spatial and temporal control of transgene expression in zebrafish. *PLoS One* **9**, e92217 (2014).

23. Ju, B. et al. Activation of Sonic hedgehog signaling in neural progenitor cells promotes glioma development in the zebrafish optic pathway. *Oncogenesis* **3**, e96 (2014).

24. Meuwissen, R. & Berns, A. Mouse models for human lung cancer. *Genes Dev* **19**, 643-64 (2005).